Dependence Modelling and Risk Analysis in a Joint Credit-Equity Framework

Fredrik Backman

May 2015

Abstract

This thesis is set in the intersection between separate types of financial markets, with emphasis on joint risk modelling. Relying on empirical findings pointing toward the existence of dependence across equity and corporate debt markets, a simulation framework intended to capture this property is developed. A few different types of models form building blocks of the framework, including stochastic processes describing the evolution of equity and credit risk factors in continuous time, as well as a credit rating based model, providing a mechanism for imposing dependent credit migrations and defaults for firms participating in the market. A flexible modelling framework results, proving capable of generating dependence of varying strength and shape, across as well as within studied markets. Particular focus is given to the way markets interact in the tails of the distributions. By means of simulation, it is highlighted that dependence as produced by the model tends to spread asymmetrically with simultaneously extreme outcomes occurring more frequently in lower than in upper tails. Attempts to fit the model to observed market data featuring historical stock index and corporate bond index values are promising as both marginal distributions and dependence connecting the investigated asset types appear largely replicable, although we conclude further validation remains.

Acknowledgements

There are several people without whose support and contributions this work would not have been possible. To my supervisor Boualem Djehiche at KTH, I would like to express my sincere thanks for providing much needed guidance and advice through challenging stages of the thesis. I also wish to extend my gratitude to my supervisors at Kidbrooke Advisory, Fredrik Davéus and Edvard Sjögren, for their continual encouragement and for providing valuable assistance and many helpful suggestions as the work has progressed.

Contents

1 Introduction **1**
- 1.1 Background . . . 1
  - 1.1.1 Types of Financial Risk . . . 1
  - 1.1.2 Financial Risk and Asset Pricing . . . 3
  - 1.1.3 Regulatory Requirements . . . 4
- 1.2 Objectives . . . 4
- 1.3 Scope and Limitations . . . 5
- 1.4 Disposition . . . 5

2 Mathematical Background **6**
- 2.1 Market Risk Models . . . 6
  - 2.1.1 Interest Rate Models . . . 7
  - 2.1.2 Equity Models . . . 9
- 2.2 Credit Modelling . . . 12
  - 2.2.1 Reduced Form Models . . . 13
  - 2.2.2 Rating Based Models . . . 13
  - 2.2.3 Pricing in Presence of Credit Risk . . . 15
- 2.3 Dependence Modelling . . . 16
  - 2.3.1 Linear Correlation and Concordance Measures . . . 17
  - 2.3.2 Copulas . . . 17
  - 2.3.3 Tail Dependence . . . 20
  - 2.3.4 Dependence in Credit Risk . . . 21
  - 2.3.5 Joint Equity-Credit Modelling . . . 23

3 Model **25**
- 3.1 Model Selection and Overview . . . 25
- 3.2 Carr and Wu (2010) Model . . . 26
- 3.3 Rating Based Model . . . 28
- 3.4 A Joint Framework . . . 29
- 3.5 Portfolio Application . . . 31

4 Method **32**
- 4.1 Data Analysis . . . 32
  - 4.1.1 Data Collection . . . 32
  - 4.1.2 Moments and Quantiles . . . 33
  - 4.1.3 Multivariate Analysis . . . 33
  - 4.1.4 Tail Index Measurements . . . 34
- 4.2 Process Simulation Methodology . . . 36
  - 4.2.1 CIR Process Discretization . . . 36

4.2.2 Variance-Gamma Process Discretization . . . 37
4.2.3 Stock Process Simulation . . . 38
4.3 Credit Migration Simulation Methodology . . . 39
4.3.1 Construction of Discrete Path-Dependent Migration Matrices . . . 39
4.3.2 Transformation of Stock Index Returns . . . 40
4.3.3 Copula Simulation Techniques . . . 40
4.3.4 Mapping Simulated Uniforms to Transition Outcomes . . . 41
4.4 Portfolio Evaluation along Sample Paths . . . 42
4.5 Parameter Estimation . . . 43

5 Results **44**
5.1 Data Analysis . . . 44
5.2 Model Calibration . . . 46
5.3 Portfolio Risk Simulation . . . 48
5.3.1 Risk Perspective . . . 48
5.3.2 Dependence Structure Adjustments: Migration Copulas . . . 51
5.3.3 Dependence Structure Adjustments: Variation of β . . . 58
5.3.4 Upper Tail Properties . . . 65

6 Discussion and Conclusions **68**
6.1 Summary of Findings . . . 68
6.2 Model Evaluation . . . 70
6.2.1 Strengths and Shortcomings . . . 70
6.2.2 Review of Simplifications . . . 71
6.3 Follow-up of Objectives . . . 74
6.4 Future Work . . . 75
6.5 Concluding Remarks . . . 76

Bibliography **77**

A Method for Adjusting β **80**

B Discretization Accuracy **82**

C Complementary Results **86**
C.1 Dependence Adjustments: IG Portfolio Results . . . 86
C.1.1 Complementary Plots, Migration Copula Adjustments . . . 86
C.1.2 Variation of β . . . 89
C.2 On Migration Time Windows . . . 95
C.3 Alternative Migration Conditioning . . . 97
C.3.1 Portfolio Simulation . . . 97

Chapter 1

Introduction

Over the past few decades, the financial industry has experienced a rapid growth in its need for sophisticated quantitative models in risk management and derivatives pricing. Explanations for this growing demand include derivatives markets quickly expanding in size and complexity, as well as sophistication of regulatory frameworks for financial institutions. Academia and practitioners alike have responded to the turns of the industry by means of steady advancements in financial mathematics, though at times with difficulties keeping up pace. Following the most recent financial crisis, the need for coherent and reliable mathematical models has been further highlighted.

While much of recent literature within quantitative finance has dealt extensively with the quantification and modelling of individual risk factors influencing pricing and asset allocation, less attention has been given to the analysis of dependence of risk across financial markets. The acquisition of knowledge of the interplay between disparate sources of risk, along with development of appropriate modelling tools able to capture this, are key challenges that lie ahead in order to consolidate the effectiveness of regulations and counteract the risk of future crises.

Via the construction and simulation from a joint modelling framework, the purpose of this thesis is to investigate how variations of the dependence structure between separate types of risk affect risk management calculations for portfolios consisting of several different asset classes. Specifically, focus is directed toward equity and credit risk and much of the emphasis is placed on model development. Furthermore, a discussion on what could be established empirically is undertaken aided by cross-sectional historical financial data.

In Section 1.1, we provide further background setting the scene for the thesis. Then, a number of broad thesis objectives are listed in Section 1.2 narrowed down to specifics in Section 1.3. Section 1.4 concludes this chapter by outlining how the remainder of the content is structured.

1.1 Background

The aim of this section is to further contextualize the thesis. We introduce several types of financial risk and briefly discuss the importance of modelling these for risk management and pricing purposes.

1.1.1 Types of Financial Risk

When managing financial risk, among the first questions that arises is, how can risk be quantified? Incidentally, the answer to this question varies widely depending on the type

of the risk faced. In practice, most financial institutions in need of rigorous systems for risk management face a situation where a range of different risk categories enter the picture and need to be properly accounted for.

Often included among types of financial risk are:

- Operational risk - the risk of loss caused by failure of internal processes, people or unexpected external events
- Systemic risk - the risk of loss caused by breakdown of the full financial system, or a part of it vital enough to have a severe, negative effect on the full system
- Liquidity risk - risk arising from lack of market liquidity leading to a possible loss from a trade not being effectuated

Particularly relevant to this thesis are two other types of risk, namely market risk and credit risk described in subsequent sections.

Market Risk

Market risk concerns the risk of change to values of holdings due to movements of market prices. The term can be considered an umbrella term spanning several subtypes, notably including equity, interest rates, currency and commodity risk. As a simple example, consider a long position taken in an in-the-money put option of a stock at time 0. Now, assume the value of the stock increases significantly so that at time 1, the put option is out-of-the-money. This stock movement is unfavourable for the put holder, reflecting equity risk taken and resulting in an unrealised net loss.

Further incorporated under the market risk umbrella is sometimes credit spread risk, which might appear confusing. What it captures is the risk caused from a change of the spread between market yields on treasury bonds and those on corporate bonds. The credit spread on bonds reflects both the underlying credit risk capturing the possibility of default of the issuer, and the market price of risk capturing investors' risk aversion (Jorion, 2010, ch. 11). A grey zone emerges where market and credit risks intersect. However, other definitions classify the spread risk as part of credit risk (Bielecki and Rutkowski, 2002, ch. 1), and to keep things clear that route will be followed in this thesis.

Measuring market risk involves the evaluation of the known or unknown probability distribution for the risk factors determining the value of the holdings. In case the distribution is unknown, which is usually the case, some estimation procedure has to be undertaken as well. Commonly, several risk factors are determinants for the value of the holdings, so that their joint behaviour needs to be taken into account.

Credit Risk

Credit risk is an area of finance that has recently received a large share of attention. The term describes the loss incurred to a party when a counterparty of a contractual agreement is unable to fulfil its obligation under the contract[1]. There are several quantities of interest when assessing credit risk; *probability of default* before settlement of the contract reflecting the credit quality of the counterparty; *loss given default* specifying the amount lost in case the counterparty defaults; and *exposure at default*, denoting the total amount outstanding to the counterparty at the time of default.

[1] Bielecki and Rutkowski (2002, ch. 1) distinguish between *reference* credit risk and *counterparty* credit risk, where the former refers to a risk of a reference party priced in a contract, without this party being involved in the transaction.

In order to keep track of the credit quality of market participants, formalized credit rating systems are used. Publicly available credit ratings are issued and published by credit rating agencies such as Standard & Poor's and Moody's, generally provided both with regard to issuers reflecting their overall creditworthiness, and with respect to specific financial obligations or classes of such. The latter take specific properties of the obligations, such as recovery arrangements, into account. Commonly credit ratings are classified into seven rating categories. From best to worst, these are AAA, AA, A, BBB, BB, B, CCC, occasionally with the additional inclusion of a default class D. These labels can vary slightly depending on the rating agency in question, for example Aaa instead of AAA, but are principally the same. Rating classes are sometimes further refined to include several notches of some of the aforementioned labels, such as BBB+, BBB and BBB-, reflecting minor variations in credit quality. With this refinement, 18 categories excluding default are obtained. Issuers or contracts belonging to rating classes AAA to BBB are often referred to as *investment grade*, whereas the corresponding term for the bundle of poorer rating classes (excluding default) is *speculative grade* or *high yield*.

In addition to the rating systems managed by specialized rating agencies, internal rating systems are also seeing frequent use and may be consulted by for example banks in the calculation of capital requirements.

The division into rating classes is helpful when managing portfolio risk, in particular for large portfolios, as it provides a quick overview of the overall riskiness of the portfolio. Quantities such as probability of default over a given time horizon may be estimated from the rating class of a specific asset. Therefore, credit risk modelling based on credit ratings has evolved to cover a substantial part of the literature on financial risk management. For a comprehensive overview, we refer to the book by Trueck and Rachev (2009).

1.1.2 Financial Risk and Asset Pricing

Whenever a financial asset is made available for trade, its price should be consistent with market prices. This calls for arbitrage free pricing, where the expectation of the discounted asset value at a future point in time has to be evaluated under a so-called *martingale* or *risk-neutral* probability measure. In contrast, the evolution of risk factors and asset prices in actual markets occurs under a probability measure often denoted the *physical* or *real-world* measure. While these measures might coincide, they usually do not. Typically investors demand compensation for taking larger risks, giving rise to an accentuation of the risks under the risk-neutral measure and creating what is known as market price of risk.

The probability distribution from which assets are priced will generally be unknown in closed form, and depend on one or several underlying risk factors. When there are several risk factors of relevance, a statistical model of their joint behaviour is necessary in order to obtain an accurate description of the sought distribution.

As a simple example, consider a European put option on a stock. Its value at a future point in time will depend on the movement of the stock until that time. This movement occurs in the real world, reflecting a scenario under the real-world measure. However, when valuing the option today, the expectation of the future value *discounted* to a value today further makes us have to consider all possible movements of interest rates, and all this under a risk-neutral measure. We thus deal with two separate factors of market risk in the pricing of the option: equity and interest rate risk.

Now to a more complicated example, we consider a *convertible bond* that is to be priced. A convertible bond is a corporate bond which grants the additional option of being converted into a position in the stock of the issuing company at a future point in

time. Meanwhile, corporate bonds are examples of financial instruments which are very directly linked to credit risk. The credit quality of the issuer relates to its propensity to default, in which case a recovery payment is made, lower than the bond payoff in the absence of default. A lower credit quality should therefore be directly reflected in the bond price, such that the yield is higher than that of a better rated bond. When the optionality of conversion is appended to the bond, elements of market risk separate from credit risk clearly enter as well. Thus, for correct pricing, the interplay between market and credit risks needs to be accounted for.

These examples illustrate how dependence between different sources of financial risk could naturally enter into the pricing of financial instruments and therefore is in need of modelling.

1.1.3 Regulatory Requirements

Financial institutions are obliged to comply with regulations stipulated by regulatory directives such as Solvency II, affecting insurance companies, and Basel III, directed towards banks[2]. Under Solvency II, insurance companies within the EU are required to hold sufficient buffer capital to ensure that they will be able to meet their financial obligations over the next 12 months with a probability of at least 99.5%. This directive targets the full balance sheet of the company, such that a risk analysis must incorporate all of the insurer's assets and liabilities.

The calculation of the capital requirement thus demands that all risk factors affecting the net asset value of the company be accounted for. Again, the dependence structure connecting several different risk factors becomes an important aspect to consider.

1.2 Objectives

In this section, we broadly define the thesis objectives. These are intentionally specified in a rather general manner, governing the direction of the thesis. Based on these, a demarcation detailing project specifics is presented in the next section. Towards the end of the report, in Section 6.3, each of the objectives will be reviewed and related to the work and its results.

1. **Analyse historical multivariate financial data**
   Given historical time series data from separate markets, conduct a statistical analysis raising both the behaviour of the individual series and of their dependence.

2. **Review and select relevant mathematical models**
   Review and evaluate mathematical models, emphasizing their capability to capture observed market patterns in a way well suited to the intended purpose.

3. **Construct a versatile simulation framework**
   Based on considered mathematical models, develop and construct a simulation framework capable of providing consistent generation of scenarios to be used for risk management and pricing, as much as possible admitting variation in the model specification.

[2]Basel III came into force in 2014. Solvency II is scheduled to do so in 2016.

4. **Discuss implications on risk management**
   Given variations to the modelling setup and its parameters, analyse and discuss how aggregate portfolio risk is affected and relate to reality.

1.3 Scope and Limitations

The sources of risk analysed in the thesis are credit and equity risk. Thus, any data taken should, as much as possible, reflect the movements of the corresponding risk factors and any model will be assessed based on its applicability for the setting at hand. A within-economy perspective is used throughout the thesis. Dependencies across economies are therefore not considered, rendering concepts like currency risk superfluous.

When modelling, we will consider a stock index as a proxy for the equity risk and a bond portfolio representing credit risk. As was mentioned in Section 1.1.1, credit spread movements on bonds are often considered part of market risk. However, for modelling purposes, we may use bond prices as a tool to convey information about the underlying credit risk. Further clarification is given in Chapter 3, detailing the specific application.

Interest rates are not explicitly modelled, instead the analysis and modelling is focused on excess returns of financial assets. Nonetheless, the ambition is to design the simulation framework in a flexible manner, so as to allow for additions and extensions in line with bullet 3 of the previously stated objectives. One such extension could be the inclusion of stochastic interest rates.

For the view on credit risk, we will be concerned with the modelling of probability of default and not include risk relating to contractual arrangements such as recovery covenants or associated factors, affecting loss given default.

The modelling of dependence between credit and equity risk, under the limitations mentioned, is the primary point of interest. Investigations of how dependence between the risk factors can be modelled, as well as the impact of different specifications for the extent and structure of dependence on risk management, reside at the forefront of the work.

1.4 Disposition

The remainder of the report is structured as follows. In Chapter 2, we lay out the mathematical principles underlying the work. Included here are some of the key findings in recent literature. Chapter 3 describes how the simulation framework is constructed and what models in the literature it draws from. This is followed up by details of the implementation and simulation methodology, all presented in Chapter 4. Results, both from data analysis and from simulation, are covered in Chapter 5. These are discussed in detail in Chapter 6, which also concludes the thesis by evaluating the modelling framework, reviewing objectives and providing a few suggestions for the directions future work could take. Appendices, containing complementary information, are referred to as needed.

Chapter 2

Mathematical Background

In this chapter the mathematical background for the thesis is presented. The literature underpinning the work is given a brief review, and the mathematics employed is summarized. Further theory on simulation of stochastic processes and associated concepts which closely relate to the implementation details of the project, is reviewed in Chapter 4.

We assume the reader is acquainted with mathematical concepts of statistics and risk management such as Value-at-Risk (VaR), empirical distributions and quantiles. Should that not be the case, recommended reading on the subject includes McNeil et al. (2010), Jorion (2010) and Hult et al. (2012).

Furthermore, martingale and arbitrage theory is not presented in detail. Nor are the basics of stochastic processes and stochastic differential equations. These matters are reviewed in most basic textbooks on quantitative finance, examples include Björk (2009) or the first few chapters of Brigo and Mercurio (2006).

For asset pricing, we denote the risk-neutral measure $\mathbb{Q}$ and consider an asset which at time $T > t$ has the stochastic value π_T. The price at time t is then expressed

$$\pi_t = E^{\mathbb{Q}}\left[\exp\left(-\int_t^T r_s ds\right)\pi_T|\mathcal{F}_t\right], \tag{2.1}$$

with $E^{\mathbb{Q}}$ indicating expectation is computed under $\mathbb{Q}$ and with the short interest rate given by r_t. $\{\mathcal{F}_t\}$ is a filtration collecting information of the relevant risk factors as time evolves. Real-world movements are collected under a probability measure $\mathbb{P}$. Throughout the thesis, unless otherwise stated we operate under $\mathbb{P}$ and superscripts indicating measure are attached to parameters and operators whenever the distinction between measures is necessary.

We will often deal with the special case where $\pi_T = 1$ with probability 1. This case corresponds to an idealized zero-coupon treasury bond, with zero credit risk. Denoting its value at time t by $P(t,T)$, we have

$$P(t,T) = E^{\mathbb{Q}}\left[\exp\left(-\int_t^T r_s ds\right)|\mathcal{F}_t\right]. \tag{2.2}$$

2.1 Market Risk Models

The aim of this section is to introduce some of the models that have developed in market risk management and pricing and that are relevant to this thesis.

2.1.1 Interest Rate Models

Although interest rates themselves are not modelled in this thesis, some of the models occurring in interest rate theory are applicable also for credit modelling. This also goes for stochastic volatility in equity modelling. Therefore, we address some of the fundamentals here.

The models we consider are all short rate models, representing the instantaneous return on what is considered a risk-free investment. That is, if we let B_t denote a security priced consistently with the market, given by the dynamics

$$dB_t = r_t B_t dt \tag{2.3}$$

then we may take r_t to represent the short interest rate of the market (Björk, 2009, ch. 7).

We will look into a special class of interest rate models known as affine models, defined below.

Affine Models

For the definition of affine models[1], we first introduce the concept of continuously compounded spot rate. This quantity, denoted $R(t,T)$, is given by

$$R(t,T) = -\frac{\log P(t,T)}{T-t}, \tag{2.4}$$

and can be interpreted as the constant, continuously compounded interest rate a zero-coupon treasury bond issued at time t with maturity T would accrue from t to T (Brigo and Mercurio, 2006, ch. 1).

Affine models are then defined as short rate models by which $R(t,T)$ can be expressed

$$R(t,T) = \alpha(t,T) + \beta(t,T) r_t. \tag{2.5}$$

The key feature is now that the affine structure allows bonds to be priced according to an expression of the form

$$P(t,T) = A(t,T) e^{-B(t,T) r(t)}. \tag{2.6}$$

This is verified by insertion of Equation (2.6) into Equation (2.4), resulting in

$$\alpha(t,T) = -\frac{\log A(t,T)}{T-t}, \qquad \beta(t,T) = \frac{B(t,T)}{T-t}.$$

The coefficients $A(t,T)$ and $B(t,T)$ depend on the model and its parameters. As an example of an affine model, consider the Vasicek one-factor model where interest rates are assumed to follow an Ornstein-Uhlenbeck process,

$$dr_t = \kappa(\theta - r_t)dt + \sigma dW_t. \tag{2.7}$$

In this model, the distribution of r_t conditional on r_s, $t > s$ is normal with analytical expressions for the mean and variance. It can here be shown that Equation (2.6) holds for

$$\begin{aligned} A(t,T) &= \exp\left[\left(\theta - \tfrac{\sigma^2}{2\kappa^2}\right)(B(t,T) - T + t) - \frac{\sigma^2}{4\kappa} B(t,T)^2\right], \\ B(t,T) &= \frac{1}{\kappa}\left(1 - e^{-\kappa(T-t)}\right), \end{aligned}$$

[1] By affine models, we refer to what Brigo and Mercurio (2006, ch. 3) call *affine term-structure models*

see Brigo and Mercurio (2006, ch. 3).

A potential downside of the Vasicek model is that it allows interest rates to be negative. This becomes particularly concerning when adapting interest rate models to the modelling of default intensities and volatilities. A model addressing this issue is the Black-Karasinski model, where the short rate is modelled as the exponential of an Ornstein-Uhlenbeck process, in general with time dependent coefficients. However, this model does not belong to the class of affine models and bond prices are not analytically tractable (Brigo and Mercurio, 2006, ch. 3). Instead, we turn our attention to the Cox-Ingersoll-Ross (CIR) process described below.

The Cox, Ingersoll, and Ross (1985) Process

The CIR model by Cox et al. (1985) has been a popular choice for modelling interest rates, stochastic volatility and default intensities. This is explained by its distributional characteristics, admitting a closed form representation of the future distribution as well as staying almost surely non-negative given that parameters are positive (Cox et al., 1985). Furthermore, the model belongs to the class of affine processes. In its basic form, the model can be expressed by means of the SDE

$$dr_t = \kappa(\theta - r_t)dt + \sigma\sqrt{r_t}dW_t \tag{2.8}$$

where the condition $2\kappa\theta > \sigma^2$ implies that $r_t > 0$ with probability 1. If $2\kappa\theta \leq \sigma^2$, the origin is accessible to the process. The parameters θ and κ are often called *long term mean* and *mean reversion rate* respectively, hinting at the mean-reverting mechanism of the model. The drift term pulls the process back to its long term mean θ, with κ specifying the pace at which this happens.

The CIR model is analytically tractable and offers a closed form expression for the distribution of $r_t|r_s$ for every $t > s$. Conditionally on r_s, r_t involves a non-central chi-squared distribution, see e.g. Andersen (2007) for details.

As shown in Brigo and Mercurio (2006, ch. 3), bond prices under the CIR model can be explicitly calculated according to the affine pricing formula of Equation (2.6), with $A(t,T)$ and $B(t,T)$ given by

$$\begin{aligned} A(t,T) &= \left\{\frac{2\gamma\exp[(\kappa+\gamma)(T-t)/2]}{2\gamma+(\kappa+\gamma)(\exp[(T-t)\gamma]-1)}\right\}^{2\kappa\theta/\sigma^2} \\ B(t,T) &= \frac{2(\exp[(T-t)\gamma]-1)}{2\gamma+(\kappa+\gamma)(\exp[(T-t)\gamma]-1)}, \end{aligned} \tag{2.9}$$

where $\gamma = \sqrt{\kappa^2+2\sigma^2}$.

We will encounter situations where several CIR processes are added. The simplest case of this is the two-factor CIR model,

$$r_t = x_t + y_t \tag{2.10}$$

where

$$\begin{cases} dx_t &= a_x(\theta_x - x_t)dt + \sigma_x\sqrt{x_t}dW_t^x, \\ dy_t &= a_y(\theta_y - y_t)dt + \sigma_y\sqrt{y_t}dW_t^y. \end{cases}$$

In order to retain analytic tractability one has to enforce that $\mathrm{Cor}(dW_t^x,\ dW_t^y) = 0$. In this sense, the CIR process has a limitation which it does not share with the two-factor version of the Vasicek model, where affinity is conserved under the inclusion of non-zero

instantaneous correlation between the constituent processes (Brigo and Mercurio, 2006, ch. 4).

When interest rates are given by m independent CIR processes

$$\begin{aligned} r_t &= \sum_{i=1}^{m} x_t^i \\ dx_t^i &= \kappa_i(\theta_i - x_t^i)dt + \sigma_i\sqrt{x_t^i}dW_t^i, \quad i = 1, \ldots, m \\ \mathrm{Cor}(dW_t^i,\, dW_t^j) &= 0, \quad i \neq j \end{aligned}$$

it follows from Equation (2.6) that bond prices may be expressed as

$$\begin{aligned} P(t,T) &= E^{\mathbb{Q}}\left[\exp\left(-\int_t^T r(s)ds\right)|\mathcal{F}_t\right] \\ &= E^{\mathbb{Q}}\left[\exp\left(-\int_t^T \sum_{i=1}^{m} x_i(s)ds\right)|\mathcal{F}_t\right] \\ &= \prod_{i=1}^{m} E^{\mathbb{Q}}\left[\exp\left(-\int_t^T x_i(s)ds\right)|\mathcal{F}_t\right] \\ &= \prod_{i=1}^{m} A_i(t,T)e^{B_i(t,T)x_i(t)} \end{aligned} \tag{2.11}$$

where the $A_i(t,T)$ and $B_i(t,T)$ are expressed in terms of the corresponding CIR parameters according to Equation (2.9).

For a change of measure from real-world to risk-neutral dynamics, we can preserve the CIR structure if we introduce a parameter γ specifying the market price of risk such that

$$\gamma = \frac{\kappa^{\mathbb{Q}} - \kappa^{\mathbb{P}}}{\sigma} \tag{2.12}$$

where we let superscripts $\mathbb{P}$ and $\mathbb{Q}$ denote parameters under the two measures previously defined. Following Brigo and Mercurio (2006, ch. 3), the process dynamics under $\mathbb{Q}$ then becomes

$$\begin{aligned} dr_t &= [\kappa^{\mathbb{P}}\theta^{\mathbb{P}} - (\kappa^{\mathbb{P}} + \gamma\sigma)r_t]dt + \sigma\sqrt{r_t}dW_t^{\mathbb{Q}} \\ &= \kappa^{\mathbb{Q}}\left(\frac{\kappa^{\mathbb{P}}}{\kappa^{\mathbb{Q}}}\theta^{\mathbb{P}} - r_t\right)dt + \sigma\sqrt{r_t}dW_t^{\mathbb{Q}}, \end{aligned}$$

entailing that the long term mean under $\mathbb{Q}$ satisfies

$$\theta^{\mathbb{Q}} = \frac{\kappa^{\mathbb{P}}}{\kappa^{\mathbb{Q}}}\theta^{\mathbb{P}}. \tag{2.13}$$

2.1.2 Equity Models

When modelling the evolution of a stock price, the most basic of models is the geometric Brownian motion. It began gaining large popularity with the classic paper by Black and Scholes (1973), yielding explicit pricing formulas for European options and paving the way for the concept of implied volatility, to this day seeing large-scale use. The stock dynamics is simply given by

$$dS_t = \mu S_t dt + \sigma S_t dW_t, \tag{2.14}$$

with μ and σ being constant, and leads to a log-normal distribution for the stock price.

Many studies have established empirically that the geometric Brownian motion is flawed when it comes to realistically capturing stock and stock index returns (Cont, 2001; Wu, 2006). Two major limitations are the constant volatility and the light tails of returns. Stochastic volatility and jump dynamics address these two issues and are presented below.

Stochastic Volatility

In stochastic volatility models the constant σ in Equation (2.14) is replaced by a stochastically varying diffusion coefficient $\sqrt{v_t}$, where v_t denotes the instantaneous variance rate. The dynamics for v_t is normally given by a CIR process following Heston (1993). The equity model takes the form

$$\begin{cases} dS_t &= \mu S_t dt + \sqrt{v_t} S_t dW_t^S \\ dv_t &= \kappa(\theta - v_t)dt + \sigma_v \sqrt{v_t} dW_t^v \\ \mathrm{Cor}(dW_t^s,\, dW_t^v) &= \rho \end{cases} \tag{2.15}$$

The correlation ρ is usually negative accounting for the tendency for stock returns and stock volatility to move in opposite directions (Carr and Wu, 2004). Heston (1993) showed that European options can be priced analytically under this model.

Jump Diffusions

One way of capturing heavier tails in stock returns is via the addition of a discontinuous jump component to Equation (2.14). Among the first and most famous models doing this is that by Merton (1976), where jumps are modelled by a compound Poisson process, so that

$$\frac{dS_t}{S_{t-}} = \mu dt + \sigma dW_t + dJ_t \tag{2.16}$$

where S_{t-} denotes the pre-jump value of the stock, $S_{t-} = \lim_{s \uparrow t} S_s$ and

$$J_t = \sum_{j=1}^{N_t} (Y_j - 1). \tag{2.17}$$

Here N_t is a Poisson process and Y_j are some random variables reflecting the size of the jumps (Glasserman, 2004, ch. 3). Letting τ_j denote jump times, it can be shown that

$$S_{\tau_j} = S_{\tau_j -} Y_j \tag{2.18}$$

so that Y_j represent ratios of post- and pre-jump values of the stock (Glasserman, 2004, ch. 3). This explains the subtraction of 1 in the summed terms of Equation (2.17). If Y_j are strictly positive random variables, the stock value is guaranteed to stay above zero. A common choice is lognormally distributed jump sizes.

In the vein of Bates (1996), including both stochastic volatility and jumps in the model has since become popular. This allows for rich stock return dynamics. In spite of this richness, empirical findings have suggested such a model still struggles to fully capture observed stock returns. Eraker et al. (2003) explore a further extension, including jumps in volatility as well.

The Variance-Gamma Process

The variance-gamma process introduced by Madan et al. (1998) is a Brownian motion with drift γ and variance rate σ subordinated by a gamma process. Mathematically, this is captured by

$$X_t = \gamma G_t^\nu + \sigma W_{G_t^\nu} \tag{2.19}$$

where

$$G_t^\nu \sim \Gamma\left(\frac{t}{\nu}, \nu\right). \tag{2.20}$$

A natural interpretation of the subordination is that a Brownian motion with drift γ and volatility σ is evaluated at random times given by G_t^ν. Note that $E[G_t^\nu] = t$. Using the terminology of Carr and Wu (2004), the variance-gamma process may be considered a time-changed Lévy process.

The distinguishing feature of this process is its interpretation as an infinite activity jump model, applicable to stock returns. What this means is that the number of jumps within any finite time interval is infinite. Despite having infinite activity, its variation is finite, meaning that the aggregate absolute distance travelled within any finite time interval is almost surely finite (Yu et al., 2011). The process is one in a parametric family of similar models involving a time-change known as the Carr, Geman, Madan, and Yor (2002) (CGMY) processes, also including processes of infinite variation. The characteristic function of processes within this family is known in closed form, which is helpful for example in the pricing of options (Carr et al., 2002). For the variance-gamma process as defined in Equation (2.19), the characteristic function $\phi_{X_t}(u)$ is

$$\phi_{X_t}(u) = E[\exp(iuX_t)] = \left(\frac{1}{1 - i\gamma\nu u + (\sigma^2\nu/2)u^2}\right)^{t/\nu} \tag{2.21}$$

following Madan et al. (1998).

The case we will consider is that where the logarithm of the stock price includes a variance-gamma process.

Figure 2.1 shows examples of histograms obtained from simulation of the process with different specifications of the parameters. All of the simulations are performed over a horizon $0 \leq t \leq T$ where $X_0 = 0$. Furthermore, a compensator ψt is added to the process as defined in Equation (2.19), such that $E[\exp(X_t + \psi t)] = 1$ for every t. Under this specification, $X_t + \psi t$ can be taken to represent a zero-mean jump component of the logarithm of the stock. Further details are presented in Section 4.2.2.

In Madan et al. (1998), the first four moments of the distribution of X_t are derived in closed form as functions of the parameters. As the figure indicates, ν strongly influences the peakedness of the distribution, where a higher value implies larger probabilities of very large jumps but fewer medium-sized jumps. The variance grows monotonously with the size of all three parameters, while γ controls the skewness. The lower its value, the more left-skewed the distribution. Zero γ is equivalent to zero skewness, while positive values of γ would revert the shape and lead to positive skews. Empirically, asset returns tend to be left-skewed.

Yu et al. (2011) incorporated the variance-gamma process into a stock model with stochastic volatility in a comparative study analysing the ability of four different stochastic volatility stock models to capture observed market behaviours. Of the remaining of these, two were jump diffusion models in the vein of Bates (1996) and of Eraker et al. (2003) respectively, whereas the last model was an alternative infinite-activity, infinite-variation process. Yu et al. (2011) found that the stochastic volatility variance-gamma model performed better than its competition at capturing stock returns.

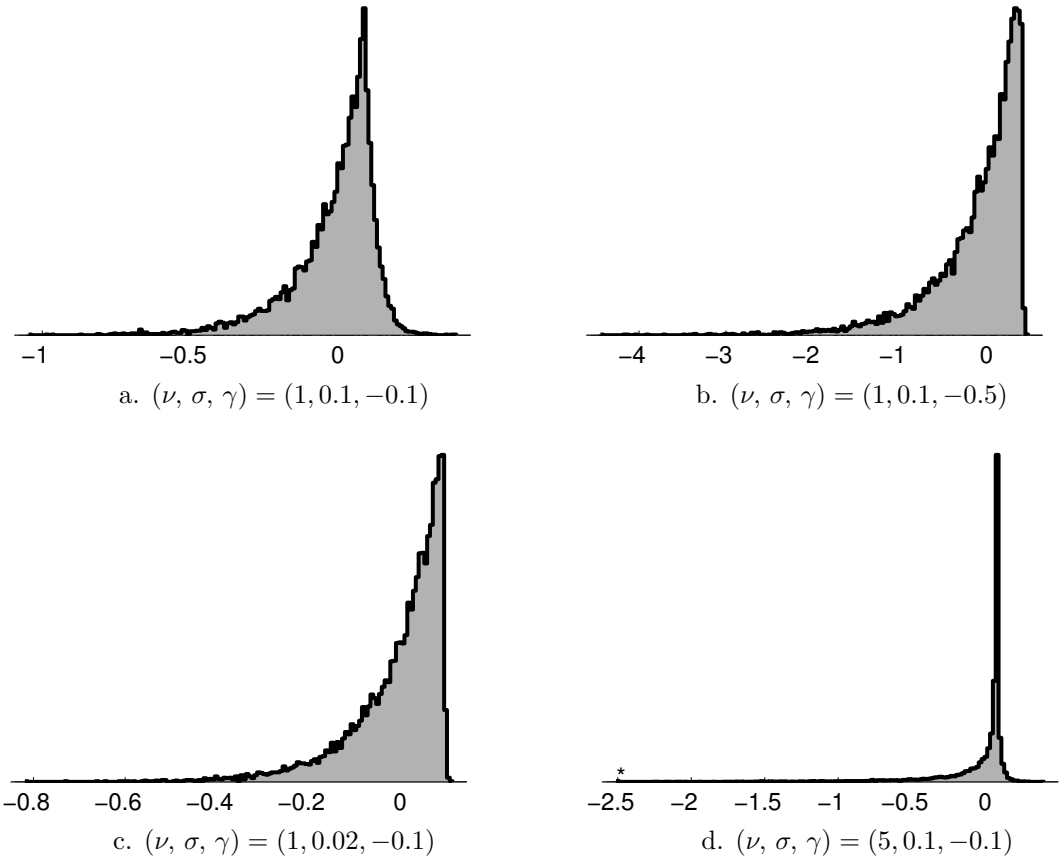

a. $(\nu, \sigma, \gamma) = (1, 0.1, -0.1)$ b. $(\nu, \sigma, \gamma) = (1, 0.1, -0.5)$

c. $(\nu, \sigma, \gamma) = (1, 0.02, -0.1)$ d. $(\nu, \sigma, \gamma) = (5, 0.1, -0.1)$

Figure 2.1: Histograms of mean-adjusted variance-gamma process simulations at time $T = 1$ for different parameter triplets. Each sample consists of $10,000$ sample paths, starting at $t = 0$ and discretized with step size $\Delta t = 1/252$. The asterisk in subfigure 2.1d indicates the left tail is truncated.

2.2 Credit Modelling

Credit risk and the modelling of such has recently undergone a surge of interest in financial mathematics. The field of credit risk modelling started with so-called structural models by Merton (1974). Later on, structural models were joined by a different branch of models called reduced form models. The two approach the modelling of the default event in a very different way. That said, there are examples of studies where basic ideas of the two approaches have been combined (Bielecki and Rutkowski, 2002, ch. 8).

In structural models, also called the firm value approach, a firm's value is modelled altogether and default is assumed to occur whenever the value falls below a threshold value, which may be deterministic or stochastic. A difficulty within this modelling framework is the measurement of the full firm value and the modelling of its evolution (Bielecki and Rutkowski, 2002, ch. 1). Since the time of default is directly linked to the evolution of the firm value, the default event is endogenously specified. Also recovery rates are endogenously determined by the firm value at default.

The models considered in this thesis are all reduced form models. Included here are also models based on credit rating classes and migrations between such, reflecting changes in credit quality.

2.2.1 Reduced Form Models

Reduced form models take very different view compared to structural models. Default is here modelled as a *completely inaccessible stopping time*, where the time of default is determined as the first jump of a Poisson process with intensity λ. In sharp contrast to structural models, the time of default is here an exogenous quantity independent of all other market information, and may come by surprise (Bielecki and Rutkowski, 2002, ch. 8). Recovery payments are also assumed to be exogenously specified.

The Poisson intensity λ may be constant or varying with time, deterministic or stochastic. In the most general case where the intensity both varies with time and is stochastic, the process is called Cox process and denoted λ_t. Models of this kind are highly prevalent in the literature on credit risk, where intensities are often modelled by some interest rate model. The stochastic default intensity is often named *hazard rate*.

We let the time of default be denoted by τ. The probability of a firm with hazard rate λ_t defaulting in $(t, t + dt)$ is

$$\mathbb{P}(\tau \in (t,\, t + dt)|\mathcal{F}_t) = \lambda_t dt \tag{2.22}$$

assuming no default has occurred by time t. Under this assumption and with $T > t$, it is shown in for example Brigo and Mercurio (2006, ch. 21) that

$$\mathbb{P}(\tau > T|\mathcal{F}_t) = E\left[\exp\left(-\int_t^T \lambda_s ds\right)|\mathcal{F}_t\right], \tag{2.23}$$

a quantity known as the survival probability.

Default intensities for firms are not observable quantities. Given observed bond prices and a parametric model for the risk factors involved in their pricing, one could theoretically deduce default intensities. However, as pointed out by Zhang et al. (2009), credit default swap (CDS) spreads tend to be better informants of the default risk, being more standardized than bonds[2]. Spreads of the latter are likely to be affected by contractual arrangements such as seniority, coupon payments and liquidity factors (Zhang et al., 2009). In disentangling credit risk, much of recent literature has therefore taken advantage of market CDS spreads.

2.2.2 Rating Based Models

To account for transitions between rating classes, Jarrow et al. (1997) pioneered a Markov chain approach assigning probabilities to credit migration events. Their model, referred to as the Jarrow-Lando-Turnbull (JLT) model, lent itself to discrete as well as continuous time settings. Credit classes are denoted by $m \in \{1, ..., M, K\}$, descending from high to poor creditworthiness, followed by the last class signifying an absorbing default state.

The standard JLT model was composed of constant, deterministic transition probabilities, thereby representing a homogeneous Markov chain. In order for the model to be consistent with varying market spreads, time-varying risk premia were considered. However, both homogeneity and Markov assumptions have later been questioned in a range of studies (Bangia et al., 2002; Truck, 2008). Various extensions relieving the model of one or both of these assumptions have been suggested. When doing so, it is at the expense of keeping the model simple.

[2] A CDS is a contract in which the seller pays a compensation to the buyer in case of default of a reference entity. In return, the buyer regularly pays the seller fixed amounts.

In the model, probabilities of rating changes are represented by means of *migration matrices*. These may be written in discrete or continuous form, where the former describes rating transition probabilities within any finite time interval and the latter contains transition intensities. Denoting the two by P and Λ, an element p_{ij} of P describes the probability of transition from rating class i to rating class j within a given time interval. Similarly, an element λ_{ij} of Λ describes the corresponding transition intensity.

Given a discrete matrix P, an associated intensity matrix Λ can be constructed trough

$$P = \exp(\Lambda), \tag{2.24}$$

where it is understood that the right-hand side represents the matrix exponential,

$$\exp(\Lambda) = I + \Lambda + \Lambda^2/2! + \Lambda^3/3! + \dots.$$

The matrix Λ is here called a generator for P. We also look at the more general case where intensity matrices are allowed to be time dependent, however restricting this time inhomogeneity to piecewise constant intensities. In this case, if Λ_s denotes the intensity matrix at time $s \in [t, T]$, having H piecewise constant segments of length Δs_h, $h = 1, \dots, H$ between t and T where s_1 is a time between t and $t + \Delta s_1$, s_2 a time between $t + \Delta s_1$ and $t + \Delta s_1 + \Delta s_2$ and so forth, a matching discrete matrix can be constructed through

$$P_{(t,T)} = \prod_{h=1}^{H} \exp\left(\Lambda_{s_h} \Delta s_h\right). \tag{2.25}$$

For general time dependent intensity matrices, where the length of the largest segment in the interval tends to zero, a similar definition exists. A review is available in Lebovic (2011).

Several conditions are imposed on the matrix elements. For every row $i = 1, \dots, K$, the sum of its elements $\sum_{j=1}^{K} p_{ij} = 1$ for any discrete time matrix and $\sum_{j=1}^{K} \lambda_{ij} = 0$ for the continuous time counterpart. Further, all elements in the discrete time matrix, as well as all off-diagonal elements in the continuous-time matrix, must be greater than or equal to zero. This last condition requires some caution, since some specifications of P do not have a valid generator Λ (Trueck and Rachev, 2009, ch. 5). This situation might arise when estimating transition probabilities historically, sometimes resulting in an economically implausible matrix due to scarcity of data calling for some modification approach, as suggested in Trueck and Rachev (2009, ch. 5). K representing an absorbing default state translates into $p_{Kj} = 0, j \leq K$, $p_{KK} = 1$ as well as $\lambda_{Kj} = 0 \; \forall j$.

Extensions of the JLT Model

An early means of incorporating time inhomogeneity in the JLT framework was explored by Lando (1999), who suggested a few different methods of modifying the historical migration matrix such that the default probabilities implied by market prices match those of the matrix. These methods essentially create risk-neutral matrices, consistent with bond prices. Referring to the historical discrete matrix and its generator as *baseline* matrices, all of the methods consist of a transformation to the baseline generator followed by application of Equation (2.24) to create market-consistent discrete matrices over different time windows. In one of these, each row i of the baseline generator is scaled by a factor $\pi_i(t)$ creating a modified generator with constant entries until time t.

Credit migration and default probabilities have been observed to vary with the state of the economy, see e.g. Bangia et al. (2002), reinforcing the previously mentioned doubts

concerning time homogeneity of migration matrices. In the literature, there are many accounts of tuning migration matrices after conditions currently prevailing in the economy. Wei (2003) implicitly conditioned credit migration matrices on a set of latent variables representing deviations from the average historical transition matrix. Further, Truck (2008) explored means of adapting transition probabilities to the business cycle by creating a model accounting for observable macroeconomic factors. By conditioning transition probabilities on generic business cycle indices, constructed separately for speculative and investment grade bonds, clear improvements in model forecasting quality compared to the previously mentioned market price adjustment methods suggested by Lando (1999) were recorded.

Letting migration probabilities vary with macroeconomic conditions in this way essentially constitutes a method for adding dependence to the rating migration processes across firms. The methodology falls under the concept of conditional independence, further described in Section 2.3.4 where we review a few common approaches to modelling dependence in credit risk.

For pricing purposes, risk-neutral matrices should be used. Several methods of transforming real-world matrices into risk-neutral ones are reviewed in Trueck and Rachev (2009, ch. 8). Among these, adjustment methods by Lando (1999) may be used. Another one was suggested in the pioneering paper by Jarrow et al. (1997), where every off-diagonal element of each non-default row of the discrete migration matrix is multiplied by a deterministic function $\pi_i(s,t)$. This function can be estimated from market prices. With this approach, the risk-neutral migration matrix will in general not preserve the Markov property.

2.2.3 Pricing in Presence of Credit Risk

Starting from Equation (2.1), consider an asset which at time T is worth

$$\pi_T = \begin{cases} \tilde{\pi}_T, & \tau > T \\ 0, & \tau \leq T \end{cases}$$

where τ is the default time. So whenever default occurs, the value is assumed to drop to zero. Then, at time t,

$$\pi_t = I(\tau > t) E^{\mathbb{Q}} \left[\exp\left(-\int_t^T r_s ds \right) \tilde{\pi}_T I(\tau > T) | \mathcal{F}_t \right], \tag{2.26}$$

where $I(\cdot)$ denotes the indicator function. Under the assumption of a reduced form approach where τ is the time of the first jump of a Poisson process with intensity λ_t, the equation can be written

$$\pi_t = I(\tau > t) E^{\mathbb{Q}} \left[\exp\left(-\int_t^T (r_s + \lambda_s) ds \right) \tilde{\pi}_T | \mathcal{F}_t \right]. \tag{2.27}$$

From this expression, it is clear that default intensities enter the pricing of assets with credit risk in a way that is completely analogous with how interest rates affect the pricing of any asset. Therefore, much of interest rate theory is applicable for credit risk modelling as previously stated.

When a JLT-esque rating based model is applied, it is not sufficient to only consider the instantaneous default intensity of the class corresponding to the asset issuer. The full risk-neutral matrix, and its possible future evolution, is relevant for the pricing. Intuitively,

a rating change prior to time T affects the propensity to default during the remainder of the term, and what ultimately matters is the cumulative default probability prior to time T.

Bond Pricing

We will now consider the pricing of corporate bonds under a few different assumptions on the payment of recovery upon default. These different recovery structures are presented in Duffie and Singleton (1999) and further investigated in Jobst and Zenios (2001). A reduced form model with hazard rate λ_t is assumed. In all of the below pricing formulas we assume default has not occurred by the time at which the bonds are priced.

Recovery of Treasury (RT) Under this recovery structure, the bond is assumed to pay a fraction δ of the face value at maturity. This is equivalent to immediately upon default being paid the same fraction of the value of a risk-free bond with the same maturity as the corporate bond, and reinvesting this amount into the risk-free bond. The bond price at time t is

$$P^d(t,T) = E^{\mathbb{Q}}\left[\delta \exp\left(-\int_t^T r_s ds\right) + (1-\delta)\exp\left(\int_t^T (r_s+\lambda_s)ds\right)|\mathcal{F}_t\right]. \tag{2.28}$$

Recovery of Face Value (RFV) Here the bond pays a fraction δ of its face value immediately upon default. The pricing formula becomes

$$P^d(t,T) = E^{\mathbb{Q}}\left[\exp\left(-\int_t^T (r_s+\lambda_s)ds\right) + \delta\int_t^T \lambda_s \exp\left(-\int_t^s (r_u+\lambda_u)du\right)ds|\mathcal{F}_t\right]. \tag{2.29}$$

Recovery of Market Value (RMV) This model by Duffie and Singleton (1999) assumes that a recovery payment corresponding to a fraction δ of the pre-default market value of the bond is made immediately upon default. The bond price at time t is then given by

$$P^d(t,T) = E^{\mathbb{Q}}\left[\exp\left(-\int_t^T (r_s+(1-\delta)\lambda_s)ds\right)|\mathcal{F}_t\right]. \tag{2.30}$$

In each of the above models recovery rates could be stochastic or deterministic, constant or varying with time. RT along with an assumption of deterministic of constant recovery rates is a common choice in the literature owing to its simplicity, though such an assumption could in principle lead to recoveries higher than the present value of the bond (Chen et al., 2008). RMV avoids this situation, while being more tractable than RFV. All of the models simplify a process which in reality is a complex matter and involves substantial negotiation between parties (Duffie and Singleton, 1999).

2.3 Dependence Modelling

In this section we will introduce some of the concepts dealing with the measurement and modelling of dependence. We further review some of the techniques that have been proposed in the literature when modelling dependence in credit risk. Conclusively, a few notes on the joint modelling of credit and equity risk are presented.

2.3.1 Linear Correlation and Concordance Measures

The most common tool used to specify and measure dependence is linear correlation. This parameter can be seen as a normalized version of the covariance describing two variables with finite variance,

$$\rho_{X,Y} = \mathrm{Cor}(X,Y) = \frac{\mathrm{Cov}(X,Y)}{\sqrt{\mathrm{Var}(X)\mathrm{Var}(Y)}}. \tag{2.31}$$

A flaw with linear correlation is that it is not invariant under non-linear increasing transformations of the random variables (Cherubini et al., 2004, ch. 3). That is

$$\rho_{X,Y} \neq \rho_{g(X),h(Y)}, \tag{2.32}$$

where $g(\cdot)$ and $h(\cdot)$ are increasing functions, unless $g(\cdot)$ and $h(\cdot)$ are both linear. As an example, if X and Y are normal random variables, and V and W are lognormal random variables such that $V = e^X$ and $W = e^Y$, then $\rho_{X,Y} \neq \rho_{V,W}$ in general. Furthermore, when estimating linear correlation from bivariate data, the sample estimator of ρ will have large or infinite variance in the case of heavy-tailed data (Hult et al., 2012, ch. 9).

As an alternative to linear correlation, there are concordance measures. These share many properties with linear correlation, such as belonging to $[-1, 1]$ and being 0 whenever two variables are independent (but not necessarily vice versa). However, contrary to linear correlation concordance measures are invariant under non-linear increasing transformations of the underlying random variables. Therefore, they are capable of isolating the dependence structure from the marginal distributions in a way linear correlation can not (Cherubini et al., 2004, ch. 3).

Two common examples of concordance measures are Kendall's tau and Spearman's rho, of which we will further define the former. Given the independent and identically distributed bivariate random variables (X, Y) and (X', Y'), Kendall's τ is defined as

$$\tau_{X,Y} = P((X - X')(Y - Y') > 0) - P((X - X')(Y - Y') < 0) \tag{2.33}$$

assuming $P(X = X') = P(Y = Y') = 0$, and is often called rank correlation (Cherubini et al., 2004, ch. 3).

For elliptical distributions[3], linear correlation and Kendall's tau are related through the formula

$$\tau = \frac{2}{\pi} \arcsin \rho. \tag{2.34}$$

When analysing bivariate time series data coming from an elliptical distribution, estimating τ and then using the above equation to obtain an estimate of ρ is likely to result in improved accuracy compared to computing the linear correlation sample estimator (Hult et al., 2012, ch. 9).

2.3.2 Copulas

Consider the bivariate random variable (X, Y) with distribution function $F(x, y)$ and continuous marginals $F_X(x)$, $F_Y(y)$. Also, let $(U, V) = (F_X(X), F_Y(Y))$, which by the

[3]Elliptical distributions include multivariate normal and t distributions, for technical details see Lindskog et al. (2003)

probability transform has standard uniformly distributed marginals. Then, it holds that

$$\begin{aligned} F(x,y) &= P(X \leq x, Y \leq y) \\ &= P(F_X(X) \leq F_X(x), F_Y(Y) \leq F_Y(y)) \\ &= P(U \leq F_X(x), V \leq F_Y(y) \\ &= C(F_X(x), F_Y(y)) \end{aligned} \tag{2.35}$$

where C denotes the *copula* of (X, Y). Analogously, this result known as Sklar's theorem holds for any multivariate random variable having continuous marginals and distribution function F . In other words, if one has knowledge of both the marginals and of the copula of a multivariate random variable, its full distribution is known.

We will continue with the bivariate case. The copula function represents a distribution function for a random variable (U, V) with standard uniform marginals. With (X, Y) as before, its full dependence structure is then captured within the copula. Given (U, V), (X, Y) is obtained by applying the quantile transform

$$(X, Y) = (F_X^{-1}(U), F_Y^{-1}(V)),$$

which also holds for discrete random variables. Within finance, copulas have emerged as a tool to handle and express dependencies deviating from normality. In fact, normality corresponds to one specific copula, representing one specific dependence structure among a broad range of admissible structures.

When considering the previously mentioned concordance measures, it can now be verified that the requirement of invariance under non-linear increasing transformations leads to

$$\tau_{X,Y} = \tau_{U,V},$$

for Kendall's tau. Due to this property, it is natural to utilize concordance measures when dealing with copulas. Fixing τ, different types of copulas are readily compared. We will soon review a few standard types, but first define the three important special cases of independence copula, with independent marginals, maximum copula, with perfect positive dependence, and minimum copula, with perfect negative dependence:

Independence copula:	$C(u, v) = uv$
Maximum copula:	$C(u, v) = \min(u, v)$
Minimum copula:	$C(u, v) = \max(u + v - 1, 0)$

With the introduction of these, the dependence of any two random variables is bounded in between the minimum and maximum copulas. Depending on the marginal distributions for some random variable (X, Y), this also imposes bounds on the linear correlation parameter which might differ from ± 1. As an example, let $(X, Y) = (Z_1, e^{Z_2})$ where Z_1 and Z_2 are standard normally distributed. In case of the maximum copula, $Z_1 = Z_2$ and $\rho_{X,Y} = (e-1)^{-1/2} \approx 0.76$. For the minimum copula, $Z_1 = -Z_2$ and $\rho_{X,Y} = -(e-1)^{-1/2} \approx -0.76$. In contrast, the value of any concordance measure is ± 1 in these cases.

We now introduce three families of copulas, Gaussian, t and Clayton.

Gaussian copula The Gaussian copula is very commonly used in applications, and is defined by

$$C(u, v) = \Phi_\rho^2(\Phi^{-1}(u), \Phi^{-1}(v)) \tag{2.36}$$

where Φ_ρ^2 denotes the bivariate standard normal distribution function with correlation parameter ρ and Φ^{-1} is the standard normal quantile function. With this copula, the

random variable $(X, Y) = (\Phi^{-1}(U), \Phi^{-1}(V))$ is standard normally distributed with linear correlation ρ. When $\rho = \pm 1$, the copula converges to the maximum and minimum copula respectively. In case $\rho = 0$, the copula is equal to the independence copula.

Student's t copula The t copula with $\nu > 0$ degrees of freedom is defined by

$$C(u, v) = t^2_{\nu,\rho}(t^{-1}_\nu(u), t^{-1}_\nu(v)) \tag{2.37}$$

where $t^2_{\nu,\rho}$ is the bivariate student's t distribution function with ν degrees of freedom and correlation parameter ρ, t^{-1}_ν the t quantile function. Like for the Gaussian copula, $\rho = \pm 1$ corresponds to the maximum/minimum copula. However, there is no value of ρ such that the independence copula is attained for finite values of ν. As ν tends to infinity, the t copula coincides with the Gaussian one.

Clayton copula The Clayton copula is part of a class of copulas known as Archimedean copulas. These are associated with a *generator* $\phi(t)$, from which the copula expression may be constructed. Such a generator must be a positive, continuous, decreasing and convex mapping on $[0, 1]$ such that $\phi(1) = 0$ and with a pseudo-inverse defined as

$$\phi^{[-1]}(v) = \begin{cases} \phi^{-1}(v), & 0 \leq v \leq \phi(0) \\ 0, & \phi(0) \leq v \leq \infty \end{cases}$$

The copula is then constructed as

$$C(u, v) = \phi^{[-1]}(\phi(u) + \phi(v)). \tag{2.38}$$

The Clayton copula with parameter $\alpha \in [-1, 0) \cup (0, \infty)$ has generator $\phi_\alpha(t)$ given by

$$\phi_\alpha(t) = \frac{1}{\alpha}(t^{-\alpha} - 1),$$

resulting in the copula expression

$$C(u, v) = \max\left((u^{-\alpha} + v^{-\alpha} - 1)^{-1/\alpha}, 0\right) \tag{2.39}$$

The parameter α is associated with Kendall's tau through

$$\alpha = \frac{2\tau}{1 - \tau}. \tag{2.40}$$

The Clayton copula coincides with the minimum copula for $\alpha = -1$ and approaches the maximum copula as $\alpha \to \infty$. In the limit where $\alpha \to 0$, it tends to the independence copula (Cherubini et al., 2004, ch. 3).

Other examples of Archimedean copulas include the Gumbel and Frank copula, having different dependence structures. The Clayton copula is here given attention due to its dependence properties. This is clarified by a simulation from this copula along with the Gaussian and t copulas at different degrees of freedom. Figure 2.2 shows the results, in particular illustrating different behaviours in the tails for the various copulas used. For the t copula, it is clear that extreme simultaneous outcomes are more prevalent than in the Gaussian case, and this in either tail including where the outcomes are at the opposite ends. The tendency appears stronger for lower degree of freedom parameter. The Clayton copula, on the other hand, behaves differently with dependency clustered in the lower tail. In the next section the concept of tail dependence is defined, providing a tool for establishing this observation mathematically. Details on how the simulation is carried out are presented in Section 4.3.3.

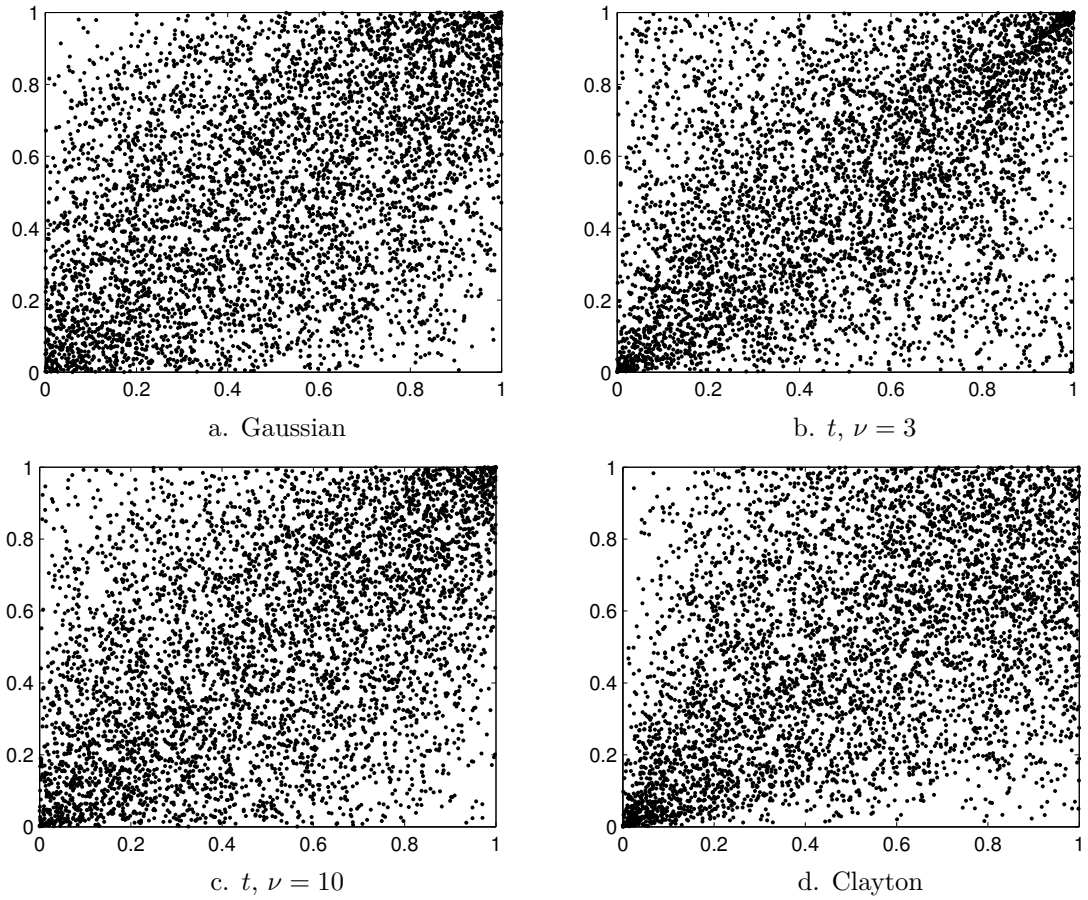

a. Gaussian b. t, $\nu = 3$

c. t, $\nu = 10$ d. Clayton

Figure 2.2: Simulations from four different bivariate copulas using a sample size of $N = 5000$. Correlation parameter $\rho = 0.5$ is used for the Gaussian and t copulas, where corresponding Kendall's tau may be computed through Equation (2.34). Insertion of this value into Equation (2.40) gives the value of α used for the Clayton copula.

2.3.3 Tail Dependence

When several stochastic quantities are involved in what is being modelled, it is often of interest to monitor their interaction in the extreme ends of the distributions. This particularly applies to finance and financial risk management. It is not uncommon that weakly correlated assets display simultaneous negative extreme movements. Tail dependence is a standardized measure capable of capturing this property. Given the bivariate random variable (X, Y) with copula C and marginal distributions F_X and F_Y, its lower tail index or tail dependence coefficient is defined as

$$\lambda_L = \lim_{u \downarrow 0} \frac{C(u,u)}{u}, \tag{2.41}$$

or equivalently,

$$\lambda_L = \lim_{u \downarrow 0} P(X < F_X^{-1}(u) | Y < F_Y^{-1}(u)).$$

An analogous definition is available for the upper tail index,

$$\begin{aligned}\lambda_U &= \lim_{u\uparrow 1} \frac{1-2u+C(u,u)}{1-u} \\ &= \lim_{u\uparrow 1} P(X > F_X^{-1}(u) | Y > F_Y^{-1}(u)).\end{aligned}$$

Tail indices can vary between 0 and 1, 0 signifying absence of tail dependence and 1 indicating perfect tail dependence. For the maximum copula, both upper and lower tail indices are equal to 1. For the Gaussian copula, it can be shown that both tail indices are zero for any copula correlation parameter ρ less than 1. The t copula, on the other hand, exhibits tail dependence in both tails for any value of the correlation parameter except $\rho = -1$. Due to symmetry, the coefficients are equal and given by

$$\lambda_L = \lambda_U = 2t_{\nu+1}\left(-\sqrt{(\nu+1)\frac{1-\rho}{1+\rho}}\right),$$

$t_\nu(\cdot)$ being the distribution function, as shown in Embrechts et al. (2003). The Clayton copula has lower tail index $\lambda_L = 2^{-1/\alpha}$ as long as $\alpha > 0$, but lacks upper tail dependence for finite α. Other Archimedean copulas differ in this respect; as an example the Gumbel copula has upper but lacks lower tail dependence (Cherubini et al., 2004, ch. 3).

2.3.4 Dependence in Credit Risk

In the literature, various different ways of modelling dependence in credit risk have been developed. Among approaches commonly seen within reduced form models, a few prominent ones are conditional independence models, contagion models and copula models. The distinction is not entirely without overlap. Elizalde (2006) gives a review of the three and their use in the modelling of dependent hazard rates and defaults. We will also direct attention towards models dealing with dependence in credit migrations, here treated under conditional independence models.

Conditional Independence

Conditional independence models lend themselves both to the simulation of correlated defaults and to rating-based models. Starting with the latter, Truck (2008) reviews two different approaches; firstly adjusting the matrix explicitly such that default probabilities match market spreads, and secondly making use of the constant, historical matrix and conditioning outcomes of these on a common index. The methods are used and their accuracy tested in a historical forecasting setting. We will have a closer look at the second approach, which Truck (2008) found performed better than the former.

Consider a baseline discrete transition matrix P of size $K \times K$, with $M = K - 1$ non-default rating classes and K representing an absorbing default state. P contains historical average transition probabilities over a given risk horizon T. Now, for a firm i belonging to rating class m, its unconditional transition probabilities over the risk horizon are represented by row m of P. The rating state at the end of the period is now expressed via a variable Y_T^i, which is here assumed to belong to the standard normal distribution. Then, its outcome can be mapped to a rating class at T by constructing the following disjoint partition of the real line:

$$(-\infty,\ \Phi^{-1}(p_{mK})],\ (\Phi^{-1}(p_{mK}),\ \Phi^{-1}(p_{mK}+p_{mM})],\ \ldots,\ (\Phi^{-1}(p_{mK}+p_{mM}+\cdots+p_{m2}),\ \infty) \tag{2.42}$$

The probability of Y_T^i falling within the first bin is now equal to p_{mK}, which is the unconditional default probability. Similarly, the probability of falling into bin $j \geq 2$ is equal to $p_{m,M+2-j}$. Therefore, a simulated value of Y_T^i is mapped to the time T rating of a firm by checking which bin it falls into, bin j mapping to rating class $M + 2 - j$.

The dependence in this enters by correlating the outcomes Y_T^i for individual firms with a common credit cycle index Z_T, which is designed such that its distribution is standard normal. This is typically done so that

$$Y_T^i = wZ_T + \sqrt{1 - w^2}X_T^i \tag{2.43}$$

where w is the weight of the index on the transition outcomes and X_T^i are standard normally distributed idiosyncratic factors, capturing risk which enters independently. Equation (2.43) is equivalent to the use of a bivariate Gaussian copula with parameter w linking the common index and firm rating outcomes. Truck (2008) constructs separate indices for investment and speculative grade bonds, using a regression and forecasting method involving a number of macroeconomic variables. As Equation (2.43) suggests, the variables $\{Y_T^i|Z_T\}_i$ are independent, explaining the notion of conditional independence. There are many variations and extensions to this approach in the literature. A recent example is Berteloot et al. (2013), who applied a sophisticated regression technique for estimation of default and migration probabilities based on historical migration data capturing momentum in rating dynamics as well as macroeconomic indicators.

A similar approach can be conducted to simulate correlated defaults, without applying a rating-based model. The binning would then be reduced to default and non-default only. Alternatively, default intensities in a continuous time setting can be modelled directly through conditional independence by letting hazard rates for individual firms be made up of sums of processes describing common state factors and idiosyncratic factors. Such a specification may also be used for the simulation of dependent default times. A review is available in Elizalde (2006).

Contagion

Contagion models make use of a different mechanism to tackle an empirical observation that conditional independence models as described above are poorly equipped to handle, namely that of default clustering. It appears the default of one firm in itself can trigger default of other firms, and that defaults tend to be clustered in time (Elizalde, 2006).

One example of a contagion model is that by Jarrow and Yu (2001), where default intensities depend on the status of other firms being modelled. To avoid what they call looping defaults, which might occur when hazard rates across firms are interlinked symmetrically, they distinguish between primary and secondary firms so that default dependence is one-way matter. Primary firm intensities are modelled using a conditional independence specification, then if one of these defaults a sharp increase for the default intensities of secondary firms is recorded.

Copula models

Copula models have seen some use in credit modelling. Relying on the limitations of using only linear correlation to describe dependence, Hamilton et al. (2001) analysed credit risk with the help of copula methods and also discussed how parametric families of copulas could be calibrated to observed data. Copulas were used to model simultaneous credit events, including defaults and rating transitions.

Meissner et al. (2013) compared different correlation approaches and their effect on CDS pricing when there is counterparty risk involved. As previously mentioned, a CDS contract fundamentally depends on the credit risk of a reference party. When there is also counterparty risk, the dependence between counterparty and reference party is relevant to the pricing. They found that different correlation approaches lead to fairly large differences in pricing. A naive approach is to just correlate Brownian motions of default processes, causing far higher CDS spreads due to weak dependence between counterparty and reference party, compared to more involved approaches such as using a fatter-tailed t copula connecting the intensities.

Interest Rates and Credit Risk

Many studies also include interest rate risk studied jointly with credit risk. The existence of dependence between interest rates and credit spreads has been settled empirically. Duffee (1998) found that short-term treasury yields and investment-grade credit spreads appear to be inversely correlated, with a more pronounced negative dependence as credit quality decreases. Duffie and Singleton (1999) described default intensities and interest rates through the use of multi-factor independent CIR processes, yielding an additive dependence structure between intensities and rates while preserving tractable bond pricing.

In Jobst and Zenios (2001) risky bonds were priced and tracked using a tree implementation to model the risk-neutral evolution of correlated interest rates and default intensities. The latter were assumed to be coupled with rating classes, rather than pertaining to individual firms. For simulation under the real measure, the tree was again used to generate economic scenarios, then rating transitions were appended using a discrete Markov chain approach with fixed, historical probabilities. These were treated separately from the interest rates and credit spread scenarios. Different recovery models, as described in Section 2.2.3, were applied. Chen et al. (2008) is another example of dependence modelled between interest rates and hazard rates, using CIR processes and fitting to market CDS spreads for a range of companies.

2.3.5 Joint Equity-Credit Modelling

Beside dependence between interest rates and credit risk, co-movements have also been observed across equity and debt markets. Particularly, stock volatility and credit spreads have been observed to interact significantly, both between individual firms as in Zhang et al. (2009) and market-wide as in Naifar (2012). Furthermore, breaking movements on stock markets down into separate volatility and jump components, research also suggests there is dependence between equity jumps and credit spreads as exemplified in both of the mentioned studies. Naifar (2012), analyzing movements of CDS index spreads and stock indices, also found that dependence between the two is asymmetric and amplified in times of financial turmoil.

Linking stock volatility with hazard rates has been done in several studies. Kovalov and Linetsky (2008) modelled hazard rates with a three-factor CIR process, with two of these describing stock stochastic volatility and interest rates while the third one was an independent addition capturing independent movements of default intensities. Furthermore, the stock process included yet another univariate Brownian motion correlated with the stochastic volatility, resulting in a four-factor specification. Under this model specification, the authors priced convertible bonds.

Another example is found in Carr and Wu (2010), modelling stock processes of individual firms by means of stochastic volatility and a variance-gamma jump process, then

linking default intensities with stochastic volatility in a similar fashion as described above. The model allowed stock options to be priced analytically, and was fit to market CDS spreads and implied volatilities on stock options simultaneously, where both real-world and risk-neutral parameters were determined through the use of Kalman filtering on historical time series data. This was done for a range of companies and led to good fits for both implied volatility surfaces and CDS spreads. The model forms a basis for the thesis, and is described in more detail in Chapter 3.

In Fontana and Montes (2014), a unified modelling framework for equity, credit and interest rate risk was devised. Default intensities as well as interest rates were defined as affine functions of stock process, volatility and underlying factors which may include macroeconomic or firm-specific variables. The specification ensured positivity of interest rates and hazard rates, as well as pricing tractability.

Chapter 3

Model

This chapter presents the choice of model and the reasons behind the choice. This is followed up by a detailed model specification, addressing all of its variations. Assumptions and simplifications are highlighted. To conclude the chapter, we describe the portfolio application studied.

3.1 Model Selection and Overview

In the selection of an appropriate model, we seek models capable of capturing rich behaviours with respect to the marginal returns of equity and debt instruments, while simultaneously allowing for dependence to enter between equity and credit risk factors in a manageable way. When setting up the framework, it is also desirable that the model is expressible in continuous time. A motivation for this is the ability to generate scenarios over arbitrary risk horizons and track the evolution of risk factors as well as asset prices along sample paths.

Aside from the ability to represent marginal returns richly, the more control we can exert over the extent and structure of dependence across equity and debt markets, the higher the model is held. In order to isolate credit and equity risks and restrict the analysis to these, we prefer models focusing on these factors, not including other risk sources.

Since we value the ability to flexibly model portfolios of varying compositions, priority is given to models targeting the behaviour of risk factors relevant to the pricing of a variety of assets, rather than to models directly focused at the time series dynamics of particular asset values such as bond spreads[1]. Discrete time models such as those described in Bangia et al. (2002) and Truck (2008), suitable to the simulation the overall creditworthiness of a portfolio but with limited ability to capture short-term market fluctuations and to generate sample paths, also hold a lower priority when looking for core building blocks. As we shall see, this type of models does however ultimately come into play in the design of the framework, owing to their capability to incorporate market-wide dependence between firms.

The model we choose as forming the basis of the framework is that by Carr and Wu (2010). This model, introduced in Section 2.3.5 and further described in Section 3.2,

[1]It should be stressed that a model describing behaviour of risk factors, calibrated after observed market prices of a certain asset type such as bond spreads, may need to be recalibrated when used with other asset types. The reason is that the way assets are modelled to depend on risk factors is likely to simplify reality, such that a particular calibration is suitable for a particular portfolio setting but requires caution when used outside of that.

lends itself to a continuous time setting featuring equity and credit risk, with substantial ability to adjust parameters for desirable behaviour of the risk factors. However, its specification of hazard rates, using CIR processes, reflects fixed long-term expectations of default probabilities so that changes in credit quality are not well represented. We therefore investigate the outlook of including rating change dynamics through a Jarrow et al. (1997) Markov chain approach, presented in Section 3.3.

Further, for multi-name portfolios a mechanism for simulating dependent migrations is investigated, as a tool to further expand the span of dependence allowed. This is essentially based on migrations through conditional independence as in Truck (2008), but with the added possibility to make use of different copula techniques. A summary of the framework, putting all pieces together, is given in Section 3.4.

3.2 Carr and Wu (2010) Model

The Carr and Wu (2010) model, targeting individual firms, contains a stock process and a hazard rate process, linked through stochastic volatility of the stock. Aside from stochastic volatility, the stock process also features a variance-gamma jump process. Whenever default occurs, the value of the stock is assumed to drop to zero. Letting Y_t denote the logarithm of the pre-default stock price, the model specification is

$$\begin{cases} dY_t &= \tilde{\mu}_t dt + \sqrt{v_t} dW_t^S + dJ_t \\ dv_t &= \kappa_v(\theta_v - v_t)dt + \sigma_v\sqrt{v_t}dW_t^v \\ dz_t &= \kappa_z(\theta_z - z_t)dt + \sigma_z\sqrt{z_t}dW_t^z \\ \lambda_t &= \beta v_t + z_t \end{cases} \tag{3.1}$$

where

$$\begin{aligned} \mathrm{Cor}(dW_t^v, dW_t^S) &= \rho, \\ \mathrm{Cor}(dW_t^S, dW_t^z) = \mathrm{Cor}(dW_t^v, dW_t^z) &= 0. \end{aligned}$$

J_t here denotes the mean-adjusted variance-gamma process, which is independent of the three Brownian motions. The modified drift process $\tilde{\mu}_t$ here includes an Itō compensator $(-v_t/2)$ for the volatility process and therefore differs from the drift of the stock process $S_t = \exp(Y_t)$. Under the risk-neutral measure, the stock drift is $r_t - q_t + \lambda_t$ with r_t denoting the short interest rate, q_t a stock dividend rate and λ_t the default intensity. The latter contains an independent component z_t, allowing independent hazard rate movements along with those following the stock volatility process. With this specification, λ_t follows a two-factor CIR process.

Dependence between credit risk and equity risk is captured primarily by the parameter $\beta \geq 0$. Note that for negative ρ and positive β, negative correlation between stock process and default intensity indirectly spreads via the volatility process. Additional dependence is imposed through λ_t entering the stock process, either via the risk-neutral drift component or by default simulation in a real-world setting.

Different dynamics of v_t and z_t are allowed under the real-world and risk-neutral measures, with market price of risk determined consistently with Equation (2.12). That is, for mean reversion rates defined differently under the two measures, we have the market prices of risk

$$\begin{aligned} \gamma_v &= \frac{\kappa_v^{\mathbb{Q}} - \kappa_v^{\mathbb{P}}}{\sigma_v}, \\ \gamma_z &= \frac{\kappa_z^{\mathbb{Q}} - \kappa_z^{\mathbb{P}}}{\sigma_z}. \end{aligned}$$

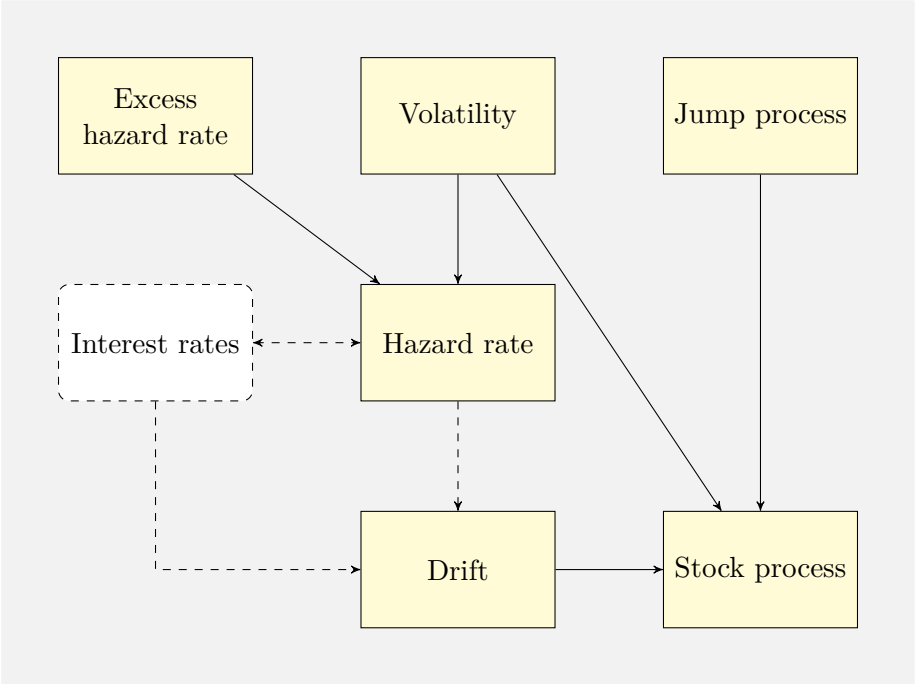

Figure 3.1: Component overview of the model described in Section 3.2. Arrows show directions of dependency between components. Dashed borders indicate the component is not implemented in the present thesis. Dashed arrows represent possible, but not strict, dependencies.

In line with Equation (2.13) we also have

$$\theta_v^{\mathbb{P}}\kappa_v^{\mathbb{P}} = \theta_v^{\mathbb{Q}}\kappa_v^{\mathbb{Q}},$$
$$\theta_z^{\mathbb{P}}\kappa_z^{\mathbb{P}} = \theta_z^{\mathbb{Q}}\kappa_z^{\mathbb{Q}}.$$

Yu et al. (2011) also suggest how a measure change of the variance-gamma jump process could be implemented, but this is not done in the present thesis since it would only affect the pricing of assets explicitly depending on the stock process, not considered here.

As opposed to Carr and Wu (2010) who fit the model to market prices, we are interested in simulation under a real-world measure. Furthermore, we will let the equity process represent a stock index, such that the default intensity does not interact in the same way with the process. More on this in Section 3.4, describing the full modelling framework.

As illustrated in Figure 3.1, it is possible to divide the model into several different blocks or components, each represented by a process or quantity of interest. A division of this kind breaks down the dependencies of the model such that components can be treated separately and some of them given as input to other blocks. When developing the method for simulation presented in Chapter 4, this will turn out to be helpful.

Furthermore, this block representation opens for high adaptability to changes and additions. An example is the variance-gamma jump process, here treated as an independent module. Exchanging this for a different jump process, such as compound Poisson, or removing it altogether is here easily done. Another example is how the stock drift enters. Specifying this as an input factor to the stock process, such that its whole evolution could be generated independently of the actual stock process, stochastic interest rates could potentially be added without too much difficulty. One way of doing so would be by following

Kovalov and Linetsky (2008), where default intensities are given by

$$\lambda_t = \alpha r_t + \beta v_t + z_t,$$

with r_t following an independent CIR process. Under such a specification, the arrow of dependency highlighted in Figure 3.1 connecting hazard rates with interest rates would be directed from the latter to the former.

In the figure, the stock volatility process is indicated as an independent component, which could be input to the stock process. The dynamics of Equation (3.1) suggest the dependency between the two is mutual rather than unidirectional. The explanation lies in that the CIR process can in fact be treated separately and have its full evolution input to the stock process simulation, as will become clear in Section 4.2.3. Expressing the dependency like this facilitates the implementation while providing for higher efficiency.

3.3 Rating Based Model

To account for varying credit qualities as well as improved applicability to a multi-name setting, we consider an extension involving several rating classes, each associated with its own hazard rate process. Let $m = 1, \ldots, M$ denote rating classes ranging from best to worst not including default. We may then define the independent processes

$$dz_t^i = \kappa_i(\theta_i - z_t^i)dt + \sigma_i\sqrt{z_t^i}dW_t^i, \quad i = 1, \ldots, M,$$

representing *excess hazard rates*, and let the default intensity for any obligor within class m be represented by

$$\lambda_t^m = \beta_m v_t + \sum_{i=1}^{m} z_t^i \tag{3.2}$$

where v_t denotes the volatility process of a common stock index on the same form as in Equation (3.1), assumed to have similar impact on all of the firms considered. With this specification, dependence between hazard rate movements across different rating classes is imposed additively, also capturing dependence with the stock index volatility in a similar way as outlined in the previous section. Moreover, as long as $\beta_m \leq \beta_n$ for $m < n$, a worse rating class is always guaranteed to have greater default probability than one of higher rating.

Now, in order to enable transitions between rating classes, we consider a continuous Markov chain approach where the default intensities of Equation (3.2) coincide with the last column entries of a time-dependent transition matrix. In order to to this, we define a baseline intensity matrix that is consistent with the long-term means of the default intensities, affecting the last columns of both the real-world and risk-neutral matrices. Under either measure, we consider the baseline intensity matrix

$$\Lambda^{\text{base}} = \begin{pmatrix} \lambda_{11} & \lambda_{12} & \cdots & \lambda_{1M} & \lambda_{1K} \\ \lambda_{21} & \lambda_{22} & \cdots & \lambda_{2M} & \lambda_{2K} \\ \vdots & \vdots & \ddots & \vdots & \vdots \\ \lambda_{M1} & \lambda_{M2} & \cdots & \lambda_{MM} & \lambda_{MK} \\ 0 & 0 & \cdots & 0 & 0 \end{pmatrix}. \tag{3.3}$$

For this to be consistent with the hazard rate process specification, the last column entries for $m = 1, \ldots, M$ must be

$$\lambda_{mK} = \beta_m \theta_v + \sum_{i=1}^{m} \theta_i. \tag{3.4}$$

The next step is to construct a time-varying intensity matrix, given this baseline. Inspired by a matrix numerical adjustment approach in Lando (1999), each row m of the baseline matrix is scaled by a factor λ_t^m/λ_{mK}. This implies that simulated instantaneous default intensities are always equal to those in the matrix, while simultaneously ensuring that the time-varying matrix is a proper intensity matrix with each row summing to zero and each off-diagonal element remaining non-negative.

Given sample paths of default intensities and fully specified baseline matrices, it is possible to superimpose credit migrations for a firm and track its rating state over a given risk horizon. This may also be done by converting the time-dependent intensity matrix to a corresponding discrete time matrix, and simulate rating scenarios from the latter. For simulation of dependent migrations across several firms, we apply the latter methodology and assume conditional independence of transitions, where discrete time matrices are conditioned on a common index. In this respect, the approach differs from that highlighted in Truck (2008), where the historical matrix is what is being conditioned on a credit cycle index, while the discrete time matrices we will be working with are those implied by sample paths of hazard rates.

Further, we let the imposition of dependent migrations be carried out with the possibility of applying different copulas. This serves as a tool to further modify the dependence structure, without casting aside the conditional independence assumption as such. In the original assumption of conditionally independent migrations, a bivariate Gaussian copula is used to create a link between migration dynamics and a common credit index. We also provide implementation for dependent migrations through student's t and Clayton copulas.

3.4 A Joint Framework

We here summarize the full simulation framework, similar to the Carr and Wu (2010) model but adapted to a market-wide setting, with a stock index and rating-based hazard rates simulated under a real-world measure, applying an added mechanism for credit rating migrations. The model bears resemblance to that studied in Jobst and Zenios (2001), involving two layers of scenario generation; economic scenarios through the evolution of stochastic processes, with rating scenarios retrospectively attached.

We consider a risk horizon $t \in (0, T]$. Letting Y_t be the logarithm of a stock index, in an economy where participants either belong to one of M non-default rating classes where 1 is the best and M the worst, or are in a default class $K = M + 1$, we have

$$\begin{cases} dY_t &= \tilde{\mu}_t dt + \sqrt{v_t} dW_t^S + dJ_t \\ dv_t &= \kappa_v(\theta_v - v_t)dt + \sigma_v\sqrt{v_t}dW_t^v \\ dz_t^i &= \kappa_i(\theta_i - z_t^i)dt + \sigma_i\sqrt{z_t^i}dW_t^i, \quad i = 1, \ldots, M \\ \lambda_t^m &= \beta_m v_t + \sum_{i=1}^m z_t^i, \quad m = 1, \ldots, M \end{cases} \tag{3.5}$$

with

$$\mathrm{Cor}(dW_t^S, dW_t^v) = \rho,$$

all other Brownian motions uncorrelated and J_t an independent variance-gamma jump process.

Furthermore, processes v_t and z_t^i have different dynamics under the real-world and

risk-neutral measure, so that

$$\gamma_v = \frac{\kappa_v^{\mathbb{Q}} - \kappa_v^{\mathbb{P}}}{\sigma_v},$$
$$\gamma_i = \frac{\kappa_i^{\mathbb{Q}} - \kappa_i^{\mathbb{P}}}{\sigma_i}, \quad i = 1, \ldots, M$$

represent constant market prices of risk. In addition to variations of the λ_t^m due to process movements, credit qualities of individual firms may also change by rating migrations. Such changes are imposed in a second step, once paths of S_t, v_t and λ_t^m are known. Given a baseline real-world intensity matrix Λ^{base} with elements λ_{mk}, and hazard rate paths λ_t^m, a time-varying matrix Λ_t is constructed by letting its elements be set to

$$\lambda_{t,mk} = \lambda_{mk} \frac{\lambda_t^m}{\lambda_{mK}}, \quad m = 1, \ldots, M, \quad k = 1, \ldots, K, \tag{3.6}$$

and $\lambda_{t,Kk} = 0$ for $k = 1, \ldots, K$. For migration simulation, we consider the partition of $(0, T]$ to

$$(t_0, t_1],\ (t_1, t_2],\ \ldots,\ (t_{J-1}, t_J]$$

with $t_0 = 0$ and $t_J = T$, and where $\Delta t_j := t_j - t_{j-1} = t_k - t_{k-1}$ for every j, k. At every t_j, $j = 1, \ldots, J$, the rating state of the firms considered is now governed by the path-dependent discrete time matrix $P_{(t_{j-1}, t_j)}$ which may be approximately constructed from the path of Λ_t through Equation (2.25). Further, this matrix is conditioned on the outcome of a common credit cycle index in $(t_{j-1}, t_j]$. Within our framework, we will let this index be represented by the stock index process, which adds another layer of dependence between credit and equity risk within the market considered. In principle, the index could be exchanged for any macroeconomic variate or combination of such assumed to have explanatory power on the rating changes of firms involved. Letting the weight of the index on firm rating transition dynamics be denoted by w, we recall Equations (2.42) and (2.43) for binning and simulation of the rating state of a firm at t_j, initially in state m at t_{j-1}. This assumes a Gaussian copula and requires mapping of the stock index path from t_{j-1} to t_j to a standard normal variable. Equivalently, if we represent the stock outcome by a uniform $U_{\text{S}}(t_{j-1}, t_j)$, a rating outcome is produced by computing

$$U(t_{j-1}, t_j) = \Phi\left(w\Phi^{-1}(U_{\text{S}}(t_{j-1}, t_j)) + \sqrt{1 - w^2}\Phi^{-1}(U_i(t_{j-1}, t_j))\right), \tag{3.7}$$

mapped to an appropiately binned partition of $(0, 1)$ further detailed in Section 4.3.4. Here, $U_i(t_{j-1}, t_j)$ is an independent standard uniform variable. In addition to the Gaussian copula, we allow student's t and Clayton copulas for the rating migration simulation, explained in Section 4.3.3.

We summarize the main steps included in simulation from the full framework, with implementation details described in Chapter 4 in the indicated sections:

1. Simulate a set of economic scenarios encompassing stock index, volatility and hazard rates (Section 4.2)

2. Conditional on hazard rate paths, construct discrete transition matrices (Section 4.3.1)

3. Convert stock index outcomes to uniforms, to be used for conditioning of rating outcomes (Section 4.3.2)

4. Simulate rating scenarios, conditional on stock index outcomes (Sections 4.3.3 and 4.3.4)

5. Map generated scenarios to portfolio values (Section 4.4)

3.5 Portfolio Application

The portfolio considered is one consisting of corporate zero-coupon bonds. The rationale for this choice is that it allows for a rather direct representation of credit risk movements, in the shape of excess returns above what a risk-free investment would yield. With stock index returns also represented as excess returns, with deterministic drift, we may study credit and equity risk isolated from interest rate risk.

Bonds are assumed to belong to one of two broad rating categories, investment grade or high yield. Upon default, an exogenously specified fraction of the market value of the bond is paid. This specification is in line with recovery of market value (RMV), mentioned in Section 2.2.3. The price of each bond is given by applying the corresponding formula, Equation (2.30), where the default intensity is that of the rating class which the bond belongs to. Assuming maturity $\mathcal{T}$ and constant recovery rate δ, and that the bond belongs to rating class m at time t, the price is thus

$$P^d(t,\mathcal{T}) = P(t,\mathcal{T})E^{\mathbb{Q}}\left[\exp\left(-\int_t^{\mathcal{T}}(1-\delta)\lambda_s^m ds\right)|\mathcal{F}_t\right],$$

which may be computed analytically under the multi-factor CIR process specification for λ_t^m. Here $P(t,\mathcal{T})$ is a discount factor, equal to the price of a zero-coupon treasury bond with the same maturity. The filtration $\{\mathcal{F}_t\}$ carries information about the stochastic processes and not of credit migrations or defaults. Beside RMV with constant recovery rates, the above equation makes use of the following simplifications:

- Interest rates are uncorrelated with default intensities, enabling the discount factor to be separated from the expectation
- Only the instantaneous default intensity is considered, neglecting transition intensities

Since we focus attention to excess returns, we will often neglect the involvement of discount factors altogether. The second bullet on the list is likely to create a bias when pricing, skewing marginal returns. However, we conjecture this bias will influence prices systematically and predictably and with little effect on the analysis of dependence between equity and credit risk.

When performing the analysis, we will further investigate bond portfolios that are continuously rebalanced. What this means is that the composition of a portfolio with respect to the rating classes and/or the maturities of the participating bonds, is regularly reset to the original state. In our case, it is natural to do so at the start of every new migration time window, adjusting for any credit migrations which might have taken place. This method favours a representation of a bond portfolio as a bond index, reflecting a certain credit quality. Take for example a portfolio consisting of 50 high yield bonds. If continuously rebalanced, this may serve as a high yield bond index. In Section 4.5, more details on the practical implementation of the rebalancing method are given.

Chapter 4

Method

In this chapter, we describe what data analyses that are made and which statistical methods that are used for this purpose. Then, the implementation of the model is presented, including all the simulation details. Finally, a note on model calibration and parameter estimation is given.

4.1 Data Analysis

While focus of this thesis is primarily on the design of the model and investigation of how risk varies with different parameter specifications, data is collected and analysed as a tool to crudely calibrate and survey the health of the model.

The analysis of data consists of data collection followed by computation of some interesting quantities relating to the marginal and multivariate distributions assumed to underlie the data. When analysing individual time series, the first four moments along with quantiles at a few different levels are empirically estimated. To do so, returns between adjacent months are considered based on closing values at the end of each month. A few reasons for picking out monthly rather than daily data, include the discrete approach to simulating dependent migrations, imposing dependence statically, as well as the rebalancing method further described in Section 4.5. Nonetheless, daily returns for the stock index will be considered. When simulating from our framework, these are not affected by bond market movements.

4.1.1 Data Collection

The data comprises time series of daily closing values of the following three bodies:

- Equity data: S&P 500 (03/01/1990 - 05/03/2015)
- Bond data: iShares iBoxx USD Investment Grade ETF (22/07/2002 - 05/03/2015)
- Bond data: iShares iBoxx USD High Yield ETF (04/04/2007 - 05/03/2015)

S&P 500 data is collected from Yahoo Finance, whereas data of the two ETFs is taken from iShares. The latter two consist of selections of USD bonds of varying maturity within the relevant rating classes, and are here taken to represent a cross section of the USD corporate debt market much like bond indices.

4.1.2 Moments and Quantiles

In case they exist, the first four moments are informative at describing the distributional characteristics of a random variable. For a given random variable X, these are specified accordingly:

$$\begin{aligned} &\text{Mean:} && \mu = E[X], \\ &\text{Variance:} && \sigma^2 = E[(X-\mu)^2], \\ &\text{Skewness:} && \gamma = \frac{E[(X-\mu)^3]}{\sigma^3}, \\ &\text{Kurtosis:} && \kappa = \frac{E[(X-\mu)^4]}{\sigma^4} - 3. \end{aligned}$$

When analysing historical data, such as daily stock index returns, we may estimate these empirically. For a sample of N observations x_i, $i = 1, \ldots, N$, of X, we use the following estimators:

$$\hat{\mu} = \frac{1}{N}\sum_{i=1}^{N} x_i \tag{4.1}$$

$$\hat{\sigma}^2 = \frac{1}{N-1}\sum_{i=1}^{N}(x_i - \hat{\mu})^2 \tag{4.2}$$

$$\hat{\gamma} = \frac{N^2}{N(N-1)(N-2)}\frac{1}{\hat{\sigma}^3}\sum_{i=1}^{N}(x_i - \hat{\mu})^3 \tag{4.3}$$

$$\hat{\kappa} = \frac{N(N+1)}{(N-1)(N-2)(N-3)}\frac{1}{\hat{\sigma}^4}\sum_{i=1}^{N}(x_i - \hat{\mu})^4 - 3\frac{(N-1)^2}{(N-2)(N-3)} \tag{4.4}$$

In addition to estimating moments, also quantiles at certain percentiles are interesting. For a sample $\{x_i\}$, we first rearrange the elements to constitute an ordered set $\{\tilde{x}_i\}$, where $\tilde{x}_1 \leq \tilde{x}_2 \leq \cdots \leq \tilde{x}_N$. The quantile $\hat{F}_X^{-1}(p)$ at p is then computed by

$$\hat{F}_X^{-1}(p) = \begin{cases} \tilde{x}_1, & p < \dfrac{1}{2N} \\ \tilde{x}_{\lfloor Np+1/2 \rfloor} + \left(\tilde{x}_{\lfloor Np+1/2 \rfloor+1} - \tilde{x}_{\lfloor Np+1/2 \rfloor}\right) \times \\ \qquad (Np + 1/2 - \lfloor Np + 1/2 \rfloor), & \dfrac{1}{2N} \leq p < \dfrac{2N-1}{2N} \\ \tilde{x}_N, & p \geq \dfrac{2N-1}{2N} \end{cases} \tag{4.5}$$

where $\lfloor x \rfloor$ is the largest integer less than or equal to x. This definition involves a linear interpolation between ordered statistics[1], whereas other alternatives might define the quantile estimator as a piecewise constant function.

4.1.3 Multivariate Analysis

The multivariate analysis consists of measurements of dependence between data series. Three quantities are of interest; linear correlation, Kendall's tau and tail index.

For a sample of observations (x_i, y_i), $i = 1, \ldots, N$ from the random variable (X, Y), we compute the linear correlation estimate by

$$\hat{\rho} = \frac{\sum_{i=1}^{N}(x_i - \hat{\mu}_x)(y_i - \hat{\mu}_y)}{\sqrt{\sum_{i=1}^{N}(x_i - \hat{\mu}_x)^2 \sum_{i=1}^{N}(y_i - \hat{\mu}_y)^2}} \tag{4.6}$$

[1]Note that the empirical quantile is not the quantile function of the empirical distribution with this definition.

and the Kendall's tau estimate by

$$\hat{\tau} = \frac{\sum_{i=2}^{N} \sum_{j<i} \{I((x_i - x_j)(y_i - y_j) > 0) - I((x_i - x_j)(y_i - y_j) < 0)\}}{n(n-1)/2} \tag{4.7}$$

where $I(\cdot)$ is the indicator function. As mentioned in Section 2.3.1, if the bivariate data comes from an elliptical distribution estimating τ and then transforming to linear correlation through

$$\hat{\rho} = \sin\left(\frac{\pi}{2}\hat{\tau}\right) \tag{4.8}$$

is likely to give improved accuracy.

4.1.4 Tail Index Measurements

In order to estimate tail dependence empirically given bivariate data, a threshold percentile level p is first defined[2]. This level is used to determine empirical quantiles for each series. Assuming we are looking at lower tail dependence, a tail index estimate is then obtained by counting the number of outcomes simultaneously falling below the respective quantile values and normalizing. Given N observations (x_i, y_i) from (X, Y),

$$\widehat{\lambda_{L,p}} = \frac{\sum_{i=1}^{N} I(x_i < \hat{F}_X^{-1}(p),\ y_i < \hat{F}_Y^{-1}(p))}{\sum_{i=1}^{N} I(y_i < \hat{F}_Y^{-1}(p))}, \tag{4.9}$$

where $I(\cdot)$ is the indicator function. This approach is also highlighted in e.g. Fortin and Kuzmics (2002) and Cherubini et al. (2004, ch. 1). When analysing upper tail dependence we would proceed similarly, looking at number of outcomes exceeding a high quantile value.

In case (X, Y) has a Gaussian copula with correlation parameter $\rho < 1$, we stated in Section 2.3.2 that upper as well as lower tail indices are zero. However, in order to see this empirically extremely low/high quantile levels are usually required. Unfortunately, the usefulness of the estimator (4.9) is dubious when p is selected so low that only a few outcomes of Y fall below the threshold, owing to small effective sample size. Therefore, tail index calculation through Equation (4.9) is more informative under the choice of a percentile level not quite so extreme, unless the sample size is enormous. Furthermore, in a VaR application a percentile level ranging from 0.005 to 0.05 is usually what is relevant, but under these choices a direct comparison to theoretical tail indices as defined in Section 2.3.3 is flawed.

For an illustration of the above, let (X, Y) be a bivariate normal variable with $\rho < 1$. We recall that both lower and upper tail indices are then equal to zero. The expectation of Equation (4.9), replacing empirical quantile functions by standard normal quantiles, is known in closed form. Assuming a low percentile level p, we may compute the quantity

$$\begin{aligned}
\lambda_{L,p} &= P(X < \Phi^{-1}(p) | Y < \Phi^{-1}(p)) \\
&= \frac{C_\rho^{\mathrm{Ga}}(p, p)}{p} \\
&= \frac{\Phi_\rho^2(\Phi^{-1}(p), \Phi^{-1}(p))}{p}
\end{aligned}$$

[2]Whenever we talk about percentile levels in this thesis, such are expressed in terms of fractions rather than percentages unless otherwise stated, so that the 0.05 level refers to the fifth percentile and similarly.

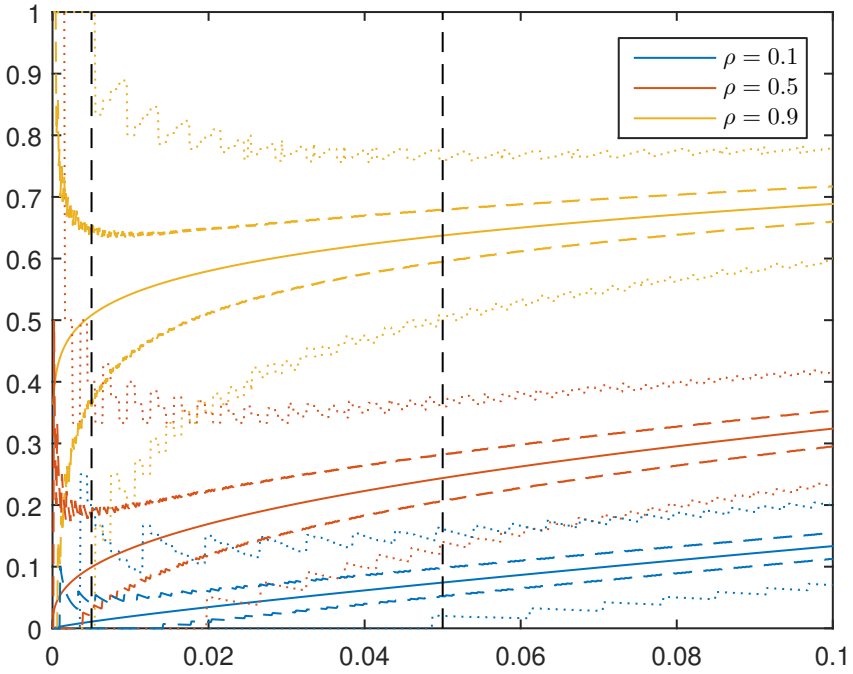

Figure 4.1: Expected lower tail index estimates from bivariate data coming from a random variable with a Gaussian copula with parameter ρ against tail index percentile levels, along with 95% confidence intervals for estimation based on samples of size N. Dotted lines correspond to confidence bounds for $N = 1000$ and dashed lines to $N = 10,000$. Vertical lines indicate the 0.005 and 0.05 percentile levels respectively.

for given correlation ρ. Using a few different values of ρ, Figure 4.1 shows how $\lambda_{L,p}$ varies with p. Further, 95% confidence intervals for estimation of $\lambda_{L,p}$ according to Equation (4.9) given a sample of size N of data coming from independent copies of (X, Y) are illustrated. These are computed by evaluating 2.5% and 97.5% quantiles of a $\text{Bin}(N_{\text{eff}}, \lambda_{L,p})$ distribution, where N_{eff} is the effective sample size,

$$N_{\text{eff}} = \sum_{i=1}^{N} I(y_i < \hat{F}_Y^{-1}(p)) = \lceil Np - 1/2 \rceil$$

with $\lceil x \rceil$ denoting the smallest integer larger than or equal to x. Evidently, estimators have high variance for small effective sample sizes. Also, unless ρ is low the convergence for $\lambda_{L,p}$ to zero occurs slowly as $p \downarrow 0$.

In order to get an idea of the strength of tail dependence for observed data, it is therefore more illuminating to pick a percentile level such that a moderately large amount of outcomes fall below the corresponding quantile value, calculate the tail index estimate according to Equation (4.9), and compare its value to what a Gaussian copula with comparable ρ would be expected to yield. If the pairs of observations reasonably enough resemble outcomes of an elliptical distribution, such a ρ is preferably determined from the Kendall's tau estimate with Equation (4.8). Fundamentally, the procedure requires fairly large sample sizes in order to be reliable.

4.2 Process Simulation Methodology

In this section, we describe the discretization schemes and algorithms used for simulation of the various stochastic processes involved. This includes the CIR process, appearing at several places in the model, the variance-gamma process and the stock index process. The discretization step size Δt is chosen to be common to all components. One process at a time is simulated, in a way largely consistent with Figure 3.1 but with the exception that several excess hazard rate processes are simulated, one for each rating class. Also, hazard rates do not participate in the stock index drift.

4.2.1 CIR Process Discretization

When sampling outcomes from the CIR process (Cox et al., 1985) at time $T > t$ conditional on information at time t, one may either sample directly from the conditional probability distribution, or by means of discretization. For the purpose of this thesis, setting up a discretization scheme is necessary in order to generate full sample paths which can be fed back to the stock process as well as the simulation of defaults and credit rating migrations.

It is then integral to discretize the process in a way that non-negativity is maintained. This becomes particularly important considering that the parameters in applications often violate the positivity constraint $2\kappa\theta > \sigma^2$ described in Section 2.1.1. There are various techniques available in the literature, where Euler and Milstein schemes described in for example Jäckel (2002) are among the simpler ones. These two, particularly the former, tend to cause issues when the process parameters are set such that the process might reach zero. When discretizing, negative values become attainable, rendering the scheme rather inappropriate. Therefore, we here apply a more sophisticated scheme known as the quadratic exponential scheme presented in Andersen (2007).

If we denote the CIR process by x_t and the discretization time step by Δt, the scheme relies on the fact that distribution of $x_{t+\Delta t}$ conditional on x_t can be well approximated by simpler distributions. For large value of x_t, the distribution of

$$\hat{x}_{t+\Delta t} = a(b + W)^2 \tag{4.10}$$

where $W \sim N(0, 1)$ closely approximates the distribution of $x_{t+\Delta t}|x_t$ for appropriately set constants a and b. Meanwhile, for small values of x_t,

$$\hat{x}_{t+\Delta t} = \begin{cases} 0, & U \leq p \\ \frac{1}{\beta} \log\left(\frac{1-p}{1-U}\right), & U > p \end{cases} \tag{4.11}$$

where U is a standard uniformly distributed variable gives a good approximation for $x_{t+\Delta t}$ conditional on x_t given appropriately set constants p and β.

The conditional mean and variance of $x_{t+\Delta t}|x_t$ are known, and the parameters a and b or p and β are determined by matching moments. A switching criterion depending on the value of x_t must be established in order to choose which of the two approaches to use. Denoting the conditional mean by m and the conditional variance by s^2, we have

$$\begin{aligned} m &= \theta + (x_t - \theta)\exp(-\kappa\Delta t) \\ s^2 &= \frac{x_t\sigma^2}{\kappa}\exp(-\kappa\Delta t)(1 - \exp(-\kappa\Delta t)) + \frac{\theta\sigma^2}{2\kappa}(1 - \exp(-\kappa\Delta t))^2. \end{aligned}$$

Letting $\psi = s^2/m^2$, Equation (4.10) is applicable for $\psi \leq 2$ while Equation (4.11) works well for $\psi \geq 1$. The constants a, b, p and β are related to m and s through

$$a = \frac{m}{1 + b^2}, \qquad b^2 = \frac{2}{\psi} - 1 + \sqrt{\frac{2}{\psi}\left(\frac{2}{\psi} - 1\right)} \tag{4.12}$$

as well as

$$p = \frac{\psi - 1}{\psi + 1}, \qquad \beta = \frac{2}{m(\psi + 1)} \tag{4.13}$$

in the two cases.

In Algorithm 1, we summarize the preceding and outline how to simulate a sample path of the CIR process. This is readily extended to efficiently simulate N sample paths.

input : step size Δt, risk horizon T, parameters (κ, θ, σ), initial value x_0
output: a sample path of the CIR process x_t

let $t = 0$, fix $\psi_C \in [1, 2]$
while $t < T$ **do**
  compute $m = \theta + (x_t - \theta)\exp(-\kappa\Delta t)$
  compute $s^2 = \frac{x_t\sigma^2}{\kappa}\exp(-\kappa\Delta t)(1 - \exp(-\kappa\Delta t)) + \frac{\theta\sigma^2}{2\kappa}(1 - \exp(-\kappa\Delta t))^2$
  compute $\psi = s^2/m^2$
  if $\psi \leq \psi_C$ **then**
    compute $b^2 = \frac{2}{\psi} - 1 + \sqrt{\frac{2}{\psi}\left(\frac{2}{\psi} - 1\right)}$
    compute $a = m/(1 + b^2)$
    simulate $W \sim N(0, 1)$
    let $x_{t+\Delta t} = a(b + W)^2$
  else
    compute $p = (\psi - 1)/(\psi + 1)$
    compute $\beta = \frac{2}{m(\psi+1)}$
    simulate $U \sim U(0, 1)$
    let $x_{t+\Delta t} = \begin{cases} 0, & U \leq p \\ \frac{1}{\beta}\log\left(\frac{1-p}{1-U}\right), & U > p \end{cases}$
  end
  let $t = t + \Delta t$
end

Algorithm 1: CIR Process Discretization and Simulation

4.2.2 Variance-Gamma Process Discretization

In order to discretize the variance-gamma jump process, we follow Yu et al. (2011) and note that increments are independent and given by

$$dX_t = \gamma G^{\nu}_{dt} + \sigma\sqrt{G^{\nu}_{dt}}W$$

where G^{ν}_{dt} belongs to $\Gamma(dt/\nu, \nu)$ and W is an independent $N(0, 1)$ variable. We mentioned in Section 2.1.2 that a compensating drift term ψt such that $E[e^{X_t+\psi t}] = 1$ should be added. This compensator could also be included as part of the stock drift process, but in order to treat the jump process independently from other parts of the model in line with Figure 3.1, we include it in this part of the simulation. Since the characteristic function

$\phi_{X_t}(u)$ is known in closed form, we have

$$\begin{aligned} e^{\psi t} &= \frac{1}{E[\exp(X_t)]} = \frac{1}{\phi_{X_t}(-i)} \\ \Leftrightarrow \quad \psi &= \frac{1}{t}\log\left((1-\gamma\nu-\sigma^2\nu/2)^{t/\nu}\right) \\ &= \frac{1}{\nu}\log(1-\gamma\nu-\sigma^2\nu/2), \end{aligned} \tag{4.14}$$

with $\phi_{X_t}(u)$ given by Equation (2.21). To conclude, simulation of an increment ΔJ_t for the mean-adjusted process from t to $t+\Delta t$ is performed by computing

$$\Delta J_t = \psi\Delta t + \gamma G + \sigma\sqrt{G}W \tag{4.15}$$

with ψ as in Equation (4.14), G simulated from $\Gamma(\Delta t/\nu,\, \nu)$ and W simulated from $N(0,1)$.

4.2.3 Stock Process Simulation

Once stochastic volatility and variance-gamma processes are simulated, they may be input to simulation of the stock process. Like for the CIR process, the scheme for this simulation is based on Andersen (2007). Since the jump process is uncorrelated with the stock Brownian motion, its evolution may be appended separately. Ignoring the jump process and the stock drift, the logarithm of the stock process discretized with step size Δt may be written

$$\begin{aligned} Y_{t+\Delta t} &= Y_t - \frac{1}{2}\int_t^{t+\Delta t} v_s ds + \int_t^{t+\Delta t}\sqrt{v_s}dW_s^S \\ &= Y_t + \frac{\rho}{\sigma_v}(v_{t+\Delta t} - v_t - \kappa_v\theta_v\Delta t) + \left(\frac{\kappa_v\rho}{\sigma_v} - \frac{1}{2}\right)\int_t^{t+\Delta t} v_s ds + \sqrt{1-\rho^2}\int_t^{t+\Delta t}\sqrt{v_s}dW_s, \end{aligned} \tag{4.16}$$

where we have let

$$\begin{pmatrix} dW_t^S \\ dW_t^v \end{pmatrix} = \begin{pmatrix} \rho dW_t^v + \sqrt{1-\rho^2}dW_t \\ dW_t^v \end{pmatrix} \tag{4.17}$$

with W_t an independent Brownian motion, and made use of

$$\begin{aligned} v_{t+\Delta t} &= v_t + \int_t^{t+\Delta t}\kappa_v(\theta_v - v_s)ds + \sigma_v\int_t^{t+\Delta t}\sqrt{v_s}dW_s^v \\ \Leftrightarrow \int_t^{t+\Delta t}\sqrt{v_s}dW_s^v &= \frac{1}{\sigma_v}\left(v_{t+\Delta t} - v_t - \kappa_v\theta_v\Delta t + \kappa_v\int_t^{t+\Delta t} v_s ds\right). \end{aligned}$$

In Equation (4.16), the two integrals need to be handled. Given v_t and $v_{t+\Delta t}$, we approximate

$$\int_t^{t+\Delta t} v_s ds \approx \frac{\Delta t}{2}(v_t + v_{t+\Delta t}). \tag{4.18}$$

As for the last integral in Equation (4.16), we first note that dv_t is independent of dW_t, as suggested by Equation (4.17). Therefore, the integral is Gaussian with mean zero and variance

$$\int_t^{t+\Delta t} v_s ds$$

by Itō isometry. Reusing the approximation (4.18) applied to the variance of the Wiener integral, it is straightforward to simulate $Y_{t+\Delta t}$, where jump and drift increments ΔJ_t and

$\int_t^{t+\Delta t} \mu_s ds$ are added to (4.16). In our case, the drift is input as a constant expected excess return, but in case a discretized drift process is used, we may use the approximation

$$\int_t^{t+\Delta t} \mu_s ds \approx \frac{\Delta t}{2}(\mu_t + \mu_{t+\Delta t}).$$

Algorithm 2 summarizes the above and describes how to simulate paths of the logarithm of the normalized stock index S_t/S_0.

input : step size Δt, risk horizon T, volatility parameters $(\kappa_v, \theta_v, \sigma_v)$, volatility path v_t, correlation ρ, drift μ_t, jump process increments ΔJ_t
output: a sample path of the logarithm Y_t of the normalized stock index process

define $k_0 = -\rho\kappa_v\theta_v\Delta t/\sigma_v$
define $k_1 = \frac{\Delta t}{2}\left(\frac{\kappa_v\rho}{\sigma_v} - \frac{1}{2}\right) - \frac{\rho}{\sigma_v}$
define $k_2 = \frac{\Delta t}{2}\left(\frac{\kappa_v\rho}{\sigma_v} - \frac{1}{2}\right) + \frac{\rho}{\sigma_v}$
define $k_3 = (1-\rho^2)\Delta t$
let $t = 0$, $Y_0 = 0$
while $t < T$ **do**
  simulate $W \sim N(0,1)$
  let $\mu = (\mu_t + \mu_{t+\Delta t})/2$
  let $Y_{t+\Delta t} = Y_t + \mu\Delta t + k_0 + k_1 v_t + k_2 v_{t+\Delta t} + \sqrt{k_3(v_t + v_{t+\Delta t})}W + \Delta J_t$
  let $t = t + \Delta t$
end

Algorithm 2: Normalized stock index process simulation

4.3 Credit Migration Simulation Methodology

We describe the main steps to simulate credit migrations in our framework. Economic scenarios encompassing sample paths of the stock index and of the instantaneous default intensities must be generated in a previous step. Although the scope within this thesis is limited to two rating classes, the methodology outlined is general.

4.3.1 Construction of Discrete Path-Dependent Migration Matrices

As previously mentioned, given a baseline intensity matrix Λ^{base} and simulated paths λ_t^m, time-dependent intensity matrices may be constructed by application of Equation (3.6). Having λ_t^m sampled at time steps Δt, we adapt the matrix construction to the discretized version of hazard rate processes and make use of midpoints between sampled values, representing approximate averages over $(t, t+\Delta t)$. Hence, the scaling factors corresponding to Equation (3.6) are set to be

$$\frac{(\lambda_t^m + \lambda_{t+\Delta t}^m)/2}{\lambda_{mK}}.$$

We assume that time windows are specified such that they fit an integral number H of process discretization steps. This will be the case for example if migration matrices are constructed on a monthly basis while process discretization is done with $\Delta t = 1/252$, with

discretization time steps corresponding to business days. Then, letting $H\Delta t = t_j - t_{j-1}$, we therefore have

$$P_{(t_{j-1},t_j)} = \prod_{h=1}^{H} \exp\left(\Lambda_{t_{j-1}+(h-1)\Delta t}\Delta t\right)$$

where Λ_t represents the intensity matrix between t and $t + \Delta t$.

4.3.2 Transformation of Stock Index Returns

In order to condition transition outcomes on movements of the stock index, it is necessary to transform the stock index returns to uniforms. Given that we have simulated N economic scenarios and constructed J discrete time transition matrices for each economic scenario in the previous step, a total of NJ returns over time windows of the type $(t_{j-1}, t_j]$, $j = 1, \ldots, J$, are obtained.

Since the stock index follows a geometric process and time windows are constructed to be of equal length, we may consider all returns jointly despite belonging to different paths and time windows. Doing so, an empirical distribution function $\hat{F}_S$ can be constructed. By applying the probability transform[3], this enables a mapping to uniforms by evaluating

$$U_S = \hat{F}_S\left(\frac{S_{t_j}}{S_{t_{j-1}}}\right). \tag{4.19}$$

Due to right continuity of the empirical distribution function, in addition to being piecewise constant with equal-sized jumps, the values U_S could take according to the above would be $1/(NJ)$, $2/(NJ)$, ..., 1. This is biased and suboptimal since the value 1 is attained. Therefore we subtract a value $1/(2NJ)$ in the assignment to uniforms, equivalent to evaluating the empirical distribution at the midpoints in discontinuous parts.

With this approach, extreme outcomes of U_S are more likely to occur in times of high volatility. A discussion on the appropriateness of the mapping is found in Appendix C.3, where we also point out an alternative method.

4.3.3 Copula Simulation Techniques

We let a parameter w represent the weight of the stock index on credit migrations for firms. This parameter governs the correlation in Gaussian and t copulas. For the latter, the dependence structure also requires that the number of degrees of freedoms ν be specified. An equivalent representation of the strength of dependence in these copulas is given by Kendall's tau,

$$\tau = \frac{2}{\pi}\arcsin w.$$

From τ, a comparable Clayton copula with parameter α may be specified through application of Equation (2.40).

Conditionally on a uniform U_S associated with the stock index and given a bivariate copula specification for the relation between the stock index and firm credit migrations, we describe how to simulate uniforms mappable to firm transition outcomes.

Conditional Gaussian Here, we simulate a uniform U_i and compute

$$U = \Phi\left(w\Phi^{-1}(U_S) + \sqrt{1-w^2}\Phi^{-1}(U_i)\right) \tag{4.20}$$

[3]The application of the probability transform is somewhat sloppy here since the empirical distribution function does not satisfy the necessary condition of being a continuous function. However, as long as the total number NJ of stock index returns is large, this becomes less of a concern.

Conditional t A technique for simulating conditionally from the bivariate t copula with ν degrees of freedom is described in Brechmann et al. (2013). The steps are as follows:

- Let $Y_S = t_\nu^{-1}(U_S)$
- Simulate $\tilde{Y}_i$ from $t_{\nu+1}(0,1)$
- Let $Y = \sqrt{\frac{\nu+Y_S^2}{\nu+1}}\sqrt{1-w^2}\tilde{Y}_i + wY_S$
- Let $U = t_\nu(Y)$

Conditional Clayton For conditional simulation from the Clayton copula we apply a method presented in Cherubini et al. (2004, ch. 6), described in the following steps:

- Simulate a uniform U_i
- Let $V = \frac{U_S^{-\alpha}+U_i^{-\alpha}-1}{U_S^{-\alpha}}$
- Let $U = \left(U_S^{-\alpha}(V-1)+1\right)^{-1/\alpha}$

4.3.4 Mapping Simulated Uniforms to Transition Outcomes

For any sample path and migration time window, there will be a discrete transition matrix P governing the probabilities of migration for the bonds in the portfolio. Assuming a transition matrix on the form

$$P = \begin{pmatrix} p_{11} & p_{12} & \cdots & p_{1M} & p_{1K} \\ p_{21} & p_{22} & \cdots & p_{2M} & p_{2K} \\ \vdots & \vdots & \ddots & \vdots & \vdots \\ p_{M1} & p_{M2} & \cdots & p_{MM} & p_{MK} \\ 0 & 0 & \cdots & 0 & 1 \end{pmatrix}, \tag{4.21}$$

then for a given bond belonging to rating class m the task is now to map simulated uniforms to an outcome in the Markov chain. Noting that uniforms with lower value should be mapped to less favourable transition outcomes for consistency with the dependence specifications, we construct the bins

$$(0,\, p_{mK}],\ (p_{mK},\, p_{mK}+p_{mM}],\ \ldots,\ (p_{mK}+p_{mM}+\cdots+p_{m2},\, 1). \tag{4.22}$$

With this ordering, a simulated uniform whose outcome belongs to bin j maps to a transition outcome to state $M+2-j$. Denoting our uniform by U, a correct transition outcome may also be immediately obtained by counting the number of bins whose right boundary is greater than or equal to U.

The upper boundary values of the bins in equation (4.22) may also be calculated

quickly for all rating classes by carrying out the matrix multiplication

$$P_U = P \cdot \begin{pmatrix} 0 & 0 & \cdots & 0 & 1 \\ 0 & 0 & \cdots & 1 & 1 \\ \vdots & \vdots & \iddots & \vdots & \vdots \\ 0 & 1 & \cdots & 1 & 1 \\ 1 & 1 & \cdots & 1 & 1 \end{pmatrix}$$
$$= \begin{pmatrix} p_{1K} & p_{1K}+p_{1M} & \cdots & p_{1K}+p_{1M}+\cdots+p_{12} & 1 \\ p_{2K} & p_{2K}+p_{2M} & \cdots & p_{2K}+p_{2M}+\cdots+p_{22} & 1 \\ \vdots & \vdots & \ddots & \vdots & \vdots \\ p_{MK} & p_{MK}+p_{MM} & \cdots & p_{MK}+p_{MM}+\cdots+p_{M2} & 1 \\ 1 & 1 & \cdots & 1 & 1 \end{pmatrix} \tag{4.23}$$

with P as in equation (4.21). Row m of P_U then contains the upper bin boundaries of rating class m, and for a bond in class m the new rating class is simply found by counting the number of values in row m exceeding or equalling the simulated uniform value U.

4.4 Portfolio Evaluation along Sample Paths

For the investigated portfolio, asset pricing relies on the specification of hazard rates and recoveries. The overall value of the portfolio is evaluated at time 0 as well as at every t_j, $j = 1, \ldots, J$. Under the recovery of market value model as in Equation (2.30), we further assume that if default for one of the bonds occurs in $(t_{j-1}, t_j]$, its value at time t_j is reduced to the fraction δ of the time t_j value the bond would have had in case of no credit transition. This is equivalent to assuming defaults may only occur at times t_j. We treat all migrations like this, letting rating states change at times t_j as governed by simulation from matrices $P_{(t_{j-1},t_j)}$.

Omitting discount factors and focusing exclusively on excess returns, the time t price of a bond maturing at $\mathcal{T}$ and being in credit class m is given by

$$\begin{aligned} P^d(t,\mathcal{T}) &= E^{\mathbb{Q}}\left[\exp\left(-\int_t^{\mathcal{T}}(1-\delta)\lambda_s^m ds\right)|\mathcal{F}_t\right] \\ &= E^{\mathbb{Q}}\left[\exp\left(-\int_t^{\mathcal{T}}\left((1-\delta)\beta_m v_s + (1-\delta)\sum_{i=1}^m z_s^i\right)ds\right)|\mathcal{F}_t\right]. \end{aligned} \tag{4.24}$$

In other words, the pricing involves the evaluation of intensities given by sums of CIR processes scaled by constants $(1-\delta)\beta_m$ and $(1-\delta)$ respectively. Letting $h \geq 0$ be a constant and x_t a CIR process with parameters (κ, θ, σ), we have

$$\begin{aligned} h dx_t &= h\kappa(\theta - x_t)dt + h\sigma\sqrt{x_t}dW_t \\ &= \kappa(h\theta - hx_t)dt + \sqrt{h}\sigma\sqrt{hx_t}dW_t, \end{aligned}$$

such that hx_t is given by a new CIR process, implying affine bond pricing through Equations (2.9) and (2.11) holds, with parameters changed according to

$$\begin{cases} x_t \to hx_t \\ \kappa \to \kappa \\ \theta \to h\theta \\ \sigma \to \sqrt{h}\sigma \end{cases} \tag{4.25}$$

4.5 Parameter Estimation

When estimating model parameters, a trial and error approach is used along with simulating from the model. Given simulated and observed paths, we compute monthly returns of the three series, from which moments, quantiles and dependence measures may be estimated as described in Section 4.1.

Regarding construction of bond portfolios, we assume the division into 50 equally weighted bonds with equal maturity and recovery arrangements connected through the chosen dependence structure offer reasonable representations of the state of the bond market. Clearly, this construction is a considerable simplification of the complex compositions associated with the investigated ETFs, containing diverse mixes of maturities, bond weights, recoveries and credit qualities.

When simulating longer sample paths, we rebalance the portfolios on a monthly basis, i.e. immediately following the possible occurrence of credit migrations. Credit ratings and maturities are reset to the original state, and gains and losses are accounted for by rescaling the positions in the portfolio, such that the portfolio values computed pre- and post-rebalancing are equal. This procedure does not alter the composition, only the size of the investment.

In order to get an idea of the uncertainty of sample estimates of statistics, which will depend on the length of time series, many sample paths are generated for a given set of parameters and all of the statistics are estimated for each scenario. This enables construction of approximate confidence intervals for statistics, from which the validity of the model parameters may be assessed. Confidence bounds at level α are evaluated empirically by computing $(1-\alpha)/2$ and $(1+\alpha)/2$ quantiles of the Monte-Carlo based estimators.

Since interest rates are not implemented and excess returns above investments into risk-free assets are modelled, while observed data contains information of actual returns, mean returns are not calibrated. Instead, emphasis is placed on whether the breadth of marginal distributions as well as dependence across markets can be captured.

Chapter 5

Results

We here present results based on analysis of market data as well as simulation from the model. First, in Section 5.1 we conduct data analysis of the available time series, from which we attempt to match parameters and use simulation to fit the model in Section 5.2.

Given fitted parameters, in Section 5.3 we perform simulation from the model in a one-year risk setting. Further, we make various adjustments to the dependence structure and investigate the implications on the analysis of risk.

5.1 Data Analysis

We start by plotting the evolutions of the three time series over the time windows at hand. Computing monthly returns of each series, we may also investigate the joint movements between stock index and bond ETF series. Figure 5.1 illustrates the evolutions, and also displays monthly joint movements by means of a scatter plot. The figure hints at the existence of dependence across the two markets. This is particularly striking when it comes to the high yield index.

In Table 5.1, we compute moments, quantiles and dependence measures for monthly returns of the series. The statistics reinforce the observation that dependence appears higher between high yield index and stock index, as compared to investment grade index and stock index. However, the figures carry considerable uncertainty due to the relatively sparsely sized data sets, especially the high yield index. In particular, the reliability of tail index estimates is questionable. When computing this as well as other measures of association, the length of the stock index sample is shortened to match the time series for the bond index with which dependence is analysed. The quantiles presented, however, make use of the full length.

For the stock index, we also briefly analyse statistics of daily log returns. Dividing the time series into several distinct time windows of equal (or close to equal) size, estimates suggest absence of stationarity, with both moments and quantiles varying greatly for different time windows along the observed path as shown in Table 5.2. Stochastic volatility appears plausible, and so does jumps given the large differences in higher order moments at similar standard deviations as is seen when four time windows are used. We however stress that as the number of business days varies between months, ranging from 15 to 23, biases are likely being created and complicating the analysis.

	S&P 500	**iBoxx IG**	**iBoxx HY**
Sample size	301	151	94
Mean ($\times 10^{-3}$)	7.076	5.489	5.909
Std. ($\times 10^{-2}$)	4.204	2.027	3.455
Volatility	0.146	0.070	0.120
Skewness	−0.631	0.044	−1.298
Kurtosis	1.289	6.736	7.549
0.02 quantile	0.908	0.954	0.927
0.10 quantile	0.954	0.987	0.969
0.90 quantile	1.057	1.026	1.037
0.98 quantile	1.087	1.040	1.084
Correlation		0.208	0.723
Kendall's tau		0.079	0.498
0.02 tail		1 (3)	1 (2)
0.10 tail		3 (15)	8 (9)
0.90 tail		1 (15)	4 (9)
0.98 tail		0 (3)	1 (2)

Table 5.1: Estimated statistics for monthly returns of S&P 500, iBoxx IG and iBoxx HY time series data. Mean values are given as subtracted by one. Volatilities are standard deviations rescaled to a yearly basis. Dependence measure estimates given describe dependence with stock index movements. Tail values show number of exceedances in the data set, with effective sample sizes displayed in parantheses. Tail index estimation according to Equation (4.9) would take the quotient of the two.

	one window	**two windows**		**three windows**			**four windows**			
	W1	W1	W2	W1	W2	W3	W1	W2	W3	W4
Length	6342	3171	3171	2114	2114	2114	1585	1586	1585	1586
Mean ($\times 10^{-4}$)	2.79	2.91	2.66	5.37	0.90	2.09	3.59	2.23	−0.36	5.69
Std. ($\times 10^{-2}$)	1.14	1.02	1.25	0.79	1.17	1.38	0.73	1.24	1.25	1.26
Volatility	0.18	0.16	0.20	0.13	0.19	0.22	0.12	0.20	0.20	0.20
Skewness	−0.24	−0.16	−0.27	−0.35	0.01	−0.33	−0.15	−0.14	−0.17	−0.38
Kurtosis	8.76	4.21	10.05	5.25	2.58	9.74	2.40	2.88	13.34	6.93
0.005 quantile	−3.97	−3.12	−4.83	−2.56	−3.50	−5.41	−2.41	−3.82	−5.02	−4.73
0.05 quantile	−1.76	−1.67	−1.88	−1.21	−1.87	−2.14	−1.19	−1.95	−1.81	−1.99
0.10 quantile	−1.19	−1.12	−1.27	−0.84	−1.41	−1.37	−0.82	−1.51	−1.30	−1.25
0.90 quantile	1.18	1.14	1.24	0.97	1.34	1.30	0.90	1.44	1.19	1.29
0.95 quantile	1.66	1.56	1.73	1.30	1.87	1.89	1.19	1.94	1.68	1.85
0.995 quantile	3.93	3.47	4.24	2.49	3.83	4.62	2.26	3.97	4.09	4.43

Table 5.2: Data analysis of daily log-returns of the S&P 500 data, with division into different time windows along the paths, where windows are denoted W# and arranged in chronological order. Volatility is computed as standard deviation times $\sqrt{252}$.

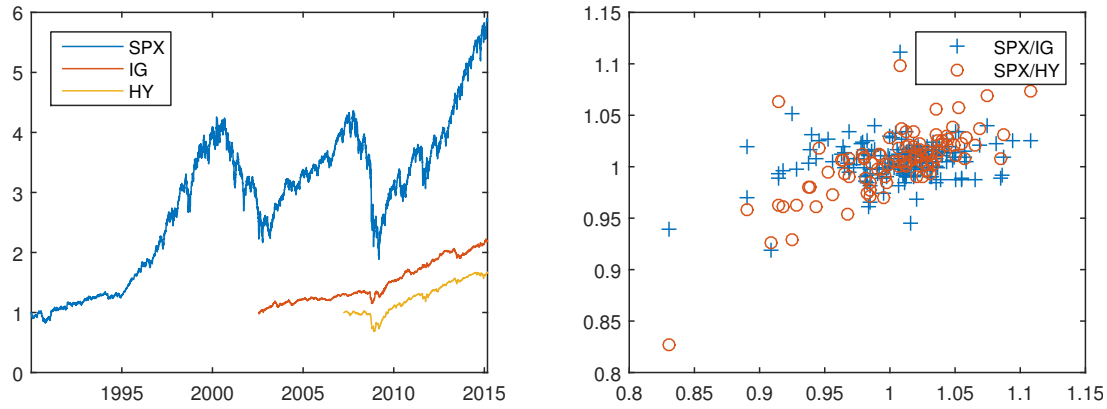

a. Normalized paths

b. Monthly returns

Figure 5.1: Observed paths of S&P 500 (SPX), the iBoxx USD investment grade ETF (IG) and the iBoxx USD high yield ETF (HY), normalized by the first observation in each series in (a). Scatter plots of monthly returns of stock index and bond ETFs whenever they are jointly observed in (b).

5.2 Model Calibration

The time horizon for simulation of sample paths from the model is set to equal that of the stock index, being the longest time series of those observed. We apply daily discretization, such that $\Delta t = 1/252$. For a discussion on this time step and on possible discretization errors resulting from this, we refer to Appendix B. An equal number of days is assigned to each month for migration simulation and portfolio rebalancing. This leads to a difference compared to the observed data sets, where the number of business days differs from one month to another by a non-negligible margin. Using observed monthly returns as the benchmark for calibration, said difference presents itself by causing an offset when comparing statistics of daily returns between observed and simulated paths.

500 paths of the same length as the observed stock index are simulated for the stochastic processes. Another 300 paths are simulated for the purpose of increasing accuracy in the conversion from monthly stock index returns to uniforms, used for the migration mapping[1]. Accumulating all simulated paths, this leads to a total sample of 241,600 monthly stock index returns mapped to uniforms.

IG and HY portfolios are constructed and rebalanced monthly in accordance with the description in Section 4.5, applying a maturity of 5 years and a recovery rate of 0.4 for all bonds. Reducing the lengths of paths of portfolio values to match observed data, we conduct statistical analysis of monthly returns for each scenario generated.

A set of parameters providing a reasonable fit is listed in Table 5.3. Applying these, the results of the statistical analysis are presented in Table 5.4. Quantities based on simulated series are presented as average values across all scenarios, with the attachment of estimated 95% confidence intervals made up by 2.5% and 97.5% quantiles of the 500 estimates for each statistic. Due to significant differences between paths belonging to different samples, in addition to limited length of each sample path, a high variation in many of the estimated quantities is observed. Higher moments display large variations and so do dependence measures.

[1]The additional 300 stock index paths are used solely to assist in the conversion to uniforms via Equation (4.19), and are thereby not used for simulation of portfolio scenarios. The total number of monthly stock index returns utilized for uniform conversion is then close to that used for the risk analysis in Section 5.3.

Discretization parameters		
sample size	N	500
time step	Δt	$1/252$
simulation horizon	T	25.17
migration window	Δt_j	$1/12$
Initial values		
volatility	v_0	0.02
IG excess hazard rate	z_0^1	0.01
HY excess hazard rate	z_0^2	0.01
Process parameters		
volatility process	κ_v	1.4
	θ_v	0.021
	σ_v	0.18
	γ_v	-2.22
stock index/volatility correlation	ρ	-0.8
stock index excess return	μ_e	0.06
variance-gamma process	ν	0.2
	σ	0.04
	γ	-0.14
IG stock volatility dependence factor	β_1	0.12
IG excess hazard rate	κ_1	1.3
	θ_1	0.0062
	σ_1	0.22
	γ_1	-5.55
HY stock volatility dependence factor	β_2	2
HY excess hazard rate	κ_2	1.2
	θ_2	0.005
	σ_2	0.2
	γ_2	-4.5
Migration parameters		
real-world baseline intensity matrix	Λ_{base}	$\begin{pmatrix} -0.026 & 0.017 & 0.0087 \\ 0.054 & -0.11 & 0.054 \\ 0 & 0 & 0 \end{pmatrix}$
IG copula		Clayton
stock index/transitions weight	w	0.3
HY copula		Gaussian
stock index/transitions weight	w	0.6

Table 5.3: Parameters for simulation from the model when attempting to fit to market data. CIR process parameters stated in terms of reversion speed (κ) and long term mean (θ) under the real-world measure, along with diffusion coefficient (σ) and market price of risk (γ).

	S&P 500		iBoxx IG		iBoxx HY	
	Obs.	Simulated	Obs.	Simulated	Obs.	Simulated
Mean ($\times 10^{-3}$)	7.08	4.82, [−0.78, 10.11]	5.49	1.25, [−1.20, 2.26]	5.91	3.78, [−2.66, 6.55]
Std. ($\times 10^{-2}$)	4.20	4.71, [3.94, 5.52]	2.03	1.93, [0.97, 3.35]	3.45	3.18, [1.94, 5.49]
Vol. ($\times 10^{-1}$)	1.46	1.63, [1.37, 1.91]	0.70	0.67, [0.34, 1.16]	1.20	1.10, [0.67, 1.90]
Skewness	−0.63	−0.34, [−0.85, 0.10]	0.04	−0.54, [−5.56, 1.20]	−1.30	−0.43, [−2.83, 1.03]
Kurtosis	1.29	1.13, [0.11, 3.14]	6.74	9.49, [1.70, 51.82]	7.55	3.70, [0.12, 16.37]
0.02 quantile	0.91	0.90, [0.87, 0.92]	0.95	0.95, [0.92, 0.98]	0.93	0.93, [0.84, 0.96]
0.10 quantile	0.95	0.94, [0.93, 0.96]	0.99	0.98, [0.97, 0.99]	0.97	0.97, [0.95, 0.98]
0.90 quantile	1.06	1.06, [1.05, 1.07]	1.03	1.02, [1.01, 1.04]	1.04	1.04, [1.03, 1.06]
0.98 quantile	1.09	1.10, [1.08, 1.12]	1.04	1.05, [1.02, 1.08]	1.08	1.07, [1.04, 1.12]
Correlation			0.21	0.14, [−0.07, 0.43]	0.72	0.58, [0.27, 0.81]
Kendall's tau			0.08	0.08, [−0.04, 0.19]	0.50	0.37, [0.16, 0.59]
0.02 tail			1	0.59, [0, 2]	1	0.80, [0, 2]
0.10 tail			3	2.81, [0, 7]	8	4.24, [1, 8]
0.90 tail			1	1.73, [0, 4]	4	3.55, [1, 7]
0.98 tail			0	0.08, [0, 1]	1	0.60, [0, 2]

Table 5.4: Estimates of statistics from observed and simulated data. Estimates from the latter constructed by taking the average and calculating approximate 95% confidence intervals based on 500 scenarios. The mean values are subtracted by one. Volatility (vol) given as standard deviation rescaled to yearly basis. Dependence measures concern the relationship between stock index and bond portfolios.

The span of admissible values which the parameters can take in order to yield results which do not provide sufficient evidence that we can reject the hypothesis that the observed data comes from the model with 95% confidence appears fairly large, by trial and error (ignoring mean values of returns). Without going into depth on all such combinations, being peripheral to the point of interest of this thesis, we note that the dependence specification can be modified. The analysis of Table 5.4 is based on a Clayton copula with weight $w = 0.3$ connecting stock index and migrations dynamics for IG portfolio bonds, while the corresponding dependence structure for stock index and HY portfolio is a Gaussian copula with weight $w = 0.6$. For an example of an alternative structure, we replace these by a t_7 copula with weight $w = 0.2$, and a Clayton copula with weight 0.3 respectively, obtaining results as in Table 5.5. It appears an acceptable fit is obtained with this specification as well.

5.3 Portfolio Risk Simulation

Instead of performing the analysis along observed and simulated paths, we here shift the perspective to focus on the distribution of stock index and bond portfolio returns at the end of a risk horizon. A one-year horizon is used throughout.

5.3.1 Risk Perspective

We run the simulation framework for a sample of size $N = 20,000$. Aside from that and the simulation horizon T being reduced to one year, parameters are held the same as those listed in Table 5.3. Like before, we simulate IG and HY portfolios with monthly rebalancing with respect both to the credit rating distribution of the constituent bonds and to their maturities. We also perform the simulations for equally constructed portfolios that are not rebalanced or adjusted during the course of the simulated time period.

Proceeding as above, we arrive at results presented in Table 5.6. For the portfolios

	S&P 500		iBoxx IG		iBoxx HY	
	Obs.	Simulated	Obs.	Simulated	Obs.	Simulated
Mean ($\times 10^{-3}$)	7.08	4.82, [−0.78, 10.11]	5.49	1.37, [−0.08, 2.06]	5.91	3.61, [−5.25, 6.87]
Std. ($\times 10^{-2}$)	4.20	4.71, [3.94, 5.52]	2.03	1.81, [0.97, 3.16]	3.45	3.21, [1.86, 6.23]
Skewness	−0.63	−0.34, [−0.85, 0.10]	0.04	0.01, [−1.69, 1.24]	−1.30	−1.02, [−5.14, 0.67]
Kurtosis	1.29	1.13, [0.11, 3.14]	6.74	5.54, [1.72, 15.66]	7.55	6.46, [−0.03, 38.96]
0.02 quantile	0.91	0.90, [0.87, 0.92]	0.95	0.96, [0.92, 0.98]	0.93	0.92, [0.79, 0.97]
0.10 quantile	0.95	0.94, [0.93, 0.96]	0.99	0.98, [0.97, 0.99]	0.97	0.97, [0.94, 0.99]
0.90 quantile	1.06	1.06, [1.05, 1.07]	1.03	1.02, [1.01, 1.04]	1.04	1.04, [1.03, 1.05]
0.98 quantile	1.09	1.10, [1.08, 1.12]	1.04	1.05, [1.02, 1.08]	1.08	1.07, [1.04, 1.11]
Correlation			0.21	0.08, [−0.09, 0.31]	0.72	0.53, [0.20, 0.74]
Kendall's tau			0.08	0.06, [−0.05, 0.17]	0.50	0.34, [0.14, 0.53]
0.02 tail			1	0.28, [0, 2]	1	0.89, [0, 2]
0.10 tail			3	2.24, [0, 6]	8	4.02, [1, 8]
0.90 tail			1	1.65, [0, 4]	4	2.82, [0, 6]
0.98 tail			0	0.06, [0, 1]	1	0.29, [0, 2]

Table 5.5: Estimates of statistics from observed and simulated data, with modified dependence structure between stock index and migration dynamics.

which are not rebalanced, rating distributions illustrated in Figure 5.3 are observed at the end of the horizon. The estimated statistics only show slight variations between portfolios that are rebalanced compared to those that are not. Slightly higher average returns and standard deviations (which may here also be interpreted as yearly volatilities) are however observed for continuously rebalanced portfolios.

		Without rebalancing		With rebalancing	
	Stock index	IG portfolio	HY portfolio	IG portfolio	HY portfolio
Mean ($\times 10^{-2}$)	6.04	2.25	5.56	2.32	6.14
Std. ($\times 10^{-2}$)	16.55	5.26	8.77	5.58	9.20
Skewness	−0.24	−3.24	−1.57	−3.17	−1.64
Kurtosis	0.02	16.70	3.88	15.90	4.67
0.005 quantile	0.60	0.76	0.70	0.74	0.69
0.05 quantile	0.78	0.92	0.89	0.91	0.89
0.10 quantile	0.84	0.96	0.94	0.96	0.94
0.90 quantile	1.27	1.06	1.14	1.06	1.15
0.95 quantile	1.32	1.06	1.16	1.06	1.16
0.995 quantile	1.45	1.06	1.17	1.07	1.19
Correlation		0.26	0.64	0.25	0.64
Kendall's tau		0.19	0.44	0.18	0.44
0.005 tail index		0.29	0.50	0.23	0.55
0.05 tail index		0.23	0.52	0.22	0.52
0.95 tail index		0.15	0.23	0.12	0.23
0.995 tail index		0.02	0.09	0.02	0.09

Table 5.6: Results from analysis of $N = 20,000$ simulated returns for stock index, IG and HY portfolios, with as well as without monthly portfolio rebalancing, over a 1-year risk horizon. Dependence measures are computed with respect to stock index returns. Means are subtracted by one.

Regarding the IG portfolio, with or without rebalancing, we see that the absolute values of skewness and kurtosis are considerably higher than for HY portfolios. This is explained by the absence of upward transition possibilities, also explaining why higher quantiles only exhibit minor differences, barely visible at two decimal places as in Table 5.6. The returns are capped at the case where no transitions occur for any of the bonds within the simulated time horizon, while IG hazard rates at the end of the horizon attain

zero.

Looking at simulated 1-year distributions of hazard rates, depicted in Figure 5.2 (subplot 5.2a) along with the distribution of returns of a bond belonging to one of the two classes throughout the horizon (subplot 5.2b), the heavily skewed and sharply capped IG return under the model is highlighted, explaining the upper quantile behaviour for the corresponding bond portfolio. Meanwhile, a wider distribution is noted for the HY hazard rate, being a higher factor CIR process. This is reflected for the HY bond. With the added possibility of both downward and upward transitions, the HY bond portfolio distribution displays a fairly high degree of variation, moreso than the IG portfolio. Histograms of the two, without and with rebalancing, are available in Figure 5.2 (subplots 5.2c and 5.2d).

The figure, along with the results in Table 5.6, indicates that the difference in risk between IG and HY portfolios is not great looking at the left tails of the two, although the left tail of the HY portfolio is heavier. When looking at the respective volatilities, the difference in risk shows clearly, with the HY portfolio displaying larger variance. Comparing to statistics of observed monthly returns in Table 5.1, quantiles as well as volatilities exhibit similar tendencies on a yearly risk horizon across the two credit qualities as those present in monthly market data. Since interest rates are left out and means are therefore not calibrated to observed data, a slight shift in levels of returns would likely be required in order to give a full account of the distributional properties. The neglect of migration risk when pricing bonds also contributes to an offset, affecting IG bonds more than HY bonds, further discussed in Section 6.2.1.

Another noteworthy observation is that upper tail dependence appears significantly weaker than its lower tail counterpart, for either portfolio. While the majority of the present chapter is devoted to analysis of overall dependence and lower tail dependence, being of higher relevance from a risk management point of view, in the concluding section we return to this observation and briefly look into the upper tail in order to further probe the full extent of model dependence properties.

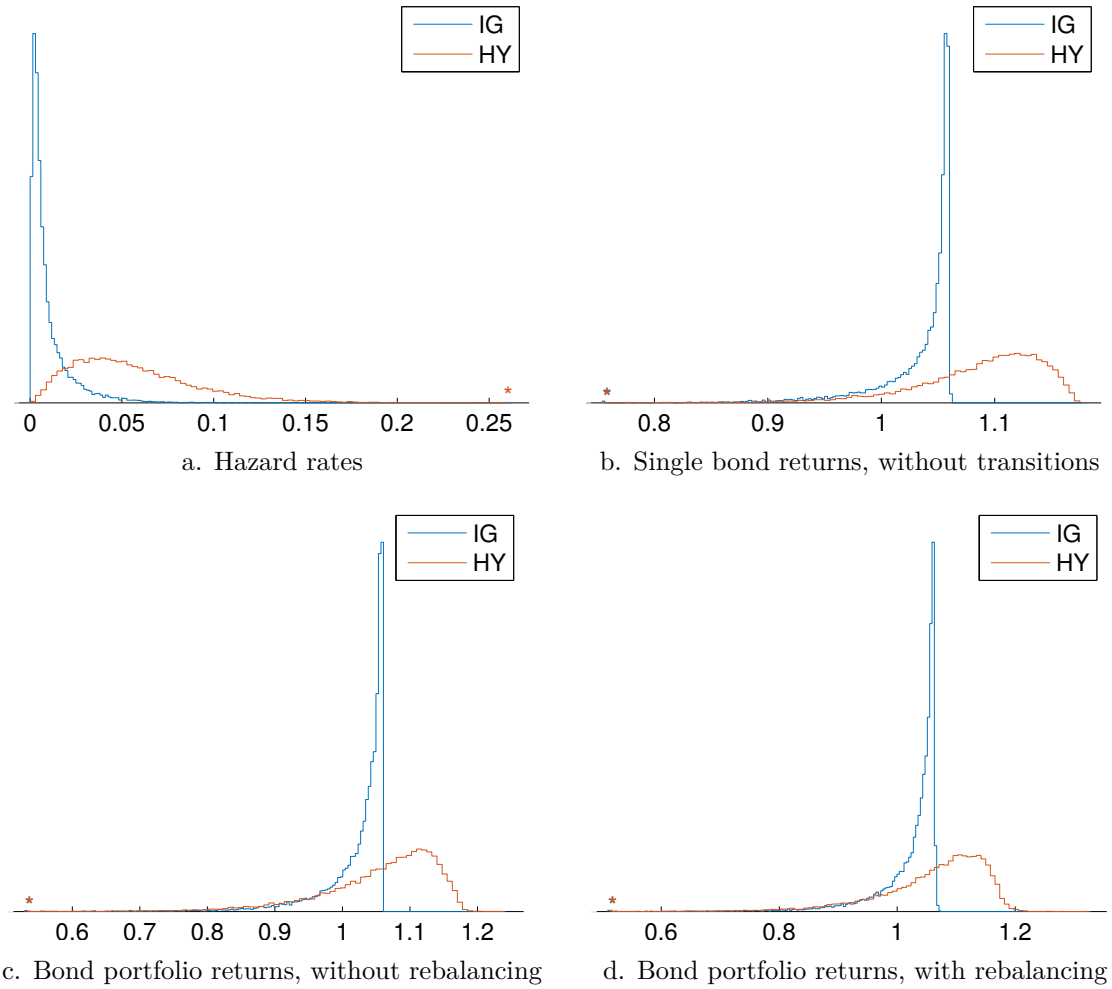

a. Hazard rates

b. Single bond returns, without transitions

c. Bond portfolio returns, without rebalancing

d. Bond portfolio returns, with rebalancing

Figure 5.2: Upper two subplots show histograms of hazard rates and single bond returns belonging to either rating class throughout the one-year risk horizon based on simulation of sample size $N = 20,000$, with parameters as in Table 5.3. Lower subplots show histograms of bond portfolio returns, with as well as without monthly rebalancing. The asterisks at the tails indicate histograms are truncated.

5.3.2 Dependence Structure Adjustments: Migration Copulas

We now turn to analysis of changes to the dependence structure. There are three primary tools with which we can control this: the parameter β affecting the relationship between stock index volatility and hazard rate processes; the weight w of stock index outcomes on migration dynamics as in Section 4.3.3; and the pairwise copula type describing the latter mechanism. Among these three, we investigate changes to the last two in this section and apply a means for systematically adjusting β in the next section. The analysis casts light on the sensitivity of the model to varying conditions, being interesting on its own, but further incentives for investigating the effects of such modifications are given by the analysis in Section 5.2, suggesting that model parameters and dependence specification can be determined quite widely while giving a reasonable account of reality.

There are also secondary parameters affecting dependence between equity and credit risk: the correlation parameter ρ between stock index and stock volatility Brownian mo-

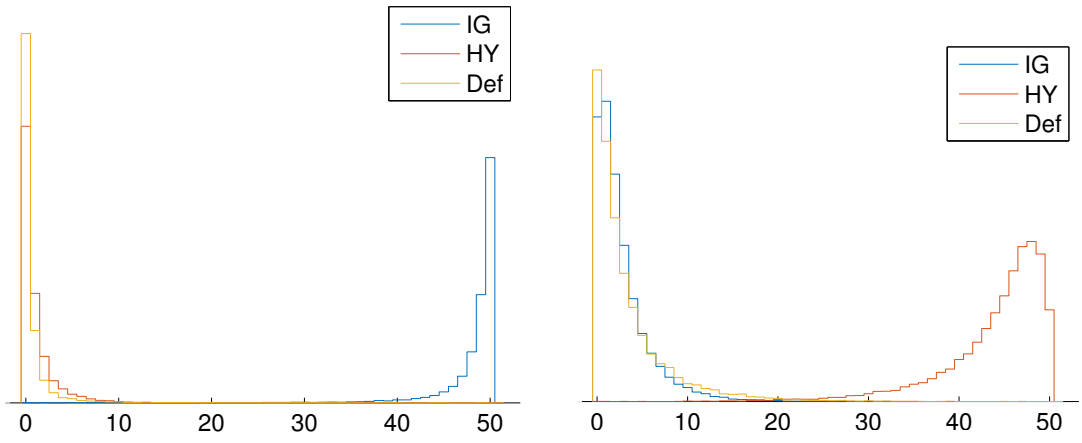

a. IG portfolio b. HY portfolio

Figure 5.3: Credit rating distributions for simulated samples of size $N = 20,000$ for IG and HY portfolios at the end of the one-year risk horizon.

tions; the amount of variance in stock index movements coming from stochastic volatility compared to the independent variance-gamma process; the time windows applied for simulating discrete-time migrations; the quantity pertaining to stock index movements upon which migration dynamics are conditioned. Of these, the first two are not adjusted since they fundamentally describe already matched stock index dynamics. We will briefly touch upon the last two in Appendix C.2 and Appendix C.3 respectively.

In the analysis, economic scenarios are simulated once with a sample size of $N = 20,000$. Looping through four different copula types, Gaussian, t_3, t_{10} and Clayton, as well as stock index migration weights in the range $0, 0.1, 0.2, \ldots, 1$, we simulate sets of independent portfolio evolution scenarios conditional on the set of economic scenarios. For the Clayton copula, weights w are transformed to a comparable Clayton parameter α as previously described. This is done for the rebalanced HY and IG portfolios, holding higher interest due to the index interpretation. Other parameters are held the same as previously.

Quantiles for the bond portfolios are calculated for each dependence specification at the 0.005 and 0.05 levels. These illustrate how the dependence in migration dynamics affects the riskiness of diversified bond portfolios. Furthermore, correlation and Kendall's tau are computed between stock index and bond portfolio returns, as well as tail index estimates at the 0.005 and 0.05 levels. Figures 5.4 and 5.5 depict how these measures vary as functions of copula and stock index transition weight for the IG and HY portfolios respectively.

Since all of the tested copulas coincide with the maximum copula for $w = 1$, where stock index returns perfectly predict the migration behaviour, diversification effects within bond portfolios are nullified at this extreme with all bonds within a rating class migrating simultaneously. This particularly affects the portfolio quantiles. At the other end of the spectrum where $w = 0$, Gaussian and Clayton copulas translate to independent migrations, whereas this is not the case for t copulas. This shines through in all of the plots, particularly for the heavier-tailed t_3 copula producing results deviating from those of other copulas at low stock index transition weights.

The significant lower tail dependence associated with a Clayton copula with parameter $\alpha > 0$ (equivalent to $w > 0$) also clearly emerges in the lower quantile plots, surpassing

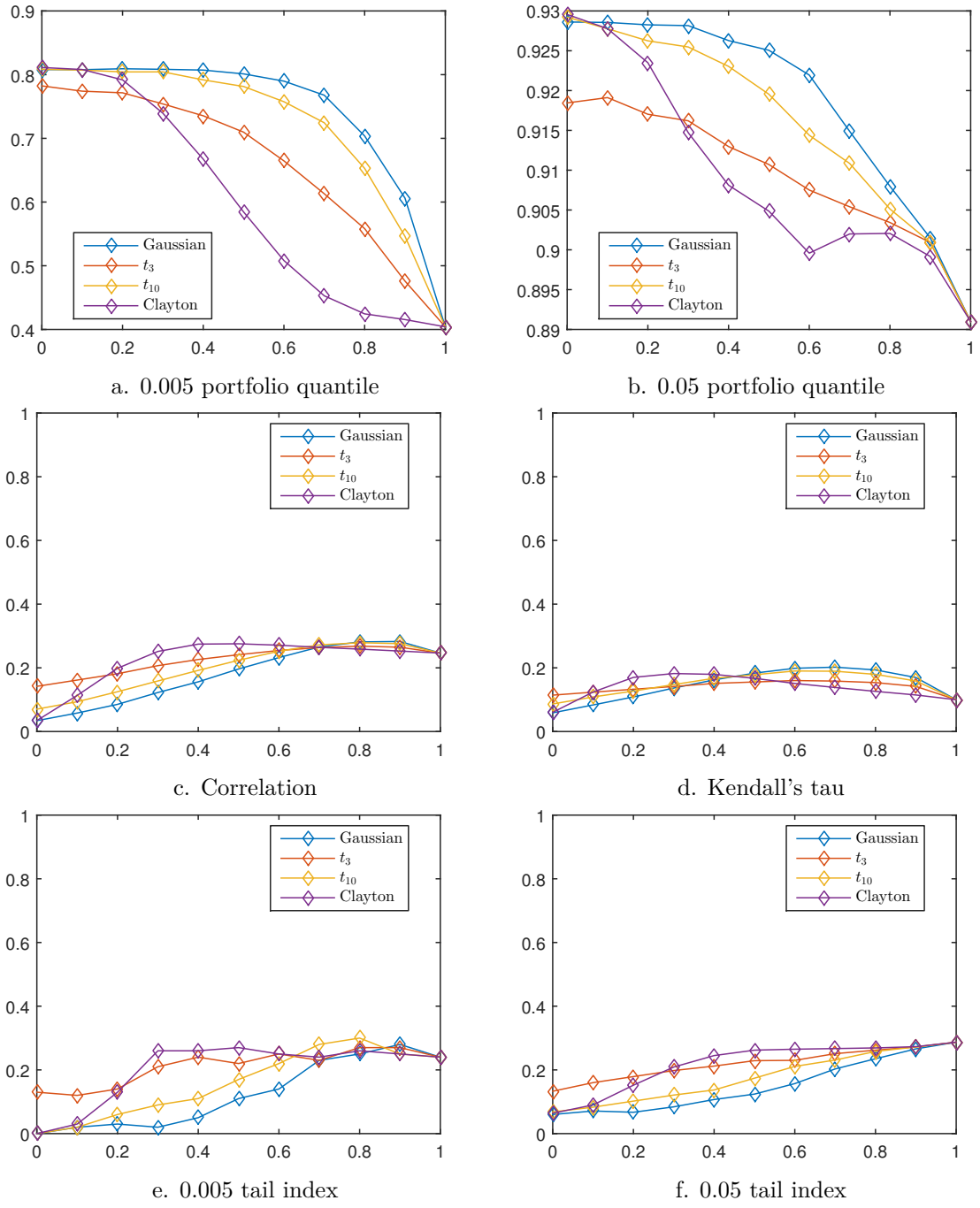

a. 0.005 portfolio quantile

b. 0.05 portfolio quantile

c. Correlation

d. Kendall's tau

e. 0.005 tail index

f. 0.05 tail index

Figure 5.4: Quantiles and dependence measures for the IG bond portfolio with monthly rebalancing, based on simulation of $N = 20,000$ economic scenarios with independent portfolio scenarios generated for each copula and stock index transition weight varying between 0 and 1 in steps of 0.1.

the t_3 copula in risk as w grows. Conversely, a Gaussian copula means a weak dependence between bonds for fixed $w < 1$ compared to other copulas, resulting in higher portfolio quantile values at the low percentages.

Turning to plots of empirical dependence measures between stock index and bond portfolios, the effect of the choice of copula family and parameter is both less obvious and

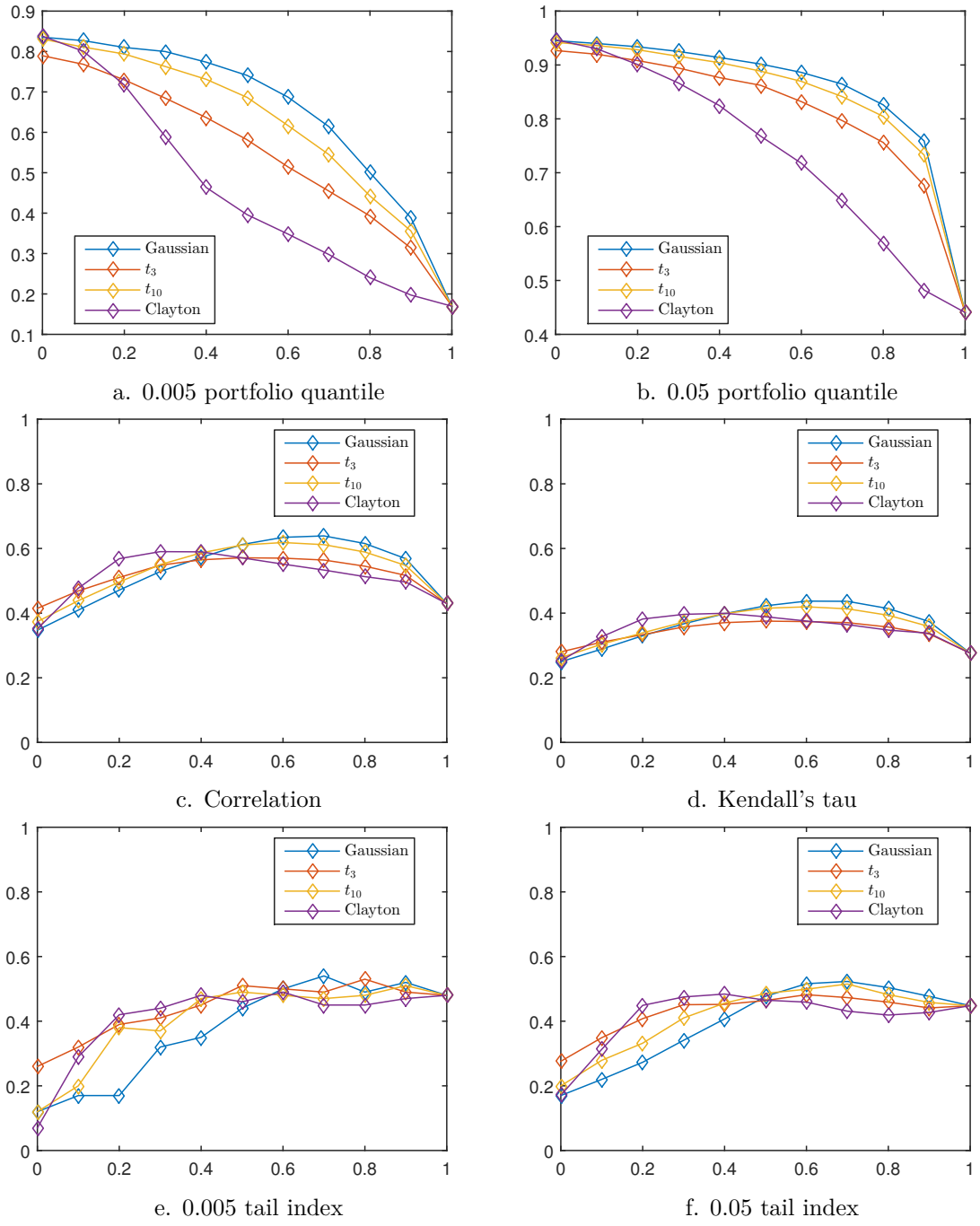

a. 0.005 portfolio quantile

b. 0.05 portfolio quantile

c. Correlation

d. Kendall's tau

e. 0.005 tail index

f. 0.05 tail index

Figure 5.5: Quantiles and dependence measures for the HY bond portfolio with monthly rebalancing, based on simulation of $N = 20,000$ economic scenarios with independent portfolio scenarios generated for each copula and stock index transition weight varying between 0 and 1 in steps of 0.1.

less decisive. The figures suggest an increase in the weight is not promptly followed by amplified dependence in future distributions, at least as indicated by the applied measures. If anything, the extent of dependence seems to peak midway through as w increases, where a flattening out or even slight diminution results as migration dependence approaches its maximum. For low values of w, t copulas induce the strongest dependence. In this regime,

the dependence induced by a Clayton copula rises sharply with w to overtake that of a t_3 copula, attaining its peak at an early stage. Correlation and Kendall's tau then appear to decrease, whereas tail index estimates at the investigated levels stabilize.

Applying a Gaussian copula for migrations, the increase in dependence between stock index and bond portfolios develops more slowly with w than what is the case for the Clayton copula. At high w, correlation, Kendall's tau and tail index estimate become on par with or exceed values observed for the other copula families.

For a more informative illustration of the shape of the dependence between stock index and bond portfolio distributions resulting from different copula specifications for the simulation of migrations, scatter plots of stock index/rebalanced HY portfolio return pairs are shown in Figure 5.6. For brevity, the first 2000 simulated pairs are used for each copula specification, and t_{10} values are omitted. The figure sheds light on why an increase in w is not necessarily equivalent to an increase of one-dimensional correlation or concordance measures. The strength of dependence that can be produced by application of migration dynamics alone is capped by the specification for the stochastic processes, and what happens as copulas for credit migrations approach the maximum copula is that more bonds in the portfolio share credit migration histories along sample paths. There are factors fundamentally limiting the dependence across equity and debt markets over the risk horizon; monthly credit migrations matrices being tuned after movements of hazard rates, imperfectly related to stock index movements; and stock index returns being sampled on a monthly basis for the mapping of migrations, whereby movements spanning the full risk horizon might not be fully reflected in the migration behaviour. Further clarification on the latter is given in Appendix C.2, where we analyse the behaviour of returns when migration time windows are set to span the full risk horizon.

For another look at the behaviour in the tails, histograms of HY bond portfolio returns conditional on stock index returns belonging to the same risk scenario falling below the estimated 0.05 quantile are found in Figure 5.7, with the same model dependence specifications illustrated as in the aforementioned scatter plots. Although empirical tail index estimates between stock index returns and bond portfolio returns may only differ slightly and in ways that are difficult to forecast between different copula choices, the shape of the conditional marginal bond portfolio distribution when the stock index fares poorly develops more predictably with the chosen dependence structure, just like the bond portfolio quantiles. As indicated in both scatter plots and histograms, clustering of defaults occurs more frequently when a Clayton copula is used compared to other types at matching values of w, explained, for example, by the higher observed frequencies around the fractional recovery payment of 0.4 in subfigures 5.7d and 5.7e.

Similar scatter plots and histograms focusing on the IG portfolio do not provide much additional insight, but are presented in Appendix C.1 for completeness.

Returning to Figures 5.4 and 5.5 for a comparison of IG and HY portfolio plots, the influence of β_m on dependence between stock index returns and bond portfolio returns becomes evident. Recalling Table 5.3, this parameter is set such that the stock index volatility process strongly contributes to the HY hazard rate process while its impact is weaker on the IG default intensity. High values of β_m seem to strongly affect the measured dependence across all investigated copulas, yielding elevated values of estimators. We elaborate on this in the subsequent section.

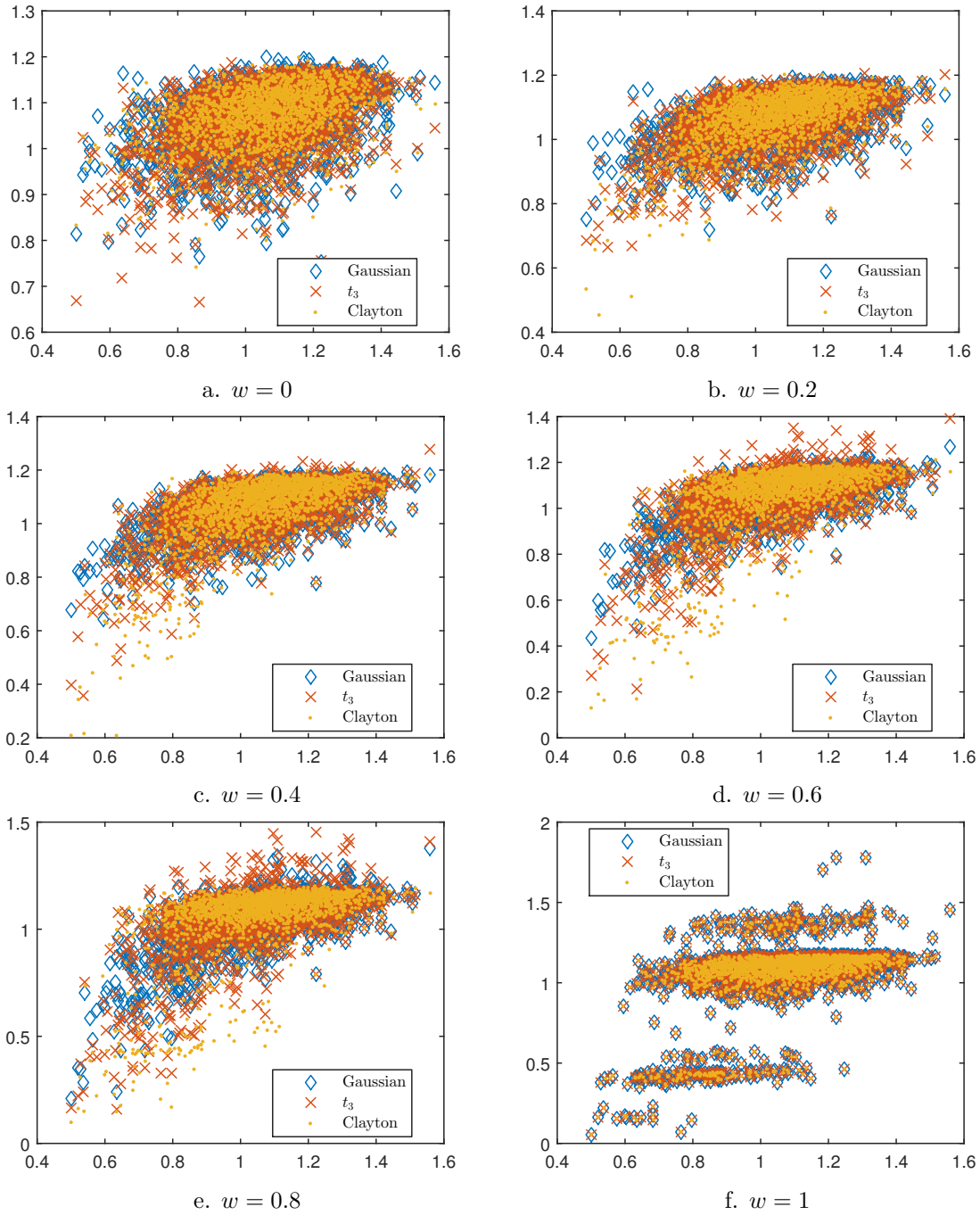

a. $w = 0$ b. $w = 0.2$

c. $w = 0.4$ d. $w = 0.6$

e. $w = 0.8$ f. $w = 1$

Figure 5.6: Scatter plots for one-year stock index returns and rebalanced HY portfolio returns, applying different copulas and weights w for the migration simulation. The first 2000 simulated observations of each pair of stock index returns/bond portfolio returns from the total sample of $N = 20,000$ bivariate returns per copula are depicted.

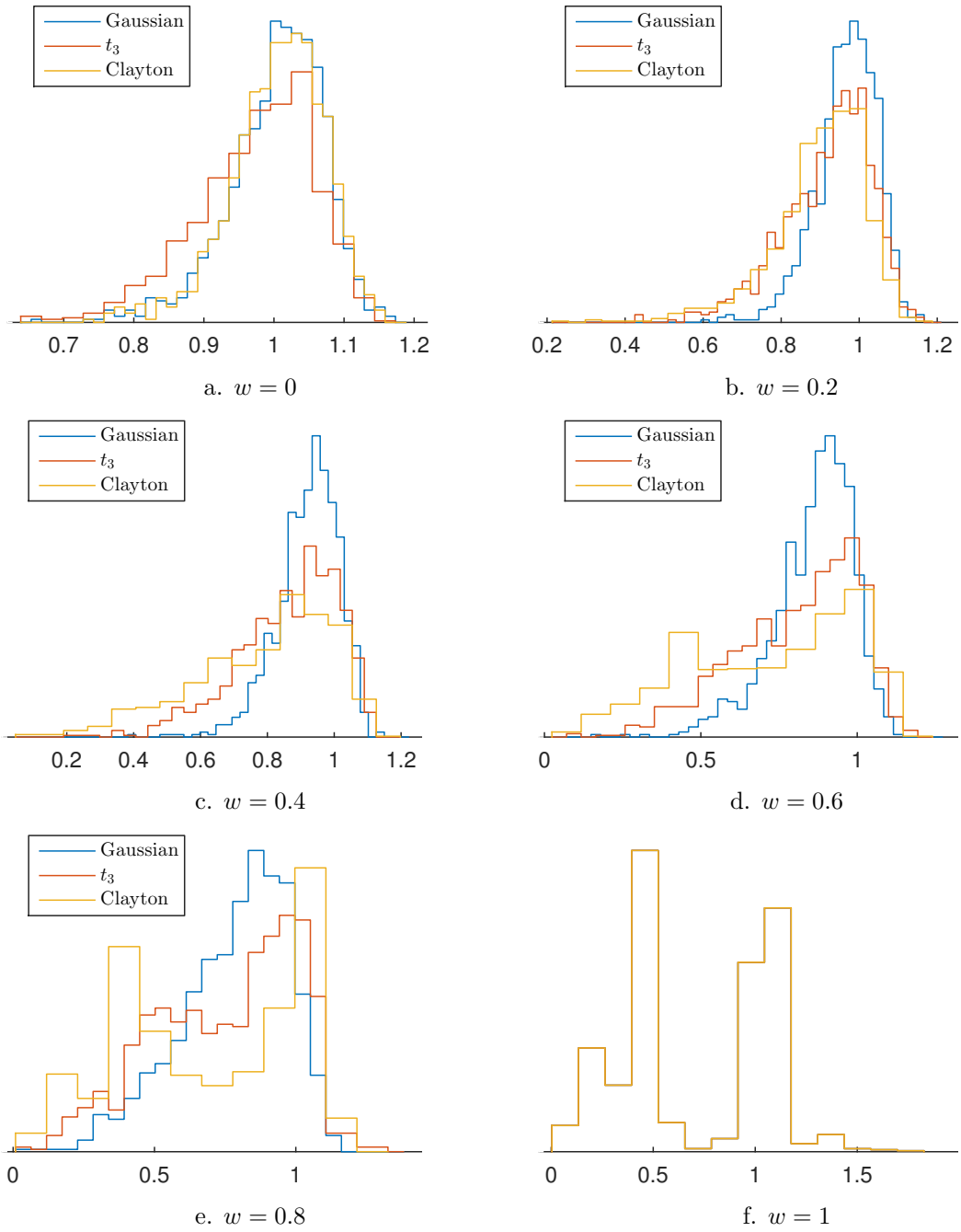

Figure 5.7: Histograms of simulated rebalanced HY portfolio returns conditional on stock index returns falling below its estimated 0.05 quantile value, where bond credit migration dynamics are connected to stock index returns through different copulas with weight w. For $w = 1$, the maximum copula is used.

5.3.3 Dependence Structure Adjustments: Variation of β

In addition to dependence modelled through the weight w of the stock index on transition dynamics and the choice of copula, we also investigate how variations to the parameter $\beta = (\beta_1,\ \beta_2)$ affect portfolio risk and dependence measures between stock index and bond portfolio. We here restrict attention to the high yield index, whose return dynamics are richer and where the pricing error appears smaller than for its investment grade counterpart.

In order to vary β while retaining both initial values and long term expectations of hazard rates, we scale the parameters of the excess default intensity processes z_t^i accordingly. We further reduce the degrees of freedom of the system by putting restrictions on the parameters. The expected bond portfolio returns are governed by market price of risk of the stock volatility process, so that levels and higher moments of returns are sidelined in favour of a focused review of the dependence structure. A description of the details of the method applied for the parameter adjustments is available in Appendix A.

We cycle through n sets of values of β, such that

$$\beta^{(i)} = h_i \beta^{\max}, \qquad h_i = \frac{i-1}{n-1}, \qquad i = 1, \ldots, n,$$

where $\beta^{\max}$ corresponds to the case

$$\lambda_t^m = \beta_m^{\max} v_t.$$

For each β, we simulate a sample of size $N = 20,000$ of economic scenarios. Like previously, portfolio scenarios are appended to each economic scenario, where we let transition dynamics be related to monthly stock index returns through the use of different bivariate copulas with weights varying from 0 to 1 in steps of 0.1. We focus on the bond index representation of the portfolio, i.e. with rebalancing to the original composition at the start of each new month.

For the simulation, we use $n = 5$ different sets of values for β. We further try out three different copulas, Gaussian, t_3 and Clayton for mapping of migrations following Sections 4.3.3 and 4.3.4. Stock and volatility parameters are held the same as previously, along with discretization parameters and the real-world baseline intensity matrix. Regarding excess hazard rate parameters, we replace κ_1, θ_1, κ_2 and θ_2 in Table 5.3 by $\bar{\kappa}_1$, $\bar{\theta}_1$, $\bar{\kappa}_2$ and $\bar{\theta}_2$ serving as baseline parameters which are rescaled in each β case. Other CIR parameters, as well as initial values for the excess hazard rate processes, are derived for each case following Appendix A.

In Figure 5.8, we plot correlation, Kendall's tau, and tail index estimates at the 0.005 and 0.05 levels between stock index returns and HY portfolio returns as functions of copula and β setting. As was noted in the previous section, most of the dependence measures experience a significant upward shift with increased influence of the stock volatility process on hazard rates, and this effect permeates all copula specifications. The only exception, providing less conclusive evidence, is the 0.005 tail index. Here, uncertainties arising from small effective sample size (100 per dependence specification) give rise to somewhat distorted results. As for the variation of dependence measures with migration weights, we observe similar effects as in the previous section with a peak occurring somewhere midway through the spectrum for every copula type, β case and estimated measure, followed by constancy to a mild decline as migration copula dependence approaches its maximum.

Figure 5.9 shows how bond portfolio quantiles at the 0.005 and 0.05 levels vary with the choice of β and with the copula. Differences in β result in a spread of quantile estimates, where higher dependence through β implies lower values. While this spread is tangible,

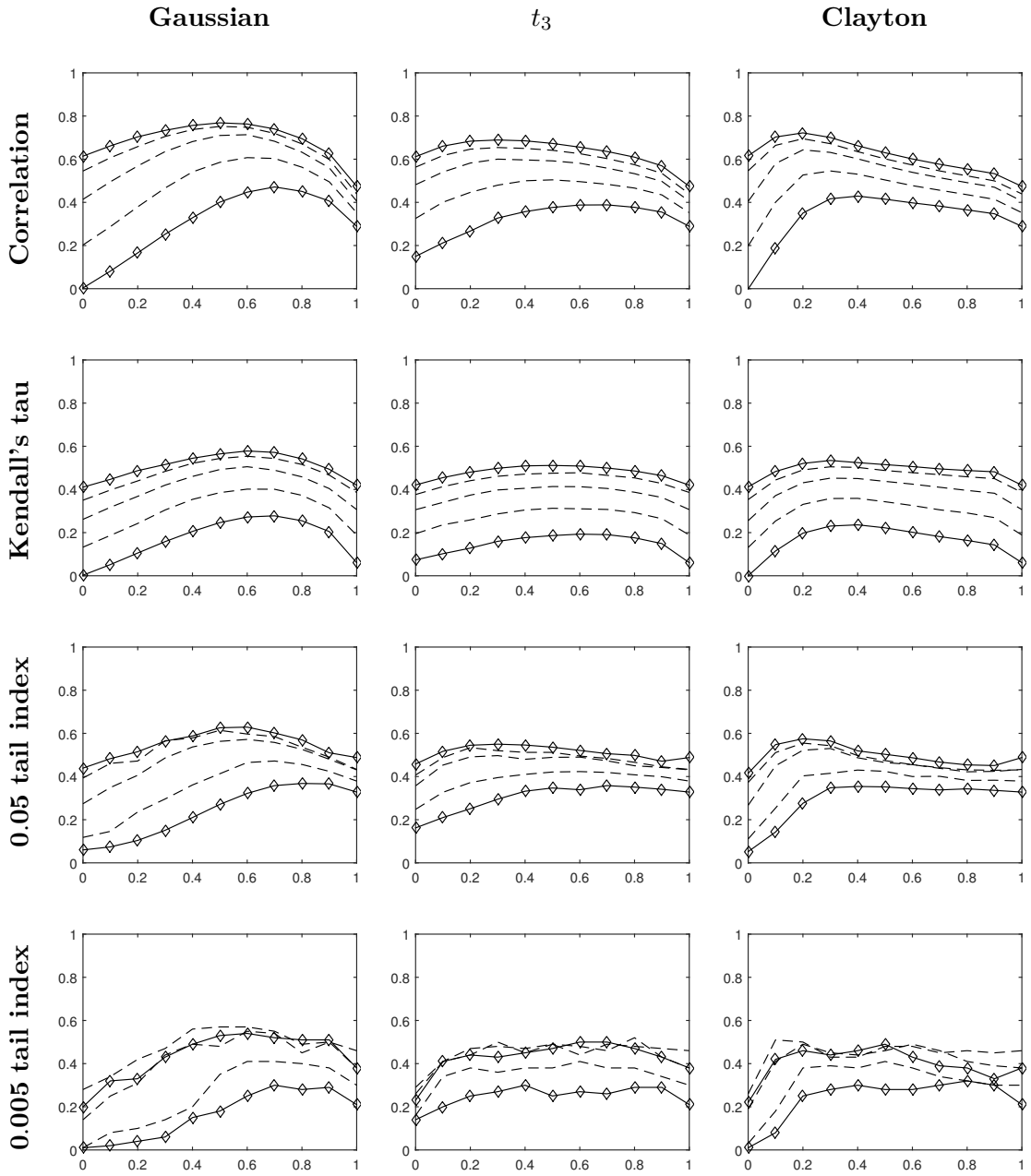

Figure 5.8: Empirical estimates of dependence measures between one-year stock index returns and HY rebalanced bond portfolio returns, against different values of the weight w of monthly stock index returns on bond rating migrations on horizontal axes, linked with different copula types. In each subplot, the uppermost, solid lines correspond to the case $\beta = \beta^{\max}$, whereas the lowermost, solid lines correspond to $\beta = \beta^{\min}$. Dashed lines represent results from intermediate cases.

reflecting differences in the lower tail behaviour of bond portfolios, the gist of the effect is still controlled by the choice of copula.

The 0.05 quantile displays a large gap depending on how β is set when the maximum

copula is applied for migrations. For the minimum β case, the quantile value is not only significantly larger than for the other cases investigated, but also exceeds estimated values at the same level of β when weaker copulas are applied. A model peculiarity when the maximum copula is used is highlighted. The low quantile values observed result from a simultaneous default of all firms involved in the portfolio in at least one of the migration time windows, occurring in at least 5% of the simulated scenarios. For the minimum β case, this happens less than 5% of the time, such that the 0.05 quantile reflects a scenario where there is not a single default during the risk horizon. An illustration is given in Figure 5.10, showing the percentage of cases where all bonds in the portfolio experience simultaneous default during the risk horizon as a function of β case. This is an increasing function, reflecting how higher β values entail hazard rates and stock index move in opposite directions more frequently (due to the negative correlation between stock index and volatility Brownian motions), resulting in transition matrices being more likely to have large migration probabilities when there are negative stock index movements.

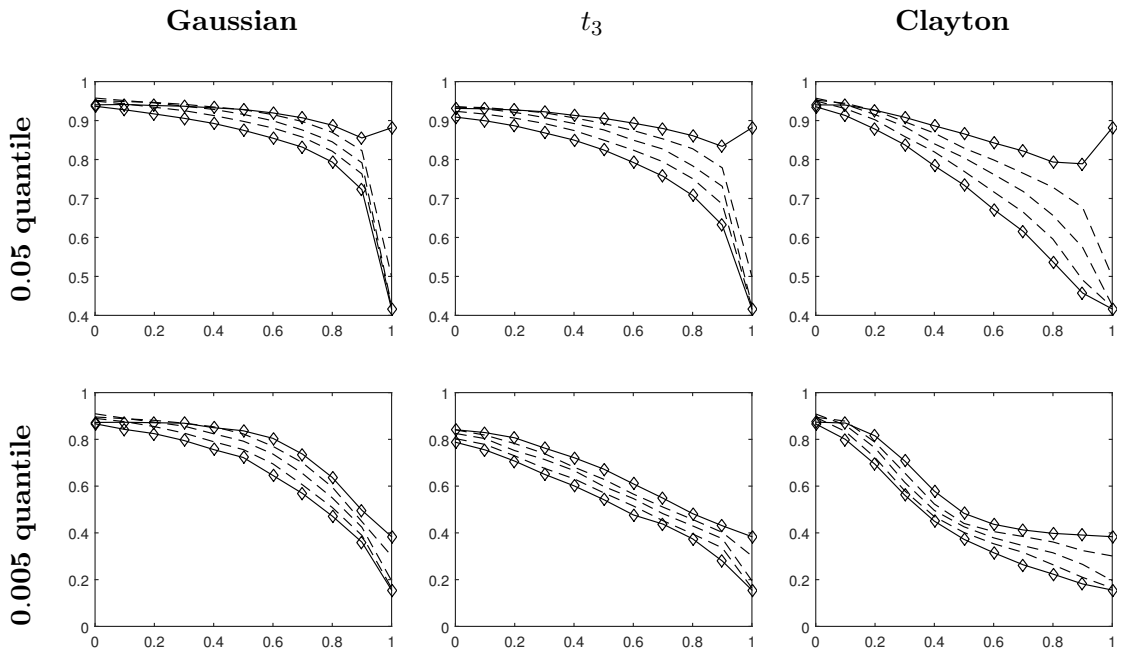

Figure 5.9: Estimated quantiles for one-year rebalanced HY portfolio returns against different values of the weight w of monthly stock index returns on bond rating migrations on horizontal axes, linked with different copulas. In each subplot, the uppermost, solid lines correspond to the case $\beta = \beta^{\min}$, whereas the lowermost, solid lines correspond to $\beta = \beta^{\max}$. Dashed lines represent results from intermediate cases.

It is worth noting that the model, with fixed secondary parameters as mentioned in the introductory paragraph of Section 5.3.2, can only produce so much dependence between stock index and bond portfolio returns. Even the maximum β case, where hazard rate movements are perfectly correlated with the stock volatility process, is incapable of producing dependence above a certain threshold lying well below the maximum in spite of the imposition of dependent credit rating migrations.

For another visualization of how different values of β and the copula specification

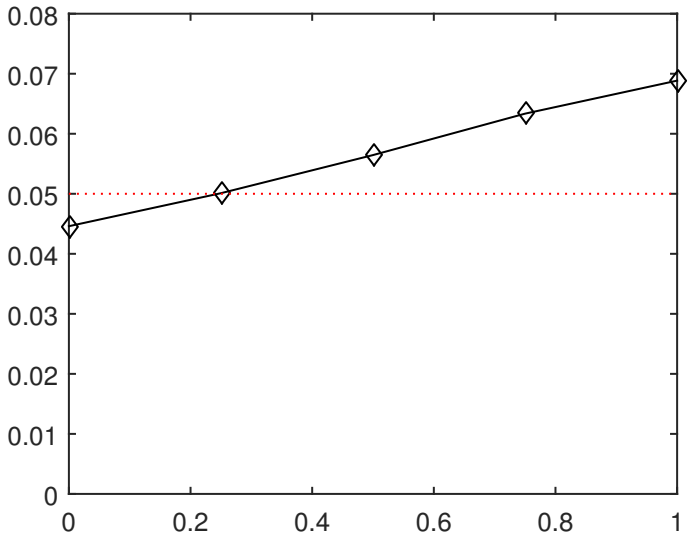

Figure 5.10: Fractions of simulated scenarios where all bonds in the rebalanced HY portfolio with migrations related to monthly stock index returns via the maximum copula default simultaneously at least once during the risk horizon, as a function of h where $\beta = h\beta^{\max}$. The dashed red line corresponds to a level of 5%.

affect the bivariate distribution of stock index/bond portfolio returns, we develop scatter plots of the first $2,000$ return pairs in each sample and display the cases of minimum β, intermediate β and maximum β and similarly for copula weights, displayed in Figure 5.11. The higher overall dependence with higher β is particularly well captured by the plots, while the impact of the copula choice for migrations on the shape of the distribution shines through in similar fashion as discussed in Section 5.3.2.

In Table 5.7, we present empirical correlation and Kendall's tau estimates between stock index returns and bond portfolio returns for a few different choices of β and copula. Table 5.8 further shows tail index estimates at levels 0.005 and 0.05 for the corresponding dependence specifications. The latter table also makes use of the estimates in the first one and constructs 95% confidence intervals for tail index estimates under the hypothesis that the return pairs have tails on par with a bivariate random variable with a Gaussian copula. That is, for given parameter specification and simulated sample of size N of stock index/bond portfolio return pairs, the correlation estimate $\hat{\rho}$ is used to construct confidence intervals for tail index estimators based on N draws from a bivariate standard normal random variable with correlation $\hat{\rho}$, proceeding as in Section 4.1.4. Also, using the Kendall's tau estimate $\hat{\tau}$, similar confidence intervals are constructed replacing $\hat{\rho}$ by $\sin(\hat{\tau}/2)$, being a valid and preferred approach when bivariate data represents independent outcomes of a bivariate random variable with elliptical distribution as mentioned in Section 2.3.1.

The purpose of Table 5.8 is to get an idea of how strong the model implied lower tail dependence is, given model implied correlation or Kendall's tau, for different parameter specifications. A comparison to standard normal tail dependence can provide clues as to whether return pairs have lower tail dependence or not, and also give an idea of the strength of lower tail dependence in case it exists. The table indicates the model tends to produce return pairs having lower tail dependence for a wide variety of different dependence specifications. A number of observations:

- Applying the independence copula (Gaussian or Clayton at $w = 0$) for migrations,

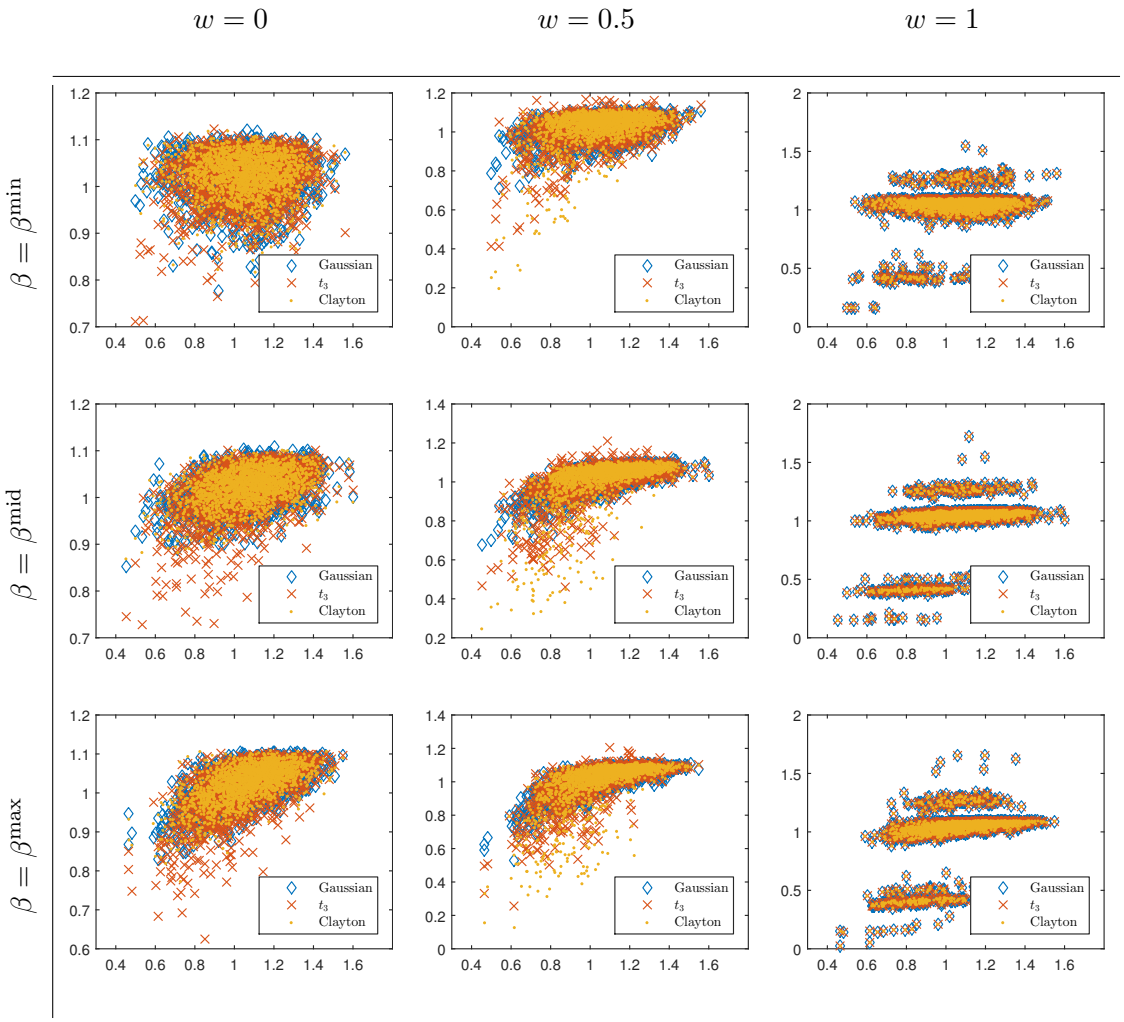

Figure 5.11: Scatter plots of 2000 simulated stock returns and corresponding simulated rebalanced HY portfolio returns where transition dynamics are given by different copulas. Different sets of values of β are used, where $\beta^{\mathrm{mid}} = \beta^{\max}/2$.

there is possible lower tail dependence produced as β increases. The tendency is weak, though, and in particular for the case $\beta = \beta^{\max}$ we see that tail index estimates at the 0.005 level are not significantly different from bivariate normal. However, since they are at the 0.05 level, a likely reason for this is that sample sizes are simply too small, resulting in wide confidence intervals at low percentiles. When $\beta = \beta^{\min}$ and the independence copula is applied, stock index returns and bond portfolio returns appear independent, which is reasonable given the construction of the model.

- Applying a Gaussian copula for the simulation of migrations, the increase in correlation parameter w results in overall stronger dependence in return pairs for the cases listed in the table. Tail index estimates also increase at a similar rate as correlation and Kendall's tau do. For $w = 0.3$ and $w = 0.6$ lower tail dependence seems to prevail for all β cases, with the possible exception of $\beta = \beta^{\min}$ and $w = 0.3$.

- For the t_3 copula, with $w = 0$ dependence is present across all β specifications.

This also includes lower tail dependence, with the only question mark appearing at $\beta = \beta^{\max}$ as indicated in the 0.005 level entry, brushing the upper confidence bound for what the tail index estimator on matching bivariate normal data would yield. Again, since the 0.05 value is placed significantly outside the confidence interval, this is likely an effect of the sample size.

- When a t_3 copula with correlation parameter $w = 0.3$ is used, the overall tendency is that tail index estimates of return pairs are far stronger than for the Gaussian copula at $\beta = \beta^{\min}$, and roughly equal for the other β cases. The latter cases also display weaker correlation and Kendall's tau estimates, such that the strength of tail dependence is arguably higher. Applying $w = 0.6$ instead of 0.3 for the simulation of migrations seems to have a minor effect on dependence in return pairs as given by these measures.

- The dependence exhibited in return pairs, as conveyed by the listed measures, is stronger at $w = 0.3$ compared to at $w = 0.6$ with the use of a Clayton copula; a finding that holds in all β cases investigated. A disparity between $\hat{\rho}$ and linear correlation estimation through transformation of $\hat{\tau}$ arises with increasing β and w, where the latter technique gives higher values, as is seen by comparing levels of confidence intervals for the two methods. Using the latter becomes increasingly questionable due to the shape of the distribution of bivariate returns. Looking only at confidence intervals associated with tail index estimation for bivariate normals of correlation $\hat{\rho}$, lower tail dependence in return pairs resulting from migration modelling via a Clayton copula (assuming $w > 0$) does not differ greatly from that observed when a t_3 copula is applied.

- The effect of an increase of β from β^{mid} to $\beta^{\max}$ on tail indices is small for all copulas except those having $w = 0$ (looking at the 0.05 level). Meanwhile, this change in β leads to higher correlation and concordance across all copula specifications. It appears stronger tail dependence is therefore attained when β is not at its maximum.

		Gaussian		t_3		Clayton	
		$\hat{\rho}$	$\hat{\tau}$	$\hat{\rho}$	$\hat{\tau}$	$\hat{\rho}$	$\hat{\tau}$
$\beta = \beta^{\min}$	$w = 0$	0.00	0.00	0.15	0.07	−0.00	−0.00
	$w = 0.3$	0.25	0.16	0.33	0.16	0.42	0.23
	$w = 0.6$	0.45	0.27	0.39	0.19	0.40	0.20
$\beta = \beta^{\text{mid}}$	$w = 0$	0.41	0.26	0.48	0.31	0.40	0.26
	$w = 0.3$	0.64	0.42	0.60	0.40	0.63	0.45
	$w = 0.6$	0.71	0.51	0.58	0.41	0.54	0.42
$\beta = \beta^{\max}$	$w = 0$	0.61	0.41	0.61	0.42	0.62	0.41
	$w = 0.3$	0.73	0.52	0.69	0.50	0.70	0.53
	$w = 0.6$	0.76	0.58	0.66	0.51	0.60	0.51

Table 5.7: Empirically estimated linear correlations $\hat{\rho}$ and Kendall's tau $\hat{\tau}$ between simulated stock index and rebalanced HY bond portfolio one-year returns. Three different sets of values for β used, where $\beta^{\min} = 0$ and $\beta^{\text{mid}} = \beta^{\max}/2$, as well as three different copulas with weight w between stock index outcomes and rating migration dynamics.

Tail index estimates at $p = 0.005$

		Gaussian		t_3		Clayton	
		$\widehat{\lambda_{L,p}}$	Normal	$\widehat{\lambda_{L,p}}$	Normal	$\widehat{\lambda_{L,p}}$	Normal
$\beta = \beta^{\min}$	$w = 0$	0.01	[0.00, 0.02] [0.00, 0.02]	0.14	[0.00, 0.04] [0.00, 0.04]	0.01	[0.00, 0.02] [0.00, 0.02]
	$w = 0.3$	0.06	[0.00, 0.06] [0.00, 0.06]	0.27	[0.01, 0.09] [0.00, 0.06]	0.28	[0.02, 0.12] [0.01, 0.10]
	$w = 0.6$	0.25	[0.03, 0.13] [0.02, 0.12]	0.27	[0.02, 0.11] [0.01, 0.08]	0.28	[0.02, 0.11] [0.01, 0.08]
$\beta = \beta^{\text{mid}}$	$w = 0$	0.14	[0.02, 0.12] [0.02, 0.11]	0.26	[0.04, 0.15] [0.03, 0.14]	0.19	[0.02, 0.12] [0.02, 0.11]
	$w = 0.3$	0.44	[0.10, 0.25] [0.09, 0.24]	0.50	[0.09, 0.23] [0.08, 0.21]	0.45	[0.10, 0.25] [0.12, 0.27]
	$w = 0.6$	0.55	[0.16, 0.33] [0.16, 0.33]	0.48	[0.08, 0.21] [0.09, 0.23]	0.49	[0.06, 0.18] [0.10, 0.24]
$\beta = \beta^{\max}$	$w = 0$	0.20	[0.09, 0.24] [0.09, 0.23]	0.23	[0.09, 0.23] [0.09, 0.24]	0.22	[0.09, 0.24] [0.09, 0.23]
	$w = 0.3$	0.43	[0.18, 0.35] [0.17, 0.34]	0.43	[0.14, 0.30] [0.15, 0.32]	0.44	[0.15, 0.31] [0.19, 0.36]
	$w = 0.6$	0.54	[0.20, 0.38] [0.23, 0.42]	0.50	[0.12, 0.27] [0.16, 0.33]	0.43	[0.09, 0.23] [0.16, 0.33]

Tail index estimates at $p = 0.05$

		Gaussian		t_3		Clayton	
		$\widehat{\lambda_{L,p}}$	Normal	$\widehat{\lambda_{L,p}}$	Normal	$\widehat{\lambda_{L,p}}$	Normal
$\beta = \beta^{\min}$	$w = 0$	0.06	[0.04, 0.07] [0.04, 0.07]	0.16	[0.07, 0.11] [0.06, 0.10]	0.05	[0.04, 0.06] [0.04, 0.06]
	$w = 0.3$	0.15	[0.10, 0.14] [0.10, 0.14]	0.29	[0.13, 0.18] [0.10, 0.14]	0.35	[0.17, 0.22] [0.14, 0.19]
	$w = 0.6$	0.32	[0.19, 0.24] [0.17, 0.22]	0.34	[0.16, 0.21] [0.12, 0.16]	0.34	[0.16, 0.21] [0.13, 0.17]
$\beta = \beta^{\text{mid}}$	$w = 0$	0.27	[0.17, 0.22] [0.16, 0.21]	0.36	[0.21, 0.26] [0.20, 0.25]	0.27	[0.17, 0.22] [0.16, 0.21]
	$w = 0.3$	0.49	[0.31, 0.37] [0.29, 0.35]	0.50	[0.28, 0.34] [0.27, 0.33]	0.53	[0.30, 0.36] [0.32, 0.38]
	$w = 0.6$	0.57	[0.37, 0.44] [0.37, 0.44]	0.49	[0.27, 0.33] [0.28, 0.34]	0.46	[0.24, 0.30] [0.30, 0.35]
$\beta = \beta^{\max}$	$w = 0$	0.44	[0.29, 0.35] [0.28, 0.34]	0.46	[0.29, 0.35] [0.29, 0.35]	0.41	[0.29, 0.35] [0.28, 0.34]
	$w = 0.3$	0.56	[0.39, 0.45] [0.38, 0.45]	0.55	[0.35, 0.41] [0.37, 0.43]	0.56	[0.36, 0.42] [0.40, 0.47]
	$w = 0.6$	0.63	[0.42, 0.48] [0.45, 0.51]	0.52	[0.32, 0.38] [0.38, 0.44]	0.49	[0.28, 0.34] [0.37, 0.44]

Table 5.8: Tail index estimates between stock index returns and high yield bond index returns at $p = 0.005$ and $p = 0.05$ for simulated samples of size $N = 20,000$. Three different sets of values for β used as well as three different copulas with weight w between stock index outcomes and monthly rating migration dynamics. 95% confidence intervals for tail index estimators based on N independent outcomes a standard normal bivariate random variable, with correlation given by $\hat{\rho}$ (upper) and by $\sin((\pi/2)\hat{\tau})$ (lower), are calculated and presented alongside the tail index estimates.

5.3.4 Upper Tail Properties

As was noted in the final paragraph of Section 5.3.1, upper tail dependence in stock index/bond portfolio return pairs when simulation is carried out over a risk horizon with parameters as in Table 5.3 appears far weaker than the corresponding lower tail dependence. In this section, we investigate whether this observation remains under modifications to the dependence structure. We use the previously generated samples for different migration copulas and values of β, and focus on tail index estimates at the 0.95 and 0.995 levels, where effective sample sizes are 1000 and 100 respectively.

In Figure 5.12, upper tail index estimates are plotted as functions of dependence setting. Clearly, the previous observation is reinforced, with upper tail indices being remarkably low across all dependence settings, especially at the 0.995 level, which suggests absence of tail dependence in the theoretical sense of Section 2.3.3. At the 0.95 level, the choice of β in particular affects index estimates with values increasing with β. However, as correlation and concordance in return pairs also appears to grow monotonously with β, it is not fully clear how β affects the tail dependence when seen in conjunction with the return correlation.

Another clue to the tendency of weak upper tail dependence is provided from a glance back at Figure 5.11, in particular looking at the maximum copula scatter plots. The most extreme yearly positive stock index outcomes, more often than not, are accompanied with HY bond portfolio returns that do not stand out in any noticeable way.

Further establishing the above, Table 5.9 presents upper tail index estimates for various cases and compares to the values a bivariate normal variable with matching correlation/Kendall's tau would be expected to give. Here, the absence of upper tail dependence is indisputable, where the convergence of the tail index $\lambda_{U,p}$ to zero as $p \uparrow 1$ appears to occur significantly faster than that which is the case for the bivariate normal variable. We also note that, if anything, the gap between upper tail index estimates and corresponding bivariate normal confidence intervals at matching correlation/concordance seems to widen slightly with increasing β.

Part of the explanation for this consistently recurring asymmetry between lower and upper bivariate tails, as it seems regardless of choice of copula for mapping of migrations, lies in the numerical adjustment method used for constructing path-dependent migration matrices. In times of low hazard rates, *all* transition intensities are scaled down, tuning down the probability of positive credit rating change. Unless β is at its minimum case, positive stock movements are more likely to accompany low hazard rates, leading to overall lower rating migration probabilities and vice versa. However, since upper tail dependence is consistently low even for $\beta = \beta^{\min}$, often falling short of what is expected from a bivariate normal random variable, the adjustment method alone can not explain the tendency. Another reason likely originates in how tail index estimates are calculated and how migrations affect the return distribution. For a HY bond, an upward migration has a much smaller effect on the portfolio value than what does a default event. When extreme stock index returns spread to the bond portfolio in the form of multiple migrations, a much stronger impact is exerted on empirical dependence measures when defaults occur than when rating upgrades do.

The question is then whether the effect persists as strongly for the IG portfolio. For an IG bond, a simultaneous downscale of all migration probabilities means that the bond is more likely to preserve its high credit quality. The results of this analysis are left out of this section and instead presented in Appendix C.1.2, but the conclusion is that upper tail dependence is absent across all dependence specifications here as well, also appearing weaker than a bivariate variable with Gaussian copula, but less convincingly so than for

the HY portfolio.

To conclude this section, we note that at the process level, dependence between hazard rates and stock index is fundamentally limited to a Gaussian structure, the way stock index is linked to its volatility. With the addition of jumps, the dependence is diluted, and particularly so in the tails with large stock index movements coming from jumps having no effect on hazard rates. When migration dynamics are imposed, the dependence is strengthened between stock index and bond movements, but the effect mostly shows in the lower tail since downward migrations have stronger impact on returns than upward migrations for the HY portfolio, whereas for the IG portfolio only downward migrations are possible. This explains why both portfolios display lack of upper tail dependence with the stock index, converging to zero seemingly faster than a bivariate normal variable of matching correlation.

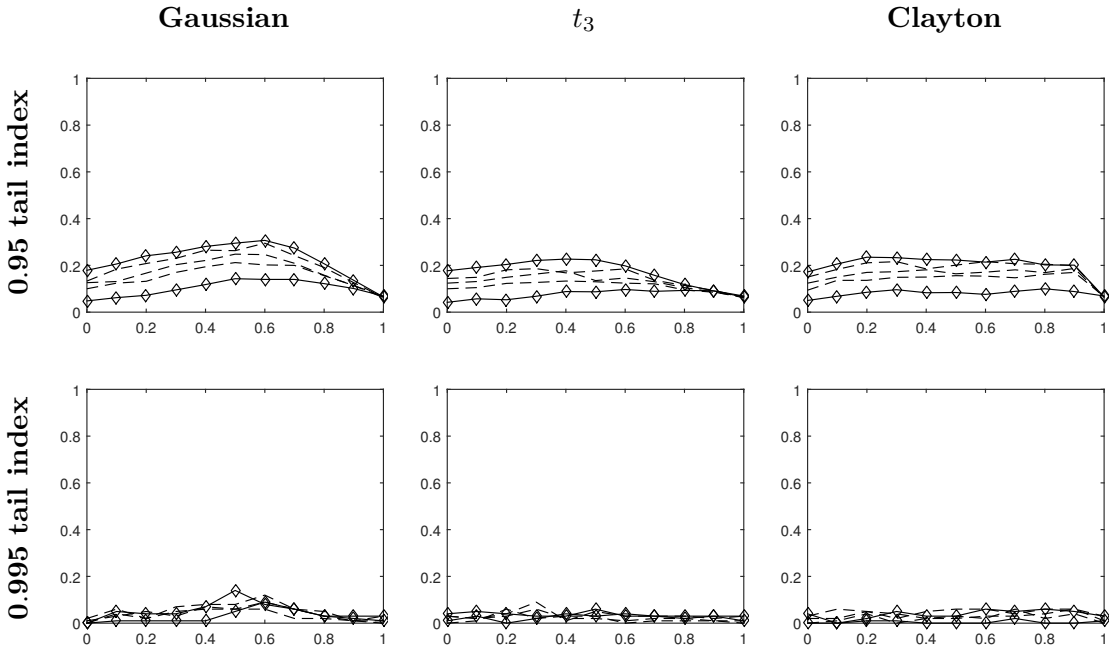

Figure 5.12: Estimated upper tail indices at the 0.95 and 0.995 levels between stock index returns and rebalanced HY bond portfolio returns over an investigated one-year horizon, as functions of β case and copula with weight w on the horizontal axis. Different lines correspond to different β cases, solid lines representing the minimum and maximum case respectively, while dashed lines map to intermediate cases. At the 0.95 level, the lowermost lines illustrate the case $\beta = \beta^{\min}$, moving upward for increasing β.

Tail index estimates at $p = 0.95$

		Gaussian		t_3		Clayton	
		$\widehat{\lambda_{U,p}}$	Normal	$\widehat{\lambda_{U,p}}$	Normal	$\widehat{\lambda_{U,p}}$	Normal
$\beta = \beta^{\min}$	$w = 0$	0.05	[0.04, 0.07] [0.04, 0.07]	0.04	[0.07, 0.11] [0.06, 0.10]	0.05	[0.04, 0.06] [0.04, 0.06]
	$w = 0.3$	0.10	[0.10, 0.14] [0.10, 0.14]	0.07	[0.13, 0.18] [0.10, 0.14]	0.10	[0.17, 0.22] [0.14, 0.19]
	$w = 0.6$	0.14	[0.19, 0.24] [0.17, 0.22]	0.10	[0.16, 0.21] [0.12, 0.16]	0.08	[0.16, 0.21] [0.13, 0.17]
$\beta = \beta^{\text{mid}}$	$w = 0$	0.13	[0.17, 0.22] [0.16, 0.21]	0.12	[0.21, 0.26] [0.20, 0.25]	0.12	[0.17, 0.22] [0.16, 0.21]
	$w = 0.3$	0.20	[0.31, 0.37] [0.29, 0.35]	0.16	[0.28, 0.34] [0.27, 0.33]	0.17	[0.30, 0.36] [0.32, 0.38]
	$w = 0.6$	0.25	[0.37, 0.44] [0.37, 0.44]	0.15	[0.27, 0.33] [0.28, 0.34]	0.17	[0.24, 0.30] [0.30, 0.35]
$\beta = \beta^{\max}$	$w = 0$	0.18	[0.29, 0.35] [0.28, 0.34]	0.18	[0.29, 0.35] [0.29, 0.35]	0.17	[0.29, 0.35] [0.28, 0.34]
	$w = 0.3$	0.26	[0.39, 0.45] [0.38, 0.45]	0.22	[0.35, 0.41] [0.37, 0.43]	0.23	[0.36, 0.42] [0.40, 0.47]
	$w = 0.6$	0.31	[0.42, 0.48] [0.45, 0.51]	0.20	[0.32, 0.38] [0.38, 0.44]	0.21	[0.28, 0.34] [0.37, 0.44]

Tail index estimates at $p = 0.995$

		Gaussian		t_3		Clayton	
		$\widehat{\lambda_{U,p}}$	Normal	$\widehat{\lambda_{U,p}}$	Normal	$\widehat{\lambda_{U,p}}$	Normal
$\beta = \beta^{\min}$	$w = 0$	0.00	[0.00, 0.02] [0.00, 0.02]	0.01	[0.00, 0.04] [0.00, 0.04]	0.00	[0.00, 0.02] [0.00, 0.02]
	$w = 0.3$	0.01	[0.00, 0.06] [0.00, 0.06]	0.02	[0.01, 0.09] [0.00, 0.06]	0.01	[0.02, 0.12] [0.01, 0.10]
	$w = 0.6$	0.09	[0.03, 0.13] [0.02, 0.12]	0.04	[0.02, 0.11] [0.01, 0.08]	0.00	[0.02, 0.11] [0.01, 0.08]
$\beta = \beta^{\text{mid}}$	$w = 0$	0.01	[0.02, 0.12] [0.02, 0.11]	0.00	[0.04, 0.15] [0.03, 0.14]	0.00	[0.02, 0.12] [0.02, 0.11]
	$w = 0.3$	0.03	[0.10, 0.25] [0.09, 0.24]	0.02	[0.09, 0.23] [0.08, 0.21]	0.00	[0.10, 0.25] [0.12, 0.27]
	$w = 0.6$	0.06	[0.16, 0.33] [0.16, 0.33]	0.00	[0.08, 0.21] [0.09, 0.23]	0.03	[0.06, 0.18] [0.10, 0.24]
$\beta = \beta^{\max}$	$w = 0$	0.00	[0.09, 0.24] [0.09, 0.23]	0.04	[0.09, 0.23] [0.09, 0.24]	0.04	[0.09, 0.24] [0.09, 0.23]
	$w = 0.3$	0.04	[0.18, 0.35] [0.17, 0.34]	0.03	[0.14, 0.30] [0.15, 0.32]	0.05	[0.15, 0.31] [0.19, 0.36]
	$w = 0.6$	0.08	[0.20, 0.38] [0.23, 0.42]	0.03	[0.12, 0.27] [0.16, 0.33]	0.06	[0.09, 0.23] [0.16, 0.33]

Table 5.9: Tail index estimates between stock index returns and high yield bond index returns at $p = 0.95$ and $p = 0.995$ for simulated samples of size $N = 20,000$. Three different sets of values for β used as well as three different copulas with weight w between stock index outcomes and monthly rating migration dynamics. 95% confidence intervals for tail index estimators based on N independent outcomes a standard normal bivariate random variable, with correlation given by $\hat{\rho}$ (upper) and by $\sin((\pi/2)\hat{\tau})$ (lower) taken from Table 5.7, are calculated and presented alongside the tail index estimates.

Chapter 6

Discussion and Conclusions

In this final chapter, we evaluate the model and further discuss the most important findings of Chapter 5. Section 6.1 summarizes the findings while Section 6.2 highlights strengths and shortcomings of the model as well as reviewing and discussing the simplifications used in the work. In Section 6.3, objectives stated in Section 1.2 are followed up, leading up to a number of suggestions for future work listed in Section 6.4. Section 6.5 concludes the thesis.

6.1 Summary of Findings

We here briefly review the most important findings of the previous chapter.

Based on the analysis of observed market data, it is reasonable to assume there exist positive co-movements between equity and debt markets just like previous studies on the subject have deduced. Looking at the evolutions of stock index as well as investment grade and high yield bond ETFs, the tendency is particularly striking as concerns dependence between stock index and high yield ETF, highlighted in Table 5.1. Due to scarcity of data, it is difficult to draw profound conclusions on tail dependence between monthly movements of stock index and bond ETFs.

As for the model, it appears to be able to provide a reasonable fit to observed data. The high number of model parameters can be specified rather widely while admitting simulated monthly returns to exhibit similar distributional characteristics as those observed in markets. One aspect that by trial and error proved rather difficult to capture with consistency was the high dependence between stock index and high yield index, while simultaneously maintaining the rather low observed dependence between stock index and investment grade index. It should be stressed the trial and error method applied here serves as a means to render a coarse fit to reality, whereas a more involved calibration and model validation method could likely be useful to more accurately evaluate the adequacy of the model. This would also require that interest rates be modelled, which they are not in the present thesis.

Retaining model parameters but shifting the perspective to a one-year risk analysis, forming the main point of interest of the thesis and being the topic of Section 5.3, it was found that the HY portfolio distribution under the model is wider than the IG counterpart due to both having more factors in the underlying CIR process, as well as offering upward transition possibilities. The IG portfolio return distribution is sharply capped and heavily skewed, owing to the nature of the process specification while downward migrations add weight to the left tail of the distribution. Looking at lower bond portfolio quantiles, the HY portfolio indeed turned out to be riskier than the IG portfolio, albeit not by a huge

margin, indicated in Table 5.6. Looking at volatilities, the difference is however significant. The pricing error resulting from neglect of credit migration risk is likely to cause a bias in returns, especially for the IG portfolio where the cumulative default probability under the risk-neutral measure is undervalued when pricing according to Equation (4.24).

Dependence structure adjustments

When modifying the dependence structure connecting stock index and bond portfolio, first with respect to the pairwise copula describing migration dynamics as in Section 5.3.2, and secondly with respect to the parameter β linking stock index volatility with hazard rates as in Section 5.3.3, it was found that variations of the copula seem to greatly affect the one year distributions of marginal bond portfolio returns. Lower quantiles, presented in Figures 5.4 and 5.5 for IG and HY portfolios respectively, clearly illustrate this. Higher copula dependence generally implies more extreme lower quantile values. Likewise, the type of copula also greatly influences these values. Heavier-tailed copula types such as Clayton and t_3 result in significantly heavier left tails of bond portfolio return distributions.

As for the dependence between stock index and bond portfolios, measured by correlation, Kendall's tau and tail index estimates presented in Figures 5.4 and 5.5 as functions of the migration copula, the effect of changing the latter comes out as less predictable. Heavier-tailed copula types seem to yield greater cross-sectional dependence for lower copula parameters (i.e. the weight w), whereas lighter-tailed analogues are more influential on dependence measures at higher w, eventually even surpassing heavier-tailed types for comparable w. We made a point the measures themselves are perhaps not fully informative, being one-dimensional, while scatter plots and conditional histograms available in Figures 5.6 and 5.7 respectively shed more light on the overall shape of return distributions. From these, the impact of applying different copulas for migrations emerges more clearly.

When varying β along with the migration copula specification, results illustrate higher values of β scale up cross-sectional dependence across all copula settings, visualized in Figure 5.8. A similar result holds for lower bond portfolio quantiles, with higher dependence through β generally giving rise to more extreme quantile values as seen in Figure 5.9. Here, however, the choice of migration copula appears to carry more weight than does the way β is set.

Looking at how lower tail dependence in stock index/bond portfolio return pairs varies as function of dependence setting, Table 5.8 indicates there likely is lower tail dependence for virtually any dependence setting barring an independence specification. Values obtained generally exceed those expected for outcomes of a bivariate standard normal random variable with comparable correlation or concordance. While the choice of copula here might have small impact on the level of significance with which this occurs, with heavier-tailed copulas showing slightly more convincing tendencies of yielding lower tail dependence in return pairs, applying anything other than the independence copula is likely to result in similar conclusions.

Conclusively, the choice of migration copula appears to have high importance on the shape of marginal bond portfolio distributions, but is less influential on the cross-sectional dependence on a 1-year risk horizon. Lower tail dependence exceeding the standard normal case prevails for a multitude of dependence settings, whereas the dependence in upper tails just as consistently is on the opposite end of the spectrum, converging to zero as the percentile level approaches 1 faster than a bivariate random variable with Gaussian copula. This asymmetry between the tails, clearly highlighted in Tables 5.8 and 5.9 for stock index/HY bond portfolio return pairs and in Appendix C.1.2 for stock index/IG bond portfolio return pairs, most importantly stems from the fact transitions to defaults

have a far more decisive impact on bond portfolio returns than do migrations between non-default rating classes. Thereby, any dependence added when migration dynamics are present mostly shows in the lower tail.

6.2 Model Evaluation

Backed by Chapter 5, we here attempt to qualitatively discuss the performance of the model, highlighting its strengths and weaknesses. The simplifications used are reviewed, with the intent of addressing their impact on the results as well as lifting possible relaxations and modifications of these.

6.2.1 Strengths and Shortcomings

First off, we note that the model is capable of richly producing various types of bivariate distributions, both as concerns the dependence across equity and debt markets, and with respect to marginal distributions. The moderately high number of parameters, summarized in Table 5.3, contributes to this flexibility. The original model by Carr and Wu (2010), as described in Section 3.2, also featured a large number of parameters without accommodating a rating migration mechanism. In their paper, the model appeared to provide a good fit to observed firm-specific cross-sectional market prices (of stock options and CDS spreads) as well as their time series behaviour for a range of firms. The addition of migrations, with simulation under a real-world measure for risk analysis explored in this work, makes for an adaptation more suitable to the purpose of this thesis.

One desirable property that follows from the rating-based hazard rate specification, where hazard rates belonging to poorer rating classes feature a larger number of underlying CIR processes, is that marginal bond return distributions showcase larger variability for poorly rated bonds. Figure 5.2 illustrates this. While an already highly rated bond can only grow so much in value over any given time horizon, reflected in the capped and left-skewed return distribution, a positive credit change for a poorly rated bond fundamentally changes long-term expectations of default risk, leading to larger positive returns over the risk horizon.

Furthermore, applying rating-based hazard rates rather than firm-specific rates provides for a market-wide modelling setup. A large number of firms may be jointly modelled with this setup, while the dependence between them is also accounted for via dependent migrations. Even though the size of the model is fairly large, streamlining the behaviour of individual firms in this way equals a large reduction in number of parameters to keep track of in comparison to what would be the case with each firm having its own set of parameters.

Another benefit relates to the implementation, where any portfolio composed of assets depending on the risk factors studied could in principle be evaluated and tracked along any arbitrary risk horizon. While we have focused on simple assets, facilitating the study of dependence of risk factors, the framework developed contains all pieces necessary to perform pricing and risk management of more complex assets and portfolios.

Concerning model weaknesses, as previously pointed out the interest rates should ideally be included. For proper calibration and validation, this would be a near mandatory addition. With that said, it is promising that marginal distributions of both stock index returns and bond portfolios as well as their dependence are replicable to such a high degree even in the absence of interest rates being modelled, in the sense that the breadth of distributions appear capturable. Inclusion of interest rates is unlikely to compromise that

property; if anything it would enhance the richness of the model.

The complexity of the model makes fitting to market data a tricky matter. The trial and error approach applied here does not converge to an optimal solution, nor does it readily allow for model validation by any other means than qualitative discussion. An automated model calibration and validation technique would be advantageous, preferably preceded by the inclusion of interest rates in the model.

Other drawbacks lie in the model specification itself. We have noted dependence is capped from the behaviour of stochastic processes. The involvement of the variance-gamma process makes for richer stock index movements, and the presence of jumps in the equity market is empirically established. Treating the process as an independent component, however, is somewhat of a limitation impeding the attainable cross-sectional dependence. When attempting to fit the model to market data, this especially manifested itself in the difficulties of consistently generating high correlations between monthly stock index and HY bond index movements, while keeping the diversity of the stock index marginal distribution. While the migration conditioning partly resolves this, assigning importance to stock index jumps on the credit rating state of bonds, the analysis has highlighted that a substantial fraction of the dependence across markets comes from the process specification regardless of how strongly one links bond migrations to the equity market via the choice of copula.

The matrix adjustment method, shaping migration probabilities after process paths, comes with both benefits and drawbacks. While other studies, such as Jobst and Zenios (2001), held migration matrices constant over a simulation horizon where stochastic processes were allowed to vary, the present thesis attempts to enforce alignment between simulated process paths and the migration behaviour of firms. The cost of this is the neglect of credit migrations when pricing, where ideally bond pricing should take the full risk-neutral migration matrix into consideration. The pricing mismatch is likely to cause a shift in level of returns, while having little effect on other distributional characteristics. Either way, inconsistencies between process movements and migration probabilities or in way of pricing offsets are inclined to follow when one attempts to combine stochastic processes for hazard rates with the use of migration matrices.

The technique applied here also deviates slightly from those reviewed in Truck (2008), by combining adjustment of matrix entries with conditioning outcomes on a common index. In Truck (2008), these are considered to be separate methods. The conditioning is equivalent to shifting the actual transition probabilities bonds are exposed to, possibly offsetting the process alignment with migration matrices. However, the method contributes to the primary purpose of the model, in that it creates a tool for further dependence adjustments.

6.2.2 Review of Simplifications

In previous section, we already named a few of the simplifications, most importantly leaving out interest rates and the disregard of migration dynamics when pricing bonds. While the two of these are significant, they do not undermine the conclusions of the work to any considerable degree. We here summarize and discuss other simplifications and assumptions.

Rating-based modelling The application of a rating-based model for modelling of default and credit migration probabilities significantly reduces the degrees of freedom when it comes to the behaviour of individual firms. In this thesis, we have considered two rating classes - investment grade and high yield - such that all risky bonds within

the economy have their migration probabilities described by one of two possible groups of parameters, consisting of the rating-specific hazard rates and the connection of migration behaviour to the stock index via a bivariate copula. However, as described in Section 4.3, the methodology applied caters to a division into an arbitrary number of rating classes. A refinement of this number would increase the level of idiosyncrasy for bonds, as well as leading to richer migration behaviours.

To exemplify, if a finer division of rating classes were to be implemented, the sharply capped return distribution of the investment grade bond index illustrated in Figure 5.2 would likely take a slightly different look, admitting more variation in the upper tail in particular. The reason is that such a portfolio could then feature a mix of rating classes, where upward migrations are possible for at least some of the constituent bonds. At least when looking at monthly returns of the IG ETF as presented in Table 5.1 and further depicted in Figure 5.1, there are positive outliers present in the data. The model would likely be better equipped to tackle this observation with a refined rating division.

Also, the dependence specification for migrations would possibly come through differently when analysing yearly bivariate returns assuming a higher number of rating classes. In particular, it is reasonable to expect higher cross-sectional correlations could be achieved, increasing the significance of migration dynamics as compared to the process-level dependence. For an illustration, consider the scatter plots corresponding to the maximum copula case in Figures 5.6, 5.11 or C.6. The grouping of bivariate outcomes into island-looking shapes, resulting from all bonds migrating simultaneously, would be diluted as the number of rating classes grows, with the probable result of observing higher cross-sectional correlation and concordance. Still the main conclusions are unlikely to be significantly affected by such a modification, with the asymmetry in tails still being present due to the heavy impact of default events on portfolio returns.

Rating-based models similar to the one used here commonly encompass seven rating classes, reflecting the structure of rating systems such as Standard & Poor's or Moody's (Trueck and Rachev, 2009, ch. 1). From historical data on rating migrations, baseline migration matrices can then be readily adapted. A natural alternative to the dual rating class implementation studied here would therefore be one featuring seven rating classes. The drawback that comes with this is the increased complexity, greatly turning up the number of parameters to be set.

Bond standardization As mentioned in Section 4.5, the construction of bond portfolios in this thesis has consistently been highly standardized with respect to rating classes, maturities and recovery arrangements of bonds, in addition to the already discussed division into two rating classes. Furthermore, we have looked at zero-coupon bonds only. Comparing to real bond indices or the ETFs upon which data analysis was carried out, this standardization constitutes a significant simplification, also neglecting the effect of liquidity factors or contractual arrangements on bond prices, mentioned in Section 2.2.1. In spite of this, marginal monthly return distributions as well as co-movements across markets appear to be captured quite well by this simplified model. While a different specification of maturities or recovery arrangements might lead to a shift or slightly altered shape of the return distributions, there is little reason to assume any of the main findings would deviate following such a change.

Market price of risk assumptions As for the assumptions of market price of risk, we have directly adapted the method in Carr and Wu (2010) to our model. Each CIR process involved has its own associated market price of risk parameter, held constant and

affecting the drift term as described in Section 3.4. There are a couple of simplifications associated with this method. First, we have the fact only CIR processes are affected by a change of measure, while jump dynamics remain the same. Since we do not price any assets explicitly depending on the stock index process, this carries little significance. More importantly, the constancy of market prices of risk has a real effect. The term credit spread risk commonly involves changes of investors' risk aversion, giving rise to variations in market price of risk. By keeping these constant, we have effectively removed that degree of freedom, assuming changes in credit spreads come from hazard rate movements alone.

Within the devised modelling framework, relaxing this assumption would pose a challenge on the verge of being infeasible. This both from considerably complicating the parametric setup, and due to further jeopardizing bond pricing tractability.

An alternative approach, accommodating market price of risk movements, is to adopt a constant real-world migration matrix, scaled by a stochastically varying market price of risk process in order to construct risk-neutral matrices. With an appropriate choice of such a process, the CIR process being one example, one may price bonds analytically and consistently with the credit migration risk involved, see e.g. Lando (2004, ch. 6) for details. While letting real-world migrations be governed by a constant transition matrix may be a limitation, this is partly remedied if one conditions migration dynamics on a common index in similar fashion as proposed in the thesis. With an increase of number of rating classes, such an approach might be preferable preventing the number of parameters from spiralling out of control. However, the Carr and Wu (2010) foundation of the model would also be affected, where one would likely have to let go of the process-level dependence between stock index and hazard rates.

Discretization and time step assumptions When discretizing processes and linking migration dynamics to stock index movements, we have made use of several assumptions. Looking at the CIR process, the discretization scheme suggested in Section 4.2.1 is inexact and sensitive to the choice of step size. This also affects path-dependent quantities appearing in the construction of migration matrices according to Section 4.3.1, as well as on the form

$$\int_t^{t+\Delta t} v_s ds,$$

appearing in the discretization scheme for the stock index process described in Section 4.2.3. Inevitably, a discretization error will be present. In Appendix B, we briefly examine how the error varies with the choice of step size as well as of the sample size. The main finding is that the numerical error appears small for the step size chosen, and that a longer time step would probably have been fine. It should also be noted the discretization scheme itself provides good accuracy over competitors such as Euler and Milstein, which for some parameter specifications are infeasible.

Also related to this is the choice of applying monthly time windows for migrations and portfolio rebalancing, as well as in the data analysis. In reality, the number of trading days varies from one month to another, making a case against calibrating after monthly data. However, in the analysis of cross-sectional market data as well as from a modelling standpoint the use of monthly data offers convenience. Reasons include that any daily lag effects that might be present in the data are largely mitigated and that missing observations are effectively dealt with. Regarding modelling, longer time windows applied for migration conditioning and mapping facilitates actual dependence to be imposed through a copula mechanism, due to copulas being static and thereby providing no way for dependence to enter serially. A reference is provided to Appendix C.2, where we investigate

the effects of letting migration windows be a year, spanning the full risk horizon. There is also a significant computational gain to be had from applying longer time windows for migration matrix construction and portfolio evaluation and rebalancing.

For a view on how picking out monthly data is likely to affect results, an obvious drawback is the thinning of data, ignoring intra-month movements. However, the primary negative consequence that could follow from this is that parameters are not optimally set, which is not a great concern due to the purpose of the thesis. It has little effect on the analysis of how risk varies as a function of the parameter specification.

If one would stick to the monthly analysis applied here, accounting for the variations in number of trading days between months might be advisable. Such an approach would rely on the assumption that dynamics of market prices reflect actual trading time, but might present other difficulties in the form of time series across markets not matching perfectly with respect to when they are observed. Regarding the main findings of the work, they are unlikely to be affected to any great extent from making this change.

6.3 Follow-up of Objectives

We here look back at the objectives stated in Section 1.2, and relate the work to these in an attempt to put the work into perspective.

1. **Analyse historical multivariate financial data**
   We have performed analysis on equity and debt market data, presented in Section 5.1. We have primarily focused on monthly returns in the data analysis, finding evidence indicating there is alignment in the cross-market movements, in particular coming into play for the high yield ETF studied, assumed to constitute a cross-section of the riskier side of the debt market. Bond market time series were fairly short, and in order for uncertainty in the analysis to be kept low more data should ideally be used, especially as concerns the analysis of tail dependence.

2. **Review and select relevant mathematical models**
   Since the intended purpose was to find means to analyse and model both marginal distributional characteristics and dependence across equity and debt markets, equity and credit models were studied with focus on models targeting joint dynamics. We thus landed in a variation of the model by Carr and Wu (2010) described in Section 3.2, being proven for pricing purposes as well as admitting flexibility in the sense it can be tailored to different portfolio applications. Due to the need for an adaptation to an economy-wide setting, we also considered rating-based credit models capable of producing dependent credit migrations.

3. **Construct a versatile simulation framework**
   We have constructed a framework drawing from different kinds of models, implemented in an open-ended way so as to allow for further advancements, including modifications to interest rates and stock index jumps. Other features, such as migration matrix adjustment and conditioning methods could also be readily adjusted or changed. The framework is versatile from a risk management point of view, where the parametric specification can be altered to portray a wide range of market behaviours and where any portfolio whose value revolves around the modelled risk factors could theoretically be tracked over arbitrary risk horizons. Furthermore, the framework is capable of scenario generation under a risk-neutral measure and could therefore be used for asset pricing. In the rendition developed in this thesis, a

number of limitations have been imposed, of which some could likely be successfully relaxed whereas others serve well as is, discussed in Section 6.2.2. While rigorous model validation is yet to be addressed, comparison between simulated and market observed data has shown promise.

4. **Discuss implications on risk management**
   When it comes to bond portfolio returns, we have seen that the model tends to create left-skewed distributions. Dependence between equity and credit is capped from the process specification, having stock index jumps not affecting hazard rates, and from the correlation between Brownian motions of the stock index and its volatility. Variations to the dependence at process level has only been done with respect to the parameter β, linking stock index volatility and firm hazard rates, showing that an increase of this parameter leads to increased cross-sectional dependence. The impact of other factors likely influencing the dependence at process level has not been further elaborated on.

   By linking bond rating migration dynamics to the stock index through various copula specifications, the shape of the bond portfolio return distribution is affected. Heavier-tailed copulas, in particular, result in increased bond portfolio risk looking at lower quantile values. However, the cross-sectional dependence as measured by correlation, concordance and tail index estimates is only somewhat affected by the choice of copula, and the effect only shows with consistency up to a certain level of the copula dependence parameter. The process-level dependence here appears to have more of a significant effect.

6.4 Future Work

Based on the discussion of preceding sections, we here list a few suggestions for future work.

Implement interest rates A natural extension of the model would be one encompassing stochastic interest rates. Excess returns could then be replaced by a study of actual returns and all of the distributional characteristics of returns would then be of interest to analyse, including mean levels. The primary challenge that comes with this is to specify the dependence structure of the model in a manageable way, linking the three separate risk factors of interest rate risk, equity risk and credit risk. Bypassing one of the three links might be a viable first step. As an example, the multi-factor CIR specification in Kovalov and Linetsky (2008) recited at the end of Section 3.2 may be attempted in order to provide a link between interest rates and hazard rates while largely preserving the connection between stock index and hazard rate movements. However, this would likely not fully account for the joint behaviour of equity and interest rates.

Refine model calibration and validation Assuming interest rates are specified, whether deterministically or stochastically, means of calibrating the model to market data in a refined manner could be explored. In the paper by Carr and Wu (2010), Kalman filtering was applied to time series of stock option prices and CDS spreads in order to fit parameters of stochastic processes, and a similar technique could be trialled here. The goodness of fit of the model, using a certain calibration method, should ideally be quantified looking at the out-of-sample performance. One way of doing so would be by backtesting model implied risk measures against data, as described in (McNeil et al., 2010,

ch. 2). With sophisticated validation methods in place, different model specifications as well as calibration techniques could readily be compared to one another.

Fine-tune rating based model Instead of applying two rating classes as in this thesis, extending to a more refined rating-based model with a finer credit rating division is a natural development, enhancing the richness of portfolio return behaviours. Accompanied with this, the pricing issue we have previously highlighted should be addressed. The main difficulty with an extension of number of rating classes is the increased model complexity, and in order to maintain feasibility an overhaul of the matrix adjustment method might come in handy. The latter could also provide the tool necessary in order to rectify the pricing issue, as discussed in Section 6.2.2.

Investigate effects of simplifications In order to gain an improved understanding of how the various simplifications used affect the analysis, a more thorough study would be useful, alternating the shape and form of simplifications and comparing the results. This includes the migration matrix adjustment method previously mentioned, as lining this up with other methods as in Truck (2008) and surveying their performance would be illuminating. Another example is the stock index jump dynamics, which in the current model specification is detached from the behaviour of hazard rates. We have discussed how this is likely to be a limiting factor when imposing dependence between stock index and bond portfolios, while sometimes contributing to odd distributional characteristics such as when a copula with strong dependence is used for the simulation of migrations. If one were to connect stock index jumps with hazard rates, a more informed view on the limitations of the current specification could be taken.

6.5 Concluding Remarks

The present thesis has detailed the development of a simulation framework intended for the joint modelling of disparate types of financial risk, with focus directed towards equity and credit risk. The existence of dependence across these types of markets has been established in previous studies and further reinforced here. The model implementation is flexible and appears largely capable of capturing observed market patterns, although further validation remains. Taking a one-year risk perspective and varying the model-specified dependence structure, we have seen that simulated one-year distributions of stock index returns and bond portfolio returns can take a variety of shapes, but where bivariate tails display similar properties for a wide range of dependence specifications. With the dependent credit migration dynamics modelled firms are exposed to, defaults have a large impact on bond portfolio returns, such that any additional cross-sectional dependence imposed mostly shows in the lower tail. As a result, there is considerable harmonisation in the movements of studied equity and debt instruments in the lower tail, suggesting lower tail dependence, whereas a more discordant behaviour is observed in the upper tail.

Bibliography

Leif Andersen. Efficient Simulation of the Heston Stochastic Volatility Model. Technical report, 2007.

Anil Bangia, Francis X. Diebold, André Kronimus, Christain Schagen, and Til Schuermann. Ratings migration and the business cycle, with application to credit portfolio stress testing. *Journal of Banking and Finance*, 26: 445–474, 2002.

David S Bates. Jumps and Stochastic Volatility: Exchange Rate Processes Implicit in Deutsche Mark Options. *Review of Financial Studies*, 9(1):69–107, 1996.

Koen Berteloot, Wouter Verbeke, Gerd Castermans, Tony Van Gestel, David Martens, and Bart Baesens. A novel credit rating migration modeling approach using macroeconomic indicators. *Journal of Forecasting*, 32(7):654–672, 2013.

T.R. Bielecki and M. Rutkowski. *Credit Risk: Modeling, Valuation and Hedging*. Springer Finance. Springer, 2002.

Tomas Björk. *Arbitrage Theory in Continuous Time*. Oxford university press, 3rd edition, 2009.

Fischer Black and Myron Scholes. The pricing of options and corporate liabilities. *The journal of political economy*, pages 637–654, 1973.

Eike C Brechmann, Katharina Hendrich, and Claudia Czado. Conditional copula simulation for systemic risk stress testing. *Insurance: Mathematics and Economics*, 53(3):722–732, 2013.

Damiano Brigo and Fabio Mercurio. *Interest Rate Models - Theory and Practice*. Springer Finance. Springer, Berlin, Heidelberg, Paris, 2nd edition, 2006.

Peter Carr and Liuren Wu. Time-changed lévy processes and option pricing. *Journal of Financial economics*, 71 (1):113–141, 2004.

Peter Carr and Liuren Wu. Stock options and credit default swaps: A joint framework for valuation and estimation. *Journal of Financial Econometrics*, 8(4):409–449, 2010.

Peter Carr, Hélyette Geman, Dilip B Madan, and Marc Yor. The fine structure of asset returns: An empirical investigation*. *The Journal of Business*, 75(2):305–333, 2002.

Ren-Raw Chen, Xiaolin Cheng, Frank J Fabozzi, and Bo Liu. An explicit, multi-factor credit default swap pricing model with correlated factors. *Journal of Financial and Quantitative Analysis*, 43(1):123–160, 2008.

Umberto Cherubini, Elisa Luciano, and Walter Vecchiato. *Copula Methods in Finance*. The Wiley Finance Series. Wiley, 2004.

Rama Cont. Empirical properties of asset returns: stylized facts and statistical issues. *Quantitative Finance*, 1: 223–236, 2001.

John C. Cox, Jonathan E. Jr Ingersoll, and Stephen A. Ross. A Theory of the Term Structure of Interest Rates. *Econometrica*, 53(2):385–407, March 1985.

Gregory R. Duffee. The relation between treasury yields and corporate bond yield spreads. *Journal of Finance*, 53: 2225–2241, 1998.

Darrell Duffie and Kenneth J Singleton. Modeling term structures of defaultable bonds. *Review of Financial studies*, 12(4):687–720, 1999.

Abel Elizalde. Credit risk models i: Default correlation in intensity models. *Documentos de Trabajo (CEMFI)*, (5): 1, 2006.

Paul Embrechts, Filip Lindskog, and Alexander McNeil. Modelling dependence with copulas and applications to risk management. *Handbook of heavy tailed distributions in finance*, 8(1):329–384, 2003.

Bjørn Eraker, Michael Johannes, and Nicholas Polson. The impact of jumps in volatility and returns. *The Journal of Finance*, 58(3):1269–1300, 2003.

Claudio Fontana and Juan Miguel A Montes. A unified approach to pricing and risk management of equity and credit risk. *Journal of Computational and Applied Mathematics*, 259:350–361, 2014.

Ines Fortin and Christoph Kuzmics. Tail-dependence in stock-return pairs. *Intelligent Systems in Accounting, Finance and Management*, 11(2):89–107, 2002.

Paul Glasserman. *Monte Carlo methods in financial engineering*. Applications of mathematics ; 53. Springer, New York, NY ; Berlin ; Heidelberg [u.a.], 2004.

David T Hamilton, Jessica James, and Nick Webber. Copula methods and the analysis of credit risk. *Available at SSRN 1014407*, 2001.

Steven L Heston. A closed-form solution for options with stochastic volatility with applications to bond and currency options. *Review of financial studies*, 6(2):327–343, 1993.

Henrik Hult, Filip Lindskog, Ola Hammarlid, and Carl Johan Rehn. *Risk and portfolio analysis: Principles and methods*. Springer Science & Business Media, 2012.

Peter Jäckel. *Monte Carlo Methods in Finance*. Wiley Finance. Wiley, 2002.

Robert A Jarrow and Fan Yu. Counterparty risk and the pricing of defaultable securities. *the Journal of Finance*, 56(5):1765–1799, 2001.

Robert A Jarrow, David Lando, and Stuart M Turnbull. A Markov Model for the Term Structure of Credit Risk Spreads. *Review of Financial Studies*, 10(2):481–523, 1997.

Norbert Jobst and Stavros A. Zenios. Extending Credit Risk (Pricing) Models for the Simulation of Portfolios of Interest Rate and Credit Risk Sensitive Securities. Working Paper 01-25, Wharton School Center for Financial Institutions, University of Pennsylvania, July 2001.

Philippe Jorion. *Financial Risk Manager Handbook + Test Bank: FRM Part I /*. Number del 2 in Wiley Finance. Wiley, 2010.

Pavlo Kovalov and Vadim Linetsky. Valuing convertible bonds with stock price, volatility, interest rate, and default risk. *FDIC Center for Financial Research Working Paper Series*, (2008-02), 2008.

David Lando. Some Elements of Rating-Based Credit Risk Modeling. Technical report, Department of Operations Research, University of Copenhagen, 1999.

David Lando. *Credit Risk Modeling: Theory and Applications*. Princeton University Press, 2004.

Gerald Lebovic. *Estimating Non-Homogeneous Intensity Matrices in Continuous Time Multi-State Markov Models*. PhD thesis, University of Toronto, 2011.

Filip Lindskog, Alexander McNeil, and Uwe Schmock. Kendall's tau for elliptical distributions. In *Credit Risk*. Physica-Verlag HD, 2003.

Dilip B. Madan, Peter Carr, and Eric C. Chang. The variance gamma process and option pricing. *European Finance Review*, 2:79–105, 1998.

Alexander J McNeil, Rüdiger Frey, and Paul Embrechts. *Quantitative risk management: concepts, techniques, and tools*. Princeton university press, 2010.

Gunter Meissner, Seth Rooder, and Kristofor Fan. The impact of different correlation approaches on valuing credit default swaps with counterparty risk. *Quantitative Finance*, 13(12):1903–1913, 2013.

Robert C Merton. On the pricing of corporate debt: The risk structure of interest rates*. *The Journal of Finance*, 29(2):449–470, 1974.

Robert C Merton. Option pricing when underlying stock returns are discontinuous. *Journal of financial economics*, 3(1):125–144, 1976.

Nader Naifar. Modeling the dependence structure between default risk premium, equity return volatility and the jump risk: Evidence from a financial crisis. *Economic Modelling*, 29(2):119–131, 2012.

Stefan Truck. Forecasting credit migration matrices with business cycle effects—a model comparison. *The European Journal of Finance*, 14(5):359–379, 2008.

Stefan. Trueck and Svetlozar T. Rachev. *Rating based modeling of credit risk : theory and application of migration matrices*. Elsevier Academic Press Amsterdam ; London, 2009.

Jason Z. Wei. A multi-factor, credit migration model for sovereign and corporate debts. *Journal of International Money and Finance*, 22(5):709–735, 2003.

Liuren Wu. Dampened power law: Reconciling the tail behavior of financial security returns*. *The Journal of Business*, 79(3):1445–1473, 2006.

Cindy L. Yu, Haitao Li, and Martin T. Wells. MCMC estimation of Lévy jump models using stock and option prices. *Math. Finance*, 21(3):383–422, 2011.

Benjamin Yibin Zhang, Hao Zhou, and Haibin Zhu. Explaining Credit Default Swap Spreads with the Equity Volatility and Jump Risks of Individual Firms. *Review of Financial Studies*, 22(12):5099–5131, December 2009.

Appendix A

Method for Adjusting β

As was mentioned in Section 5.3.3, when investigating the effect of β the degrees of freedom of the system are reduced in order to bring forth comparable cases for the parameter specification, altering the dependence structure while avoiding causing large side effects on the marginal behaviours of hazard rate processes. To this end, all parameters relating to the stock index process can be held the same for any specification of β, while the parameters of excess hazard rates are modified. This is done with respect to the diffusion coefficients σ_i of the z_t^i processes, to their initial values and to their market prices of risk. As a starting point, we consider the case of maximum β, i.e. the maximum possible allowed dependence between the stock index volatility process and hazard rate processes:

$$\lambda_t^m = \beta_m^{\max} v_t$$

Initial values are then

$$\lambda_0^m = \beta_m^{\max} v_0 \tag{A.1}$$

while long term means obey

$$\lambda_{mK} = \beta_m^{\max} \theta_v$$

under either measure. Thus, maximum β values may be deduced from baseline intensity matrices. In principle, this leads to different maxima depending on which measure that is considered. Permitting only one such value per process and starting from the real-world process, we thus enforce

$$\lambda_{mK}^{\mathbb{Q}} = \beta_m^{\max} \theta_v^{\mathbb{Q}} \tag{A.2}$$

which fully determines market prices of risk on excess hazard rates, as we shall soon see.

Excess hazard rate process parameters are specified in terms of baseline values $(\bar{\theta}_i, \bar{\kappa}_i, \bar{\sigma}_i)$. The latter of these is determined by letting

$$\frac{\bar{\sigma}_i^2}{2\bar{\theta}_i\bar{\kappa}_i} = \frac{\sigma_v^2}{2\theta_v\kappa_v}$$

while the two former may be set freely. This restriction leads to comparable (albeit not perfectly matching) process characteristics. Then, a scaling by constants h_i is carried out, such that both long term means and relationships between the drift and diffusion components are held the same. This leads to the equation system

$$\lambda_{mK} = \beta_m \theta_v + \sum_{i=1}^{m} h_i \bar{\theta}_i, \quad m = 1, \ldots, M,$$

which is easily solved for h_i, $i = 1, \ldots, M$. Initial values for the processes are changed accordingly,

$$\lambda_0^m = \beta_m v_0 + \sum_{i=1}^{m} z_0^i$$

which may be solved by taking advantage of Equation (A.1). By Equation (4.25), when processes are scaled with this method mean reversion rates satisfy $\kappa_i = \bar{\kappa}_i$ regardless of scaling constant as long as $\beta_i < \beta_i^{\max}$ for every i. With $\lambda_{mK}^{\mathbb{Q}}$ determined from Equation (A.2), it is then possible to compute $\theta_m^{\mathbb{Q}}$ and $\kappa_m^{\mathbb{Q}}$, $m = 1, \ldots, M$ for any β. This is done by writing

$$\lambda_{mK}^{\mathbb{Q}} = \beta_m \theta_v^{\mathbb{Q}} + \sum_{i=1}^{m} \theta_i^{\mathbb{Q}}$$

which may be solved for each $\theta_i^{\mathbb{Q}}$, and then taking advantage of the relationship between parameters under the two measures as in Equation (2.13), to obtain

$$\kappa_m^{\mathbb{Q}} = \frac{\theta_m^{\mathbb{P}}}{\theta_m^{\mathbb{Q}}} \kappa_m^{\mathbb{P}}.$$

While this method results in readily comparable cases, it is not fully ideal causing minor discrepancies in bond prices depending on which set of parameters that is being used. Setting parameters such that conditional means and variances of the multi-factor CIR processes are the same independently of which case for β that is studied would likely be an improved approach. Nonetheless, the outlined method suffices for the sake of this study.

Appendix B

Discretization Accuracy

We here briefly analyse and discuss the error caused from discretization of processes. We use a somewhat heuristic procedure based on ideas of Glasserman (2004, ch. 6). A more exhaustive treatment is available in said book and chapter.

The process discretization methodology outlined in Section 4.2 involves several instances of approximation of integrals of the type

$$\int_t^{t+\Delta t} x_s ds$$

where x_t is a CIR process discretized with step size Δt. In these cases, we replace the integral with the approximation

$$\int_t^{t+\Delta t} x_s ds \approx \frac{x_t + x_{t+\Delta t}}{2}.$$

A similar situation arises when constructing time-dependent rating transition matrices, where piecewise constant intensity matrices are constructed over intervals of length Δt, taking the average of simulated hazard rate process values at the beginning and end of these intervals to constitute default column entries. Furthermore, the process discretization scheme itself makes use of approximations when generating outcomes of $x_{t+\Delta t}$ conditional on x_t. Therefore, in order not to create large numerical errors, the discretization step size should be chosen with care.

In the thesis, we have consistently applied a step size of $\Delta t = 1/252$, such that each time step corresponds to one business day. It is common practice in financial modelling to use this step size. Nonetheless, we will have a look at the severity of the resulting error one can expect. In order to do so, we apply a one-month simulation horizon, and loop through step sizes starting at a monthly discretization, then being successively halved until reaching $\Delta t = 1/768$, corresponding to 64 steps per month. For each step size, we generate economic scenarios encompassing paths of the stock index, its volatility and hazard rate processes for investment grade (IG) and high yield (HY) rating classes in accordance with Section 4.2. We let samples range from 2500 to $40,000$ in size, in steps successively doubling the size. The reason for altering the sample size like this, is the fact there are two error sources involved; one coming from the discretization time step, and one from the sample size. Based on scenarios, we also construct path-dependent discrete migration matrices as described in Section 4.3.1, spanning the monthly horizon. Other parameters are as in Table 5.3.

For each discretization step size and sample size, we thus arrive at a set of economic scenarios, from which we may estimate desired distributional characteristics. Hence we

obtain a grid of samples, with one dimension specifying different discretization time steps and one specifying sample sizes. For each sample, we calculate estimates of means and standard deviations of the following quantities at the end of the horizon:

- The volatility process
- The stock index process
- IG and HY probabilities of default over the horizon, given by last-column entries of discrete migration matrices

When it comes to the volatility process, we may compare obtained values to analytically known CIR process means and standard deviations,

$$E[v_T] = \theta + (v_0 - \theta)\exp(-\kappa T)$$
$$\sqrt{\mathrm{Var}[v_T]} = \left(\frac{v_0\sigma^2}{\kappa}\exp(-\kappa T)(1-\exp(-\kappa T)) + \frac{\theta\sigma^2}{2\kappa}(1-\exp(-\kappa T))^2\right)^{1/2}$$

as stated in Section 4.2.1. In this case, we calculate errors as absolute difference between obtained and analytical values, normalized by the analytical values.

For the stock index process and the default probabilities, we need to proceed slightly differently as the moments are not analytically known. For each sample size, we compute absolute differences in the estimates corresponding to adjacent step sizes. These are then normalized by the estimate corresponding to the finest discretization for each sample size. The normalization is applied with the intent of getting an idea of the relative fluctuations of estimates between samples. Under the assumption that estimators are unbiased and consistent, one may expect these to approach zero as step size and sample size are increased.

Figure B.1 shows how the relative error, calculated according to the above, of means and standard deviations varies as function of step size and sample size. The figure shows that the error, both in mean and standard deviation, is for the most part below 1% for any step size and sample size trialled. Interestingly, the size of the error as obtained according to this procedure does not appear to diminish at a high rate as one increases the granularity. On the contrary, it is difficult to tell whether there is any dependence at all of the error with the step and sample size, judging by the figure. Since the errors are generally small, one could argue any discretization step size and sample size in the range examined may be used. The signs of the errors, not presented in the figure, appear randomly scattered and therefore give no hint of systematic biases in these estimates.

Turning to the stock index, Figure B.2 shows how the absolute difference in mean and standard deviation estimates of adjacent return distributions varies as the step size is reduced for different sample sizes. As in the previous figure, there is no evidence of the error being eliminated as the step size is decreased, although the sample size appears to play a bigger role here. The differences in estimates between samples are small, indicating we can not expect greatly increased accuracy with smaller step size within the examined range.

As for monthly default probabilities, where normalized differences in means and standard deviations between samples corresponding to different time steps are illustrated in Figure B.3 for different sample sizes, differences in mean values are small while standard deviations show larger discrepancies. While the observations in this figure are much the same as previously, the step size does appear to have an effect on estimates, which is

particularly seen in the subplots depicting differences in standard deviation. A step size chosen too large is likely to result in accuracy issues.

The main conclusion from these plots is that we could probably have got away with both a smaller sample size and coarser discretization as compared to what is used in the thesis. However, for the purpose of tail index estimation, the sample size should be held as large as possible.

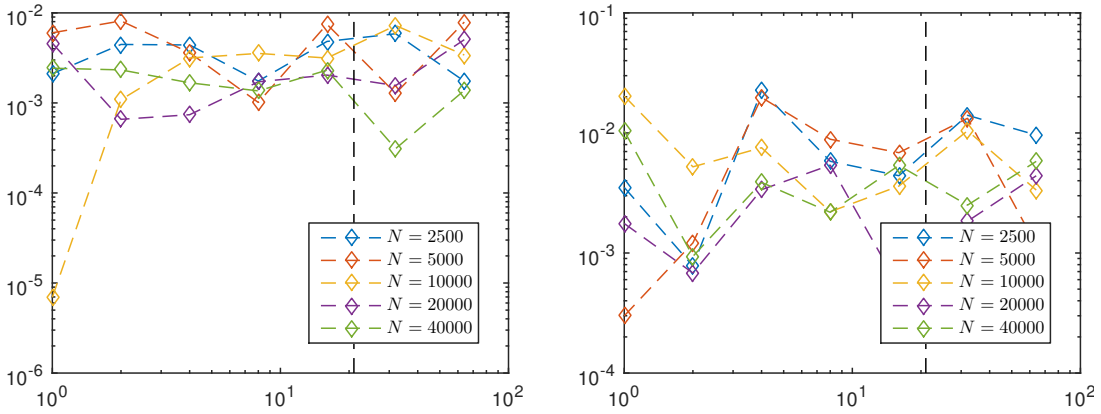

a. Means b. Standard deviations

Figure B.1: Sizes of relative errors in means and standard deviations of the one-month values of the stock index volatility process, as functions of the the number of discretization time steps in a month and of the sample size. Vertical dashed lines indicate 21 monthly steps, the value used in the thesis.

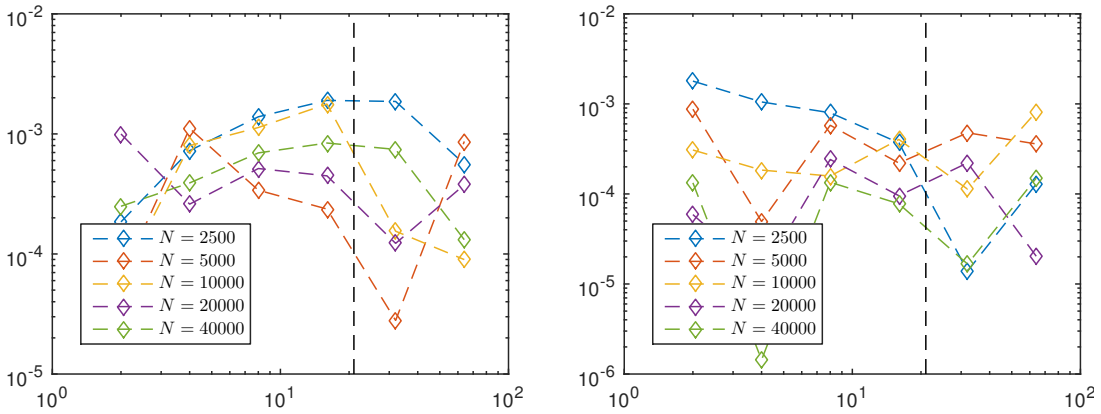

a. Means b. Standard deviations

Figure B.2: Sizes of differences between adjacent samples (with respect to discretization step size) in means and standard deviations of the simulated one-month stock index returns, as functions of the the number of discretization time steps in a month and of the sample size. The markers are placed at time steps corresponding to differences between estimates at that step size and immediately preceding, coarser, discretization. Vertical dashed lines indicate 21 steps, the value used in the thesis.

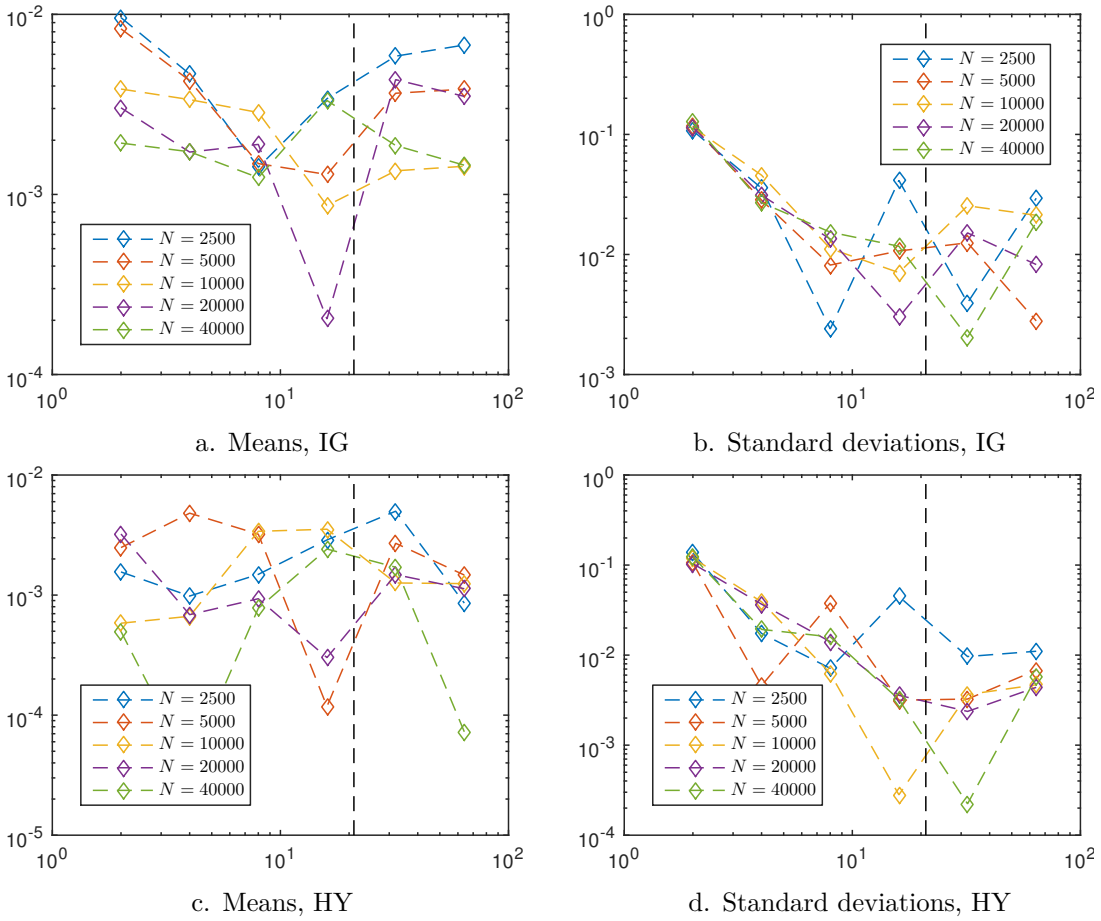

a. Means, IG

b. Standard deviations, IG

c. Means, HY

d. Standard deviations, HY

Figure B.3: Sizes of normalized differences between adjacent samples (with respect to discretization step size) in means and standard deviations of the path-dependent one-month default probabilities associated with IG and HY rating classes respectively, as functions of the the number of discretization time steps in a month and of the sample size. The markers are placed at time steps corresponding to differences between estimates at that step size and immediately preceding, coarser, discretization. Vertical dashed lines indicate 21 monthly steps, the value used in the thesis.

Appendix C

Complementary Results

This section contains additional results and plots left aside in the main presentation. The reason is that they do not convey much additional information contributing to the conclusions of the work, but they are included here for completeness.

C.1 Dependence Adjustments: IG Portfolio Results

Here, we include complementary results from the portfolio risk simulations under various dependence structures connecting stock index returns and IG portfolio returns, left out in Section 5.3.

C.1.1 Complementary Plots, Migration Copula Adjustments

Figure C.1 shows scatter plots of stock index/rebalanced IG portfolio one-year returns from the simulations in Section 5.3.2, as functions of different migration copulas. In Figure C.2, histograms of IG portfolio returns conditional on stock index returns falling below the estimated 0.05 quantile are illustrated.

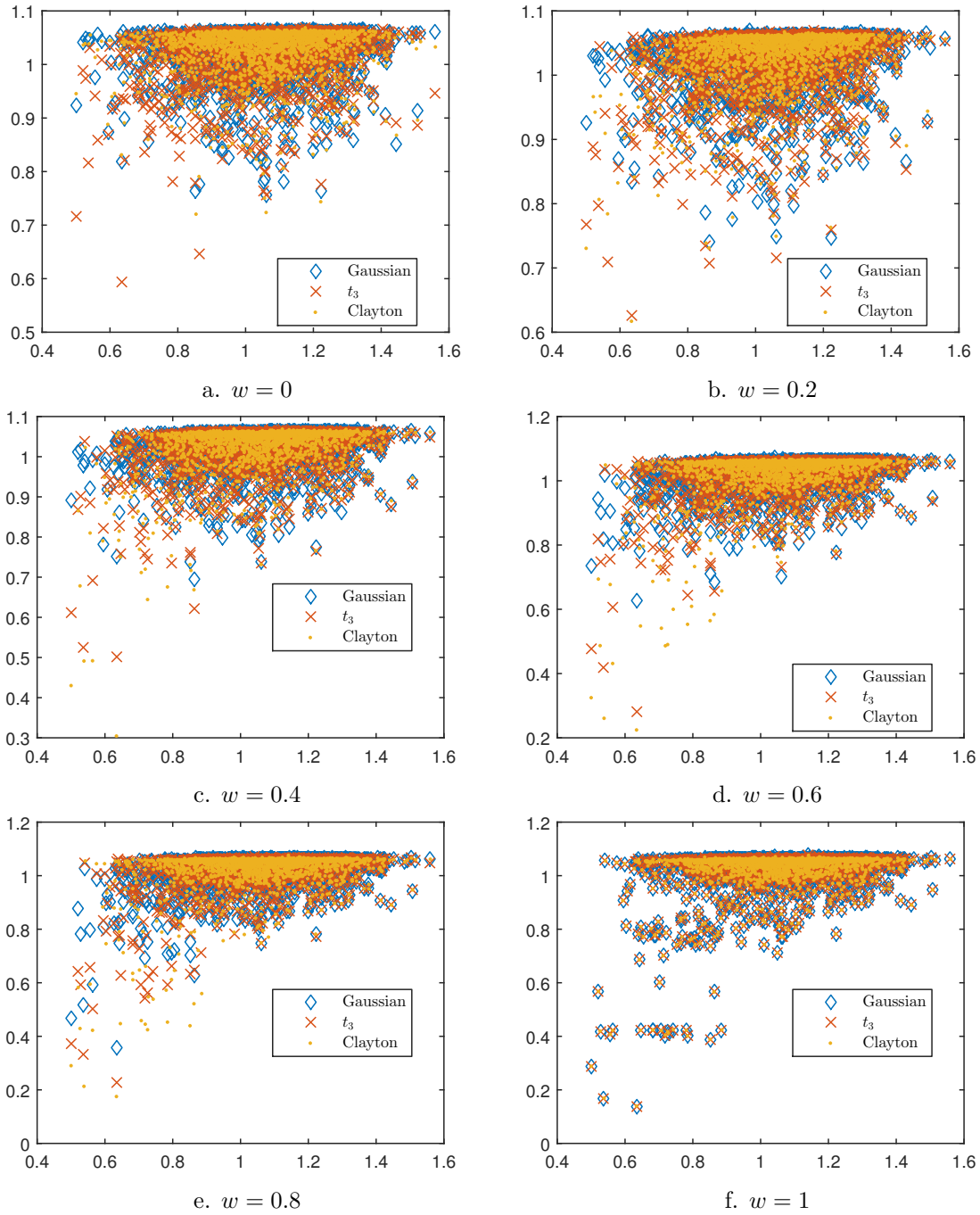

a. $w = 0$ b. $w = 0.2$

c. $w = 0.4$ d. $w = 0.6$

e. $w = 0.8$ f. $w = 1$

Figure C.1: Scatter plots for one-year stock index returns and rebalanced IG portfolio returns, applying different copulas and weights w for the migration simulation. The first 2000 simulated observations of each pair of stock index returns/bond portfolio returns from the total sample of $N = 20,000$ bivariate returns per copula are depicted.

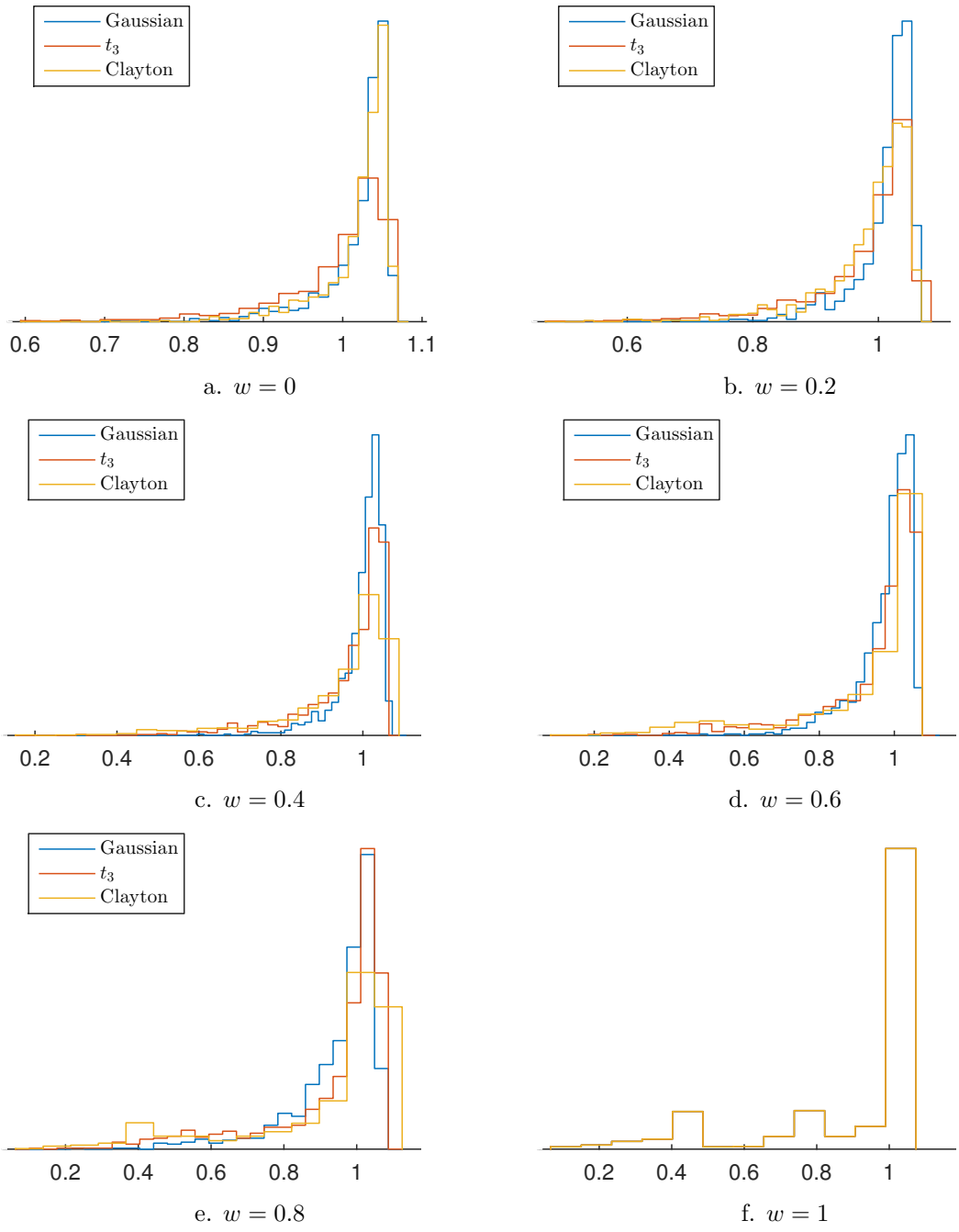

Figure C.2: Histograms of simulated one-year rebalanced IG portfolio returns conditional on stock index returns falling below its estimated 0.05 quantile value, where bond credit migration dynamics are connected to stock index returns through different copulas with weight w. For $w = 1$, the maximum copula is used.

C.1.2 Variation of β

In Section 5.3.3, we analysed how variations to the parameter β along with changes in copula governing migrations affected dependence between one-year stock index returns and corresponding returns for a monthly rebanced high yield bond portfolio, as well as dependence within the portfolio. We here present similar results for the bivariate returns of the stock index and an investment grade bond portfolio with rebalancing.

Figure C.3 shows estimates of dependence measures in stock index/IG bond portfolio return pairs. Figure C.4 shows quantile estimates at levels 0.05 and 0.005 for yearly IG portfolio returns. These plots exhibit similar features as those observed for the HY portfolio. Scatter plots showing return pairs resulting from a few different selected dependence specifications are given in Figure C.5.

Table C.1 lists return pair correlation and Kendall's tau estimates for a few different sets of values for β and the copula, with tail indices at levels 0.005 and 0.05 for corresponding dependence specifications presented in Table C.2, comparing to bivariate normal confidence intervals at matching correlation and concordance levels. Similar conclusions as those in Section 5.3.3 are drawn, with the choice of β and copula affecting stock index/bond portfolio dependence similarly for the IG portfolio as for the HY portfolio.

We also look at the upper tail index estimates, again comparing to bivariate normal with matching correlation. These results are presented in Table C.3 and support the analysis in Section 5.3.4.

		Gaussian		t_3		Clayton	
		$\hat{\rho}$	$\hat{\tau}$	$\hat{\rho}$	$\hat{\tau}$	$\hat{\rho}$	$\hat{\tau}$
$\beta = \beta^{\min}$	$w = 0$	−0.01	−0.00	0.20	0.09	−0.00	0.00
	$w = 0.3$	0.22	0.13	0.27	0.12	0.33	0.18
	$w = 0.6$	0.39	0.22	0.28	0.14	0.26	0.11
$\beta = \beta^{\text{mid}}$	$w = 0$	0.30	0.20	0.37	0.28	0.31	0.21
	$w = 0.3$	0.53	0.34	0.43	0.33	0.47	0.40
	$w = 0.6$	0.59	0.42	0.41	0.36	0.36	0.36
$\beta = \beta^{\max}$	$w = 0$	0.52	0.35	0.46	0.40	0.52	0.35
	$w = 0.3$	0.64	0.45	0.50	0.44	0.54	0.50
	$w = 0.6$	0.63	0.51	0.47	0.47	0.42	0.49

Table C.1: Empirically estimated linear correlations $\hat{\rho}$ and Kendall's tau $\hat{\tau}$ between simulated stock index and rebalanced IG bond portfolio one-year returns. Three different sets of values for β used, where $\beta^{\min} = 0$ and $\beta^{\text{mid}} = \beta^{\max}/2$, as well as three different copulas with weight w between stock index outcomes and rating migration dynamics.

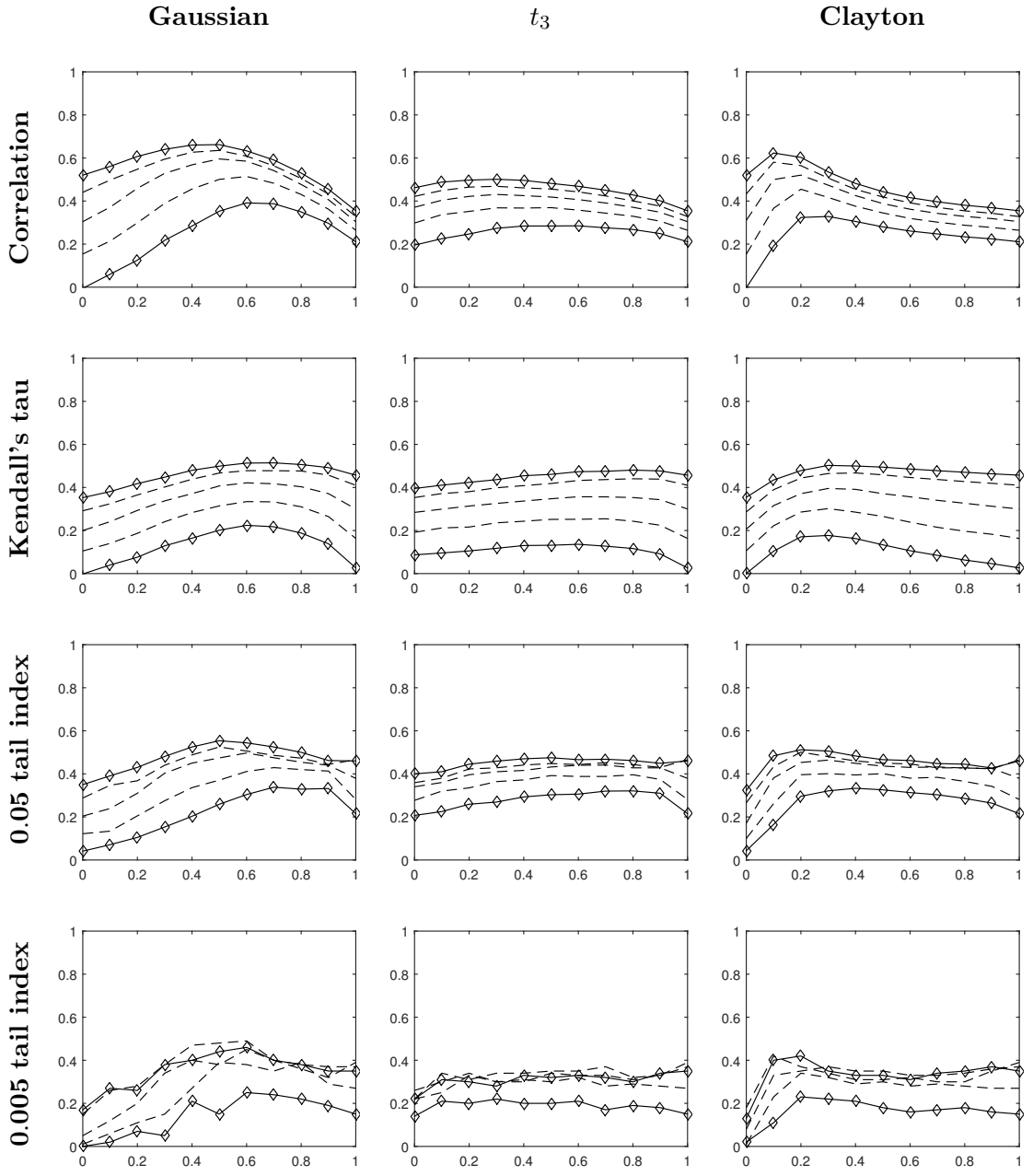

Figure C.3: Empirical estimates of dependence measures between one-year stock index returns and HY rebalanced bond portfolio returns, against different values of the weight w of monthly stock index returns on bond rating migrations on horizontal axes, linked with different copulas. In each subplot, the uppermost, solid lines correspond to the case $\beta = \beta^{\max}$, whereas the lowermost, solid lines correspond to $\beta = \beta^{\min}$. Dashed lines represent results from intermediate cases.

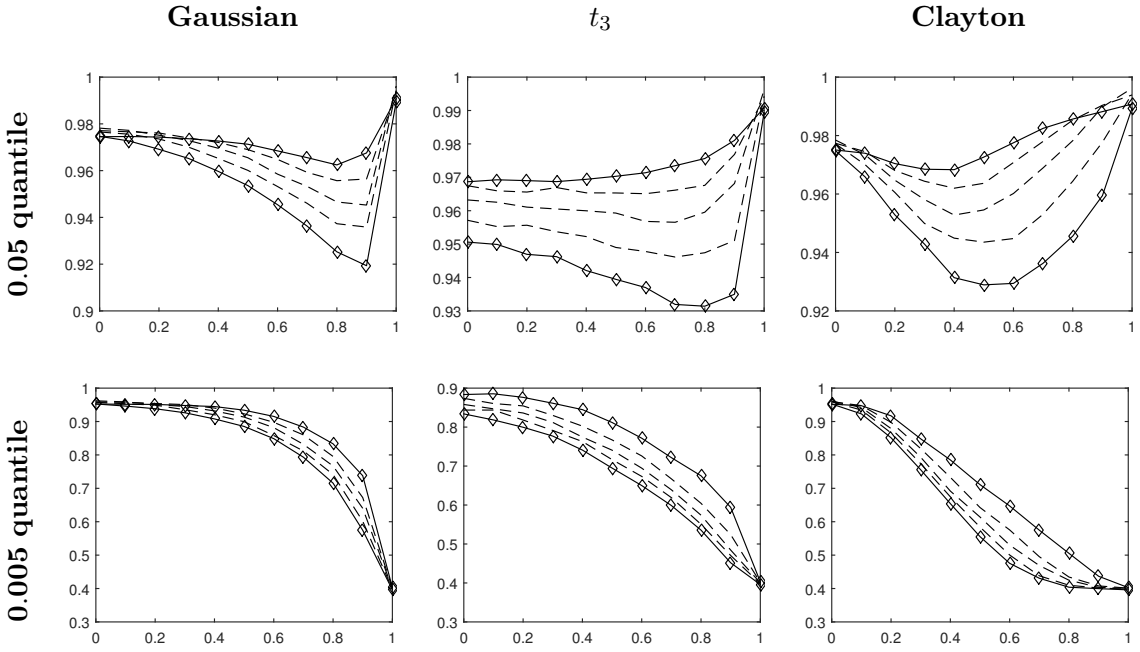

Figure C.4: Estimated quantiles for one-year rebalanced HY portfolio returns against different values of the weight w of monthly stock index returns on bond rating migrations on horizontal axes, linked with different copulas. In each subplot, the uppermost, solid lines correspond to the case $\beta = \beta^{\min}$, whereas the lowermost, solid lines correspond to $\beta = \beta^{\max}$. Dashed lines represent results from intermediate cases.

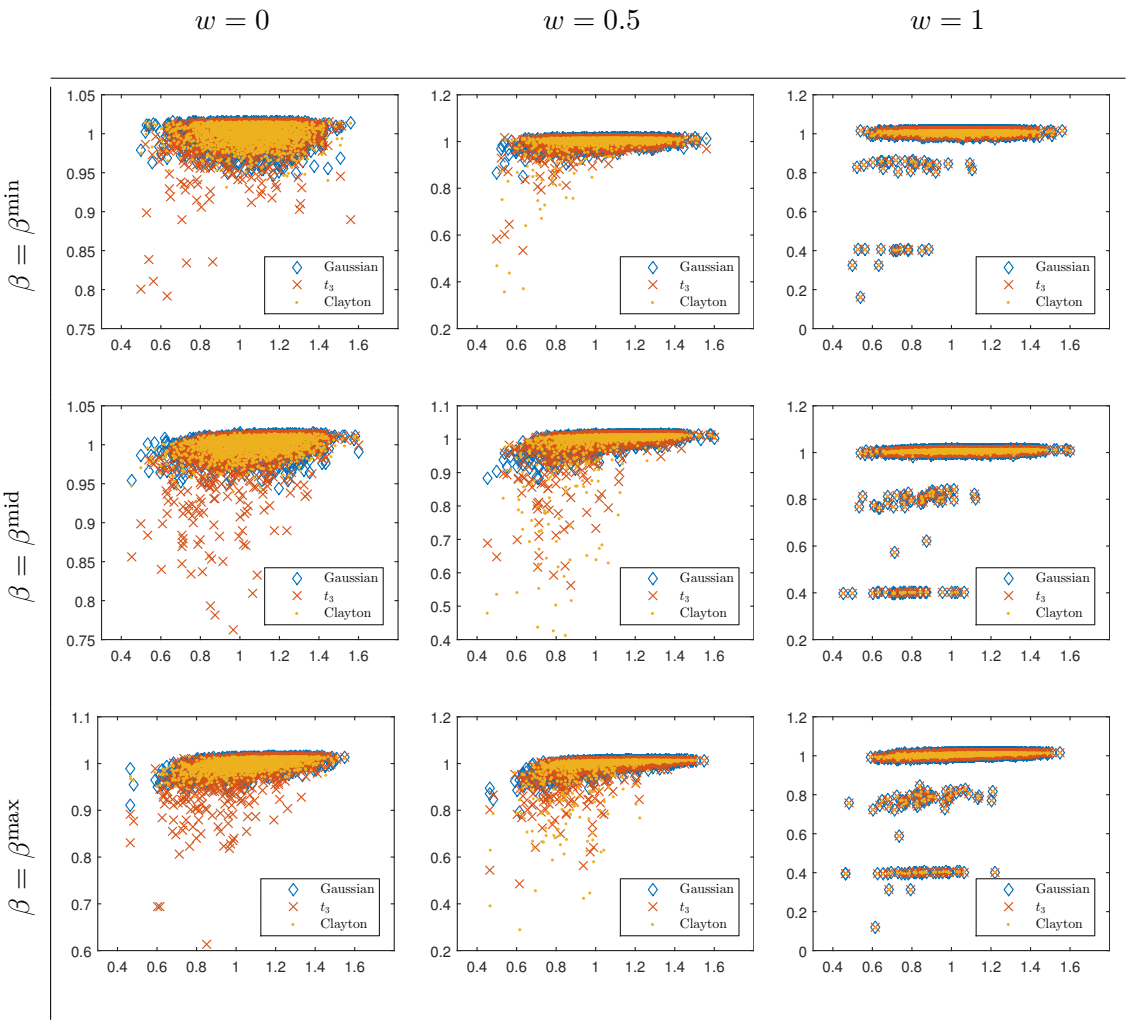

Figure C.5: Scatter plots of 2000 simulated stock returns and corresponding simulated rebalanced IG portfolio returns where transition dynamics are given by different copulas. Different sets of values of β are used, where $\beta^{\text{mid}} = \beta^{\max}/2$.

Tail index estimates at $p = 0.005$

		Gaussian		t_3		Clayton	
		$\widehat{\lambda_{L,p}}$	Normal	$\widehat{\lambda_{L,p}}$	Normal	$\widehat{\lambda_{L,p}}$	Normal
$\beta = \beta^{\min}$	$w = 0$	0.00	[0.00, 0.02] [0.00, 0.02]	0.14	[0.00, 0.05] [0.00, 0.04]	0.02	[0.00, 0.02] [0.00, 0.02]
	$w = 0.3$	0.05	[0.00, 0.06] [0.00, 0.05]	0.22	[0.00, 0.07] [0.00, 0.05]	0.22	[0.01, 0.09] [0.00, 0.07]
	$w = 0.6$	0.25	[0.02, 0.11] [0.01, 0.09]	0.21	[0.00, 0.07] [0.00, 0.06]	0.16	[0.00, 0.07] [0.00, 0.05]
$\beta = \beta^{\text{mid}}$	$w = 0$	0.05	[0.01, 0.08] [0.01, 0.08]	0.22	[0.01, 0.10] [0.03, 0.13]	0.08	[0.01, 0.08] [0.01, 0.08]
	$w = 0.3$	0.34	[0.05, 0.18] [0.05, 0.16]	0.34	[0.03, 0.13] [0.04, 0.16]	0.37	[0.04, 0.15] [0.08, 0.21]
	$w = 0.6$	0.45	[0.08, 0.21] [0.09, 0.24]	0.35	[0.02, 0.12] [0.06, 0.18]	0.33	[0.01, 0.10] [0.06, 0.18]
$\beta = \beta^{\max}$	$w = 0$	0.17	[0.05, 0.17] [0.05, 0.18]	0.22	[0.03, 0.14] [0.08, 0.21]	0.13	[0.05, 0.17] [0.05, 0.18]
	$w = 0.3$	0.38	[0.11, 0.26] [0.11, 0.26]	0.28	[0.05, 0.16] [0.10, 0.25]	0.35	[0.06, 0.18] [0.16, 0.32]
	$w = 0.6$	0.46	[0.10, 0.25] [0.17, 0.33]	0.33	[0.04, 0.14] [0.13, 0.29]	0.31	[0.02, 0.12] [0.14, 0.30]

Tail index estimates at $p = 0.05$

		Gaussian		t_3		Clayton	
		$\widehat{\lambda_{L,p}}$	Normal	$\widehat{\lambda_{L,p}}$	Normal	$\widehat{\lambda_{L,p}}$	Normal
$\beta = \beta^{\min}$	$w = 0$	0.04	[0.04, 0.06] [0.04, 0.06]	0.21	[0.09, 0.12] [0.07, 0.10]	0.04	[0.04, 0.06] [0.04, 0.06]
	$w = 0.3$	0.15	[0.09, 0.13] [0.09, 0.13]	0.27	[0.11, 0.15] [0.08, 0.12]	0.32	[0.13, 0.18] [0.11, 0.15]
	$w = 0.6$	0.30	[0.16, 0.21] [0.14, 0.19]	0.31	[0.12, 0.16] [0.09, 0.13]	0.31	[0.11, 0.15] [0.08, 0.11]
$\beta = \beta^{\text{mid}}$	$w = 0$	0.20	[0.12, 0.17] [0.13, 0.17]	0.34	[0.15, 0.20] [0.18, 0.23]	0.17	[0.13, 0.17] [0.13, 0.17]
	$w = 0.3$	0.40	[0.23, 0.29] [0.22, 0.27]	0.41	[0.18, 0.23] [0.21, 0.26]	0.46	[0.20, 0.25] [0.27, 0.33]
	$w = 0.6$	0.50	[0.27, 0.33] [0.29, 0.35]	0.44	[0.17, 0.22] [0.24, 0.29]	0.43	[0.15, 0.19] [0.24, 0.29]
$\beta = \beta^{\max}$	$w = 0$	0.35	[0.23, 0.28] [0.23, 0.29]	0.40	[0.20, 0.25] [0.27, 0.33]	0.32	[0.23, 0.28] [0.23, 0.29]
	$w = 0.3$	0.48	[0.31, 0.37] [0.32, 0.38]	0.46	[0.22, 0.27] [0.31, 0.36]	0.51	[0.24, 0.29] [0.37, 0.43]
	$w = 0.6$	0.54	[0.31, 0.36] [0.38, 0.44]	0.47	[0.20, 0.25] [0.34, 0.40]	0.46	[0.17, 0.22] [0.35, 0.41]

Table C.2: Tail index estimates between stock index returns and IG bond index returns at $p = 0.005$ and $p = 0.05$ for simulated samples of size $N = 20,000$. Three different sets of values for β used as well as three different copulas with weight w between stock index outcomes and monthly rating migration dynamics. 95% confidence intervals for tail index estimators based on N independent outcomes a standard normal bivariate random variable, with correlation given by $\hat{\rho}$ (upper) and by $\sin((\pi/2)\hat{\tau})$ (lower), are calculated and presented alongside the tail index estimates.

Tail index estimates at $p = 0.95$

		Gaussian		t_3		Clayton	
		$\widehat{\lambda_{L,p}}$	Normal	$\widehat{\lambda_{L,p}}$	Normal	$\widehat{\lambda_{L,p}}$	Normal
$\beta = \beta^{\min}$	$w = 0$	0.04	[0.04, 0.06] [0.04, 0.06]	0.05	[0.09, 0.12] [0.07, 0.10]	0.05	[0.04, 0.06] [0.04, 0.06]
	$w = 0.3$	0.07	[0.09, 0.13] [0.09, 0.13]	0.05	[0.11, 0.15] [0.08, 0.12]	0.07	[0.13, 0.18] [0.11, 0.15]
	$w = 0.6$	0.07	[0.16, 0.21] [0.14, 0.19]	0.06	[0.12, 0.16] [0.09, 0.13]	0.06	[0.11, 0.15] [0.08, 0.11]
$\beta = \beta^{\text{mid}}$	$w = 0$	0.12	[0.12, 0.17] [0.13, 0.17]	0.13	[0.15, 0.20] [0.18, 0.23]	0.12	[0.13, 0.17] [0.13, 0.17]
	$w = 0.3$	0.16	[0.23, 0.29] [0.22, 0.27]	0.13	[0.18, 0.23] [0.21, 0.26]	0.15	[0.20, 0.25] [0.27, 0.33]
	$w = 0.6$	0.17	[0.27, 0.33] [0.29, 0.35]	0.14	[0.17, 0.22] [0.24, 0.29]	0.13	[0.15, 0.19] [0.24, 0.29]
$\beta = \beta^{\max}$	$w = 0$	0.21	[0.23, 0.28] [0.23, 0.29]	0.21	[0.20, 0.25] [0.27, 0.33]	0.20	[0.23, 0.28] [0.23, 0.29]
	$w = 0.3$	0.25	[0.31, 0.37] [0.32, 0.38]	0.21	[0.22, 0.27] [0.31, 0.36]	0.24	[0.24, 0.29] [0.37, 0.43]
	$w = 0.6$	0.24	[0.31, 0.36] [0.38, 0.44]	0.22	[0.20, 0.25] [0.34, 0.40]	0.22	[0.17, 0.22] [0.35, 0.41]

Tail index estimates at $p = 0.995$

		Gaussian		t_3		Clayton	
		$\widehat{\lambda_{L,p}}$	Normal	$\widehat{\lambda_{L,p}}$	Normal	$\widehat{\lambda_{L,p}}$	Normal
$\beta = \beta^{\min}$	$w = 0$	0.01	[0.00, 0.02] [0.00, 0.02]	0.01	[0.00, 0.05] [0.00, 0.04]	0.00	[0.00, 0.02] [0.00, 0.02]
	$w = 0.3$	0.01	[0.00, 0.06] [0.00, 0.05]	0.01	[0.00, 0.07] [0.00, 0.05]	0.01	[0.01, 0.09] [0.00, 0.07]
	$w = 0.6$	0.01	[0.02, 0.11] [0.01, 0.09]	0.01	[0.00, 0.07] [0.00, 0.06]	0.01	[0.00, 0.07] [0.00, 0.05]
$\beta = \beta^{\text{mid}}$	$w = 0$	0.00	[0.01, 0.08] [0.01, 0.08]	0.00	[0.01, 0.10] [0.03, 0.13]	0.00	[0.01, 0.08] [0.01, 0.08]
	$w = 0.3$	0.01	[0.05, 0.18] [0.05, 0.16]	0.01	[0.03, 0.13] [0.04, 0.16]	0.01	[0.04, 0.15] [0.08, 0.21]
	$w = 0.6$	0.01	[0.08, 0.21] [0.09, 0.24]	0.01	[0.02, 0.12] [0.06, 0.18]	0.00	[0.01, 0.10] [0.06, 0.18]
$\beta = \beta^{\max}$	$w = 0$	0.03	[0.05, 0.17] [0.05, 0.18]	0.00	[0.03, 0.14] [0.08, 0.21]	0.03	[0.05, 0.17] [0.05, 0.18]
	$w = 0.3$	0.04	[0.11, 0.26] [0.11, 0.26]	0.02	[0.05, 0.16] [0.10, 0.25]	0.01	[0.06, 0.18] [0.16, 0.32]
	$w = 0.6$	0.02	[0.10, 0.25] [0.17, 0.33]	0.02	[0.04, 0.14] [0.13, 0.29]	0.02	[0.02, 0.12] [0.14, 0.30]

Table C.3: Tail index estimates between stock index returns and IG bond index returns at $p = 0.95$ and $p = 0.995$ for simulated samples of size $N = 20,000$. Three different sets of values for β used as well as three different copulas with weight w between stock index outcomes and monthly rating migration dynamics. 95% confidence intervals for tail index estimators based on N independent outcomes a standard normal bivariate random variable, with correlation given by $\hat{\rho}$ (upper) and by $\sin((\pi/2)\hat{\tau})$ (lower), are calculated and presented alongside the tail index estimates.

C.2 On Migration Time Windows

In the second paragraph of Section 5.3.2, we listed a number of parameters affecting dependence in the model, not directly associated with the dependence structure specification through migration copula and β. One of these is the length of time windows applied for conditioning migration dynamics on stock index outcomes. In the same section, we also mentioned that dependence is likely reduced from migration windows being constructed so as to not span the full risk horizon, which in itself limits the dependence attainable in stock index/bond portfolio return pairs.

In the present section, we have a brief look at what happens to distributions of yearly returns under modifications to the dependence structure as in Section 5.3.3, but with the difference that migration time windows are also set to one year, spanning the full risk horizon. In the maximum copula case, one may then expect stock index movements to be perfectly reflected in migration dynamics.

Looping through β values and copula specifications as before, Figure C.6 shows scatter plots of the first 2000 stock index/HY portfolio return pairs from samples of $N = 20,000$ simulated scenarios per dependence setting. Comparing the figure to Figure 5.11 is now informative, particularly looking at the maximum copula case. Clearly, the separation into clusters of outcomes depending on the portfolio migration outcome (which in the maximum copula case is shared for all bonds within the portfolio), is now very strongly correlated with the stock index outcome. However, the tendency is still imperfect in the sense that a higher stock index outcome is not always accompanied with a more favourable migration outcome, as seen in the "overlap" between clusters of outcomes along the horizontal axis. The reason is that different scenarios have different transition matrices, governed by hazard rate paths, and these are imperfectly related to stock index paths even in the maximum β case.

Remaining with the maximum copula case, it is also of interest to look at the dependence between stock index and portfolio outcomes *within* clusters. Here, all that matters is the process-level dependence as all outcomes within clusters have equal credit migration histories. The effect of β shows in the plots, being positively connected to the amount of dependence observed. However, bivariate outcomes are still far from perfectly aligned even when parameters are set to maximize dependence. The process-level parameters of correlation between stock index and volatility Brownian motions as well as the presence of the jump process here set the cap for attainable dependence.

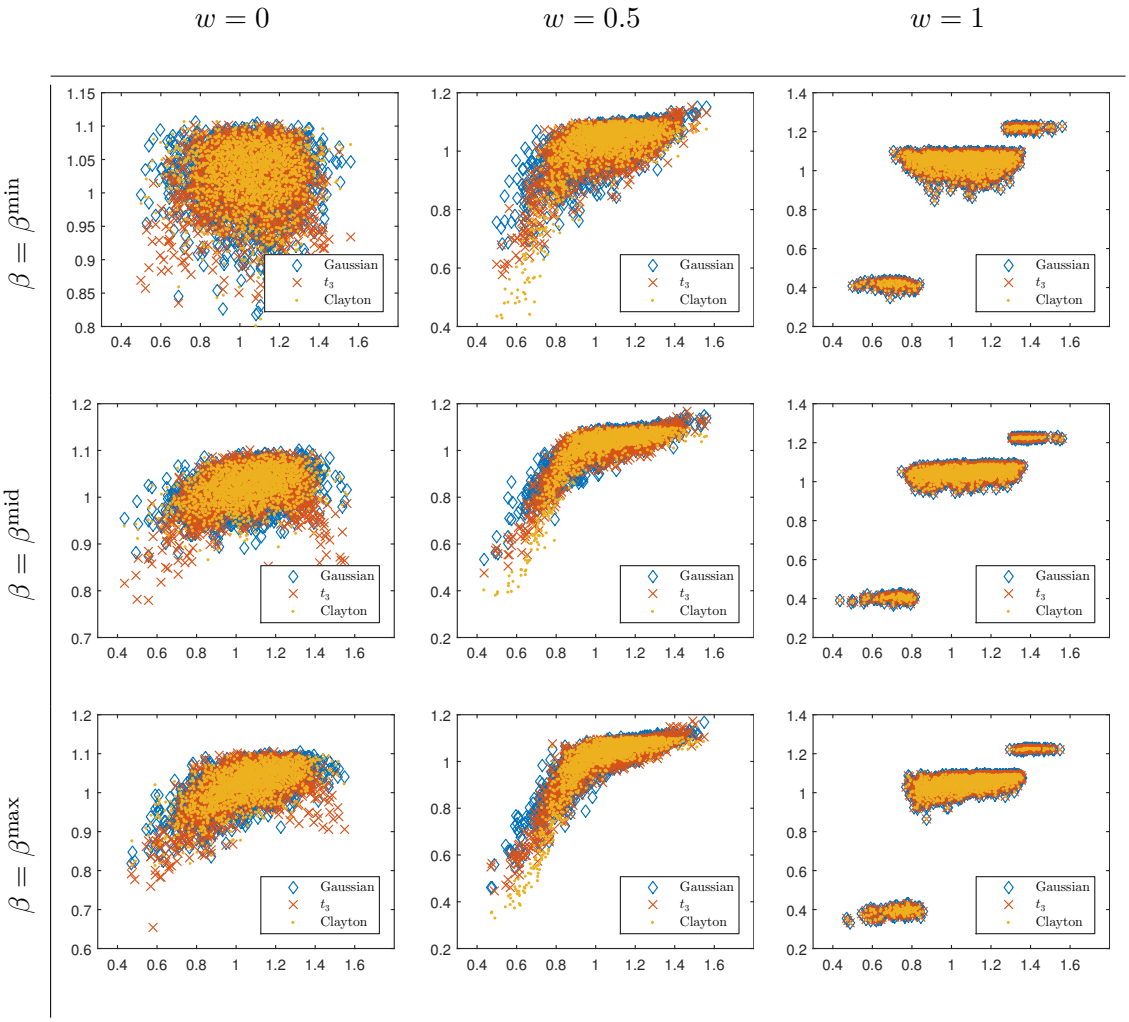

Figure C.6: Scatter plots of 2000 simulated one-year stock index returns and corresponding simulated rebalanced HY portfolio returns where transition dynamics are given by different copulas, applying discrete one-year transition matrices for migrations. Different sets of values of β are used, where $\beta^{\text{mid}} = \beta^{\max}/2$.

C.3 Alternative Migration Conditioning

The mapping of stock returns to uniforms by grouping together all sample paths and considering the empirical distribution for returns over a specified time window, has the benefit of assigning high importance to jump risk as well as increasing the credit migration frequency in periods of high stock volatility. However, due to the nature of stochastic volatility the actual distribution of stock returns over the migration time windows will vary depending on the level of volatility. That is, if we denote our migration times t_j, $j = 1, \ldots, j_T$, where t_{j_T} is the last migration time within the risk horizon, we fix j and consider the stock return $S_{t_j}/S_{t_{j-1}}$. The actual distribution of this quantity will vary depending on the value of the volatility process at t_{j-1}.

Therefore, one might argue the notion of empirical distribution is flawed in this case and that values of the uniforms will be biased toward more extreme outcomes in periods of higher volatility. An alternate route is to consider only the Brownian motion of the stock movement, where the distribution is fully known within any migration time window. This allows for construction of uniforms unaffected by stochastic volatility and analytically given from sampled stock process outcomes, but also has the disadvantage of ignoring the jump component altogether. Following this approach, we consider the quantities

$$Z = \int_{t_{j-1}}^{t_j} dW_s^S \sim N(0, t_j - t_{j-1}), \tag{C.1}$$

whereby uniforms relating to stock index movements are easily constructed according to

$$U = \Phi\left(\frac{Z}{\sqrt{t_j - t_{j-1}}}\right) \tag{C.2}$$

where $\Phi(\cdot)$ is the standard normal distribution function.

With uniforms constructed according to the above, credit migrations may be simulated by following the steps of Section 4.3.2.

C.3.1 Portfolio Simulation

We follow this alternate route to perform simulation from the framework, setting parameters according to Table 5.3, but modifying the copula for migrations much like in Section 5.3.2. Focusing on IG and HY portfolios with monthly rebalancing, we simulate $N = 20,000$ economic scenarios, attaching portfolio evolution scenarios for each copula. Applying the method described here for transforming stock index returns to uniforms, we compute lower quantiles and dependence measures and present results in Figures C.7 and C.8 for IG and HY portfolios respectively, comparing to results obtained when the standard method of Section 4.3.2 is used.

Unsurprisingly, this method leads to a weaker form of dependence within the portfolios as well as across markets, as indicated in all of the plots. The stock index jump component is here fully disconnected from any credit-side movements, contributing to more variance in stock index movements while having zero influence on bond portfolios. While the transformation of monthly stock index returns to uniforms is more analytically sound with this method, the disregard of stock index jumps is likely a drawback impeding the outlook of adapting the model to reality. However, if the model were revamped to plant dependence between equity jump component and credit risk elsewhere, such as in the behaviour of hazard rates, the approach may be assessed in a different light.

Even though the overall dependence is weaker than previously for most migration copula specifications, it is interesting to note how the conditioning method affects measures

for upper tail dependence. In Figure C.9, 0.95 and 0.995 level estimates are presented. The figure suggests that slightly higher values of upper tail dependence are obtained with this conditioning method, at least as indicated by 0.95 level plots and when a copula with higher dependence is applied for migrations, and for the HY portfolio moreso than for the IG portfolio. We recall that the influence of stock index volatility is much larger on the HY hazard rate than it is on the IG hazard rate. With this conditioning method, the level of volatility is irrelevant for the transition modelling. While a low volatility level still often comes with high stock Brownian motion movements and, in the case of high β, with low migration probabilities, a uniform constructed through Equation (C.2) is in this case more often closer to 1 than one constructed through Equation (4.19). It seems upward transitions are therefore more likely to occur jointly with large positive stock movements with this conditioning method than with the original one. Still, dependence in the upper tail appears far weaker than in the lower tail.

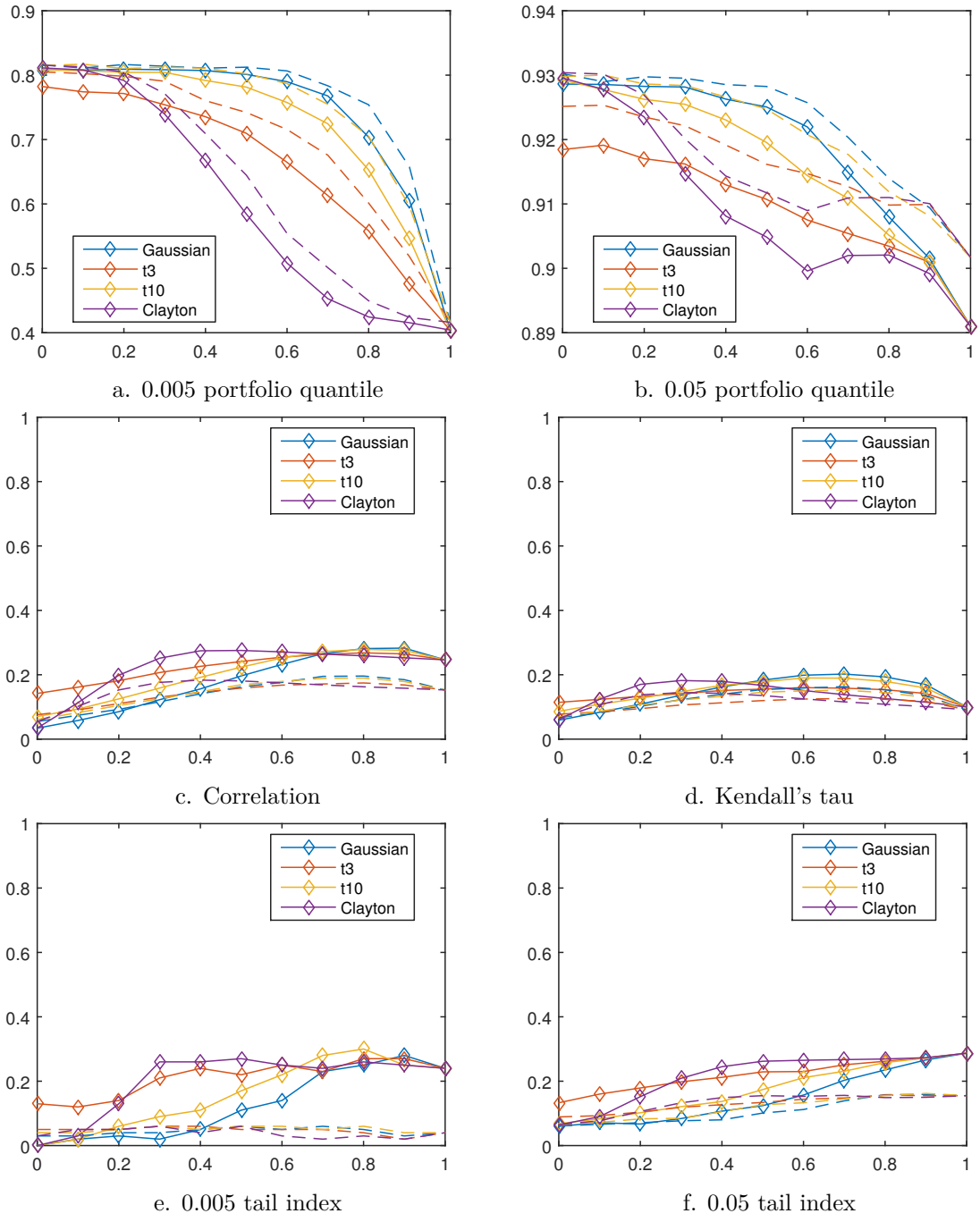

a. 0.005 portfolio quantile

b. 0.05 portfolio quantile

c. Correlation

d. Kendall's tau

e. 0.005 tail index

f. 0.05 tail index

Figure C.7: Quantiles and dependence measures for the IG bond portfolio with monthly rebalancing, based on simulation of $N = 20,000$ economic scenarios with independent portfolio scenarios generated for each copula and stock index transition weight varying between 0 and 1 in steps of 0.1. Solid lines show results when monthly stock index returns are transformed to uniforms by applying the probability transform on the empirical distribution, whereas dashed lines result from application of the alternative method described in Appendix C.3

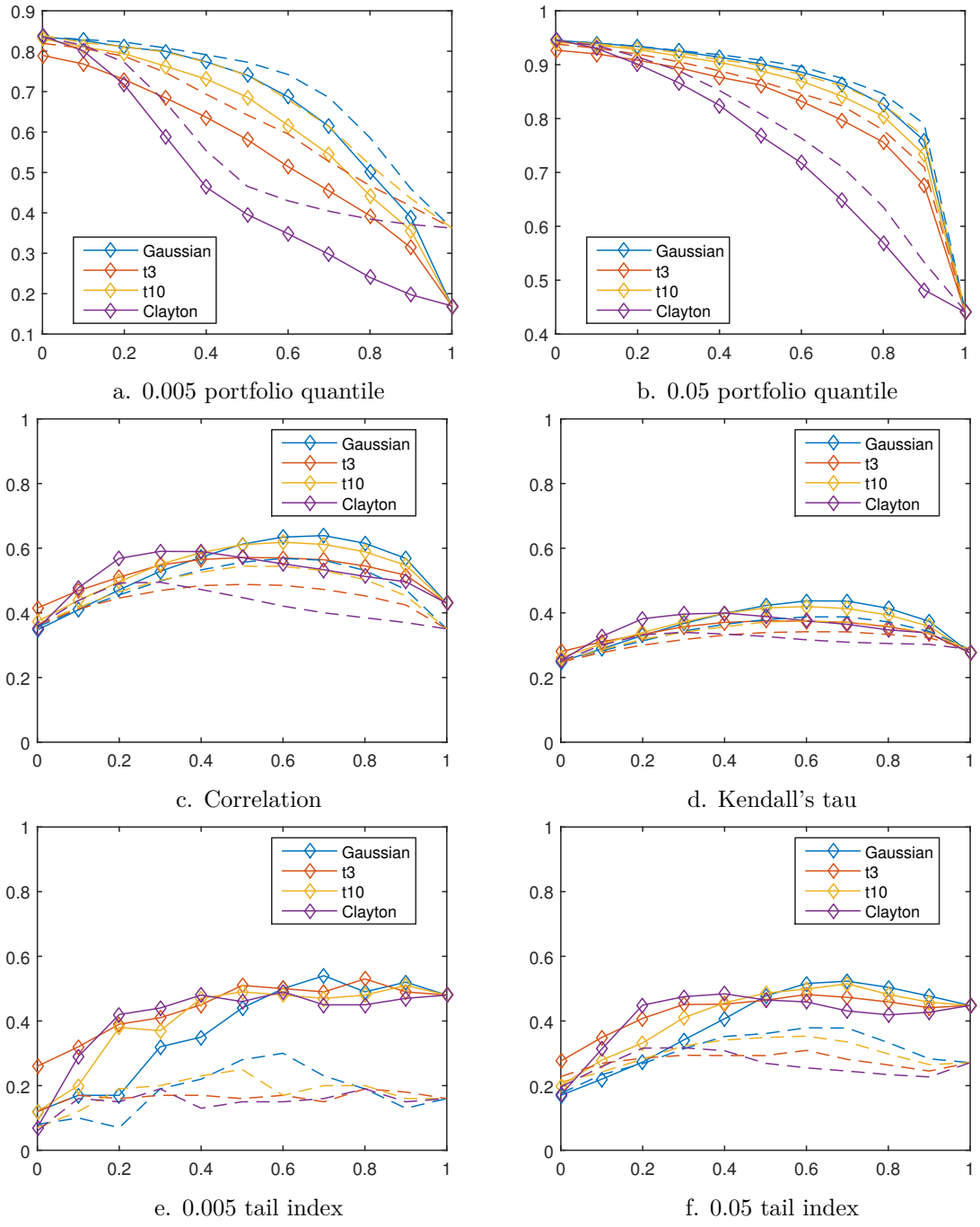

a. 0.005 portfolio quantile

b. 0.05 portfolio quantile

c. Correlation

d. Kendall's tau

e. 0.005 tail index

f. 0.05 tail index

Figure C.8: Quantiles and dependence measures for the HY bond portfolio with monthly rebalancing, based on simulation of $N = 20,000$ economic scenarios with independent portfolio scenarios generated for each copula and stock index transition weight varying between 0 and 1 in steps of 0.1. Solid lines show results when monthly stock index returns are transformed to uniforms by applying the probability transform on the empirical distribution, whereas dashed lines result from application of the alternative method described in Appendix C.3

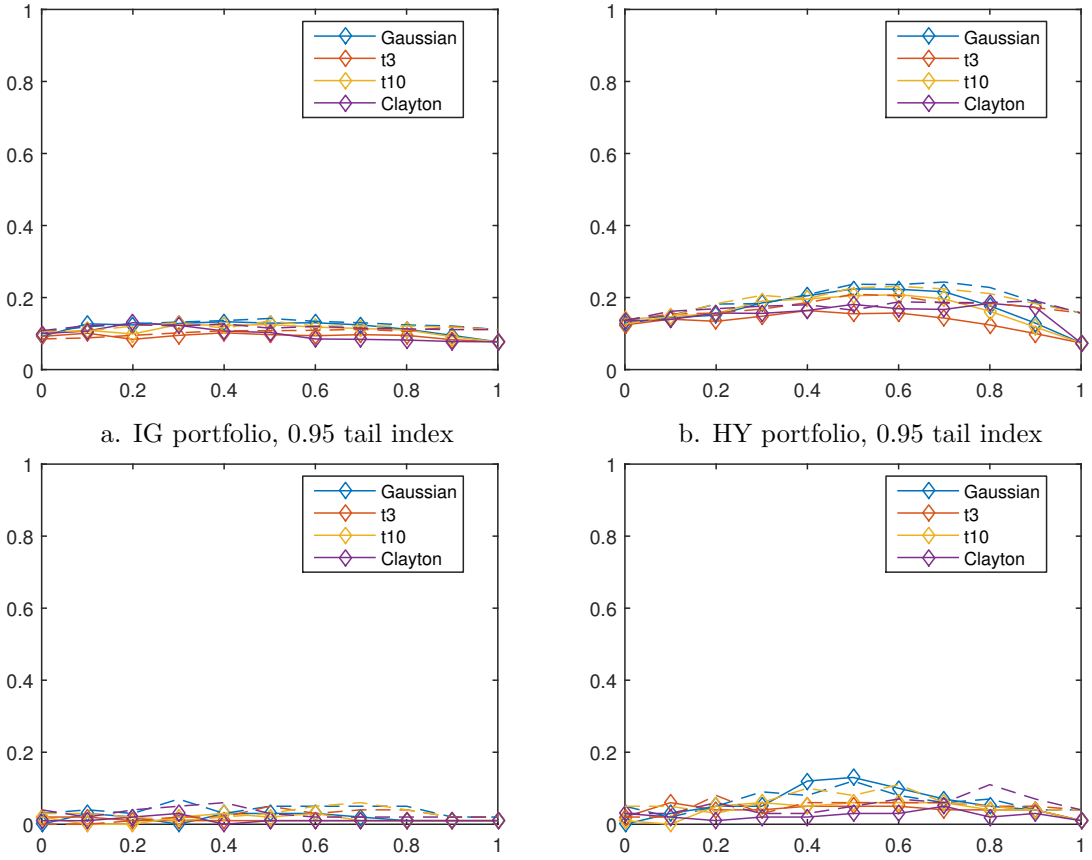

a. IG portfolio, 0.95 tail index

b. HY portfolio, 0.95 tail index

c. IG portfolio, 0.995 tail index

d. HY portfolio, 0.995 tail index

Figure C.9: Upper tail index estimates between stock index and bond potrfolio returns, based on simulation of $N = 20,000$ economic scenarios with independent portfolio scenarios generated for each copula and stock index transition weight varying between 0 and 1 in steps of 0.1. Solid lines show results when monthly stock index returns are transformed to uniforms by applying the probability transform on the empirical distribution, whereas dashed lines result from application of the alternative method described in Appendix C.3